APTAMER-BASED AFFINITY METHODS FOR MASS SPECTROMETRY

By

BASRI GULBAKAN

A DISSERTATION PRESENTED TO THE GRADUATE SCHOOL
OF THE UNIVERSITY OF FLORIDA IN PARTIAL FULFILLMENT
OF THE REQUIREMENTS FOR THE DEGREE OF
DOCTOR OF PHILOSOPHY

UNIVERSITY OF FLORIDA

2012

To my lovely family

ACKNOWLEDGMENTS

This work would not have been possible without the guidance and encouragement I received from my academic advisors, Dr. Weihong Tan and Dr. David H. Powell. I got great experience in professional aspects during my doctoral studies and grown as a better scientist. I would like to extend my thanks to Dr. Nick Polfer, Dr.David Wei and Dr.Jesse F.Gregory for their assistance and for spending their valuable time serving on my committee. I also want to thank the members of the Tan group especially Ismail, Ibrahim, Emir Judy, Mingxu, Sena, Tahir, Parag and Kwame and to Powell group especially Julia, Soledad and Noelle for their friendship and helpful advices. The help from the ICBR proteomics core lab director Dr. Sixue Chen and the scientific manager of the core lab Carolyn Diaz is also greatly appreciated. I cannot end without thanking my family for giving me the strength and the opportunity to achieve one of the most important dreams in my life.

TABLE OF CONTENTS

page

LIST OF TABLES

LIST OF FIGURES

Abstract Of Dissertation Presented To The Graduate School
Of The University Of Florida In Partial Fulfillment Of The
Requirements For The Degree Of Doctor Of Philosophy

APTAMER-BASED AFFINITY METHODS FOR MASS SPECTROMETRY

By

Basri Gulbakan

May 2012

Chair: Weihong Tan
Major: Chemistry

Capturing rare proteins and metabolites from complex biological mixtures is essential to understanding the key functions of biological systems. As such, the development of new techniques for their isolation and subsequent detection/identification by mass spectrometry (MS) is becoming increasingly more important. While identification of pure proteins and simple biological mixtures using MS has become a routine and relatively simple task utilization of this powerful tool in analyzing complex mixtures and real biological samples is still in its infancy. One approach to the analysis of complex biological samples employs chromatographic extraction and fractionation methods, before MS is performed. However, current separation methods suffer from numerous limitations, including time-consuming procedures, the difficulties involved in handling complex samples, and, especially, the lack of selective molecular isolation.

Therefore, the next best option utilizes affinity reagents tethered on a substrate which, in turn, could be used as a sample treatment tool or as a substrate to obtain direct MS readouts. A major obstacle to this strategy is finding efficient and robust capturing agents for biomarker detection. Although antibodies have been the gold

standard as capturing reagents, commercial antibodies do not exist for all proteins, and developing high- affinity and selective antibodies is very expensive and time-consuming. Moreover, since antibodies are proteins, they are very prone to irreversible degradation and cannot be easily modified. As an alternative to antibodies, aptamers provide the specificity lacking in many extraction matrixes.

This thesis discusses the development of aptamer based MS platforms. We have developed four different platforms for this purpose. First, nanowell array surfaces were prepared and applied in MS. Second graphene oxide and graphene oxide-metal conjugates were prepared and modified with aptamers. Third a unique nanoflower shaped nanostructure was developed for MS and applied for the extraction of adenosine triphosphate (ATP) in cancer cells. Finally aptamer-based affinity mass spectrometry was applied for the biomarker discovery of liver cancer. All these results demonstrate the utility of the approach for analysis of small molecules and discovery of new biomarkers in real biological samples.

CHAPTER 1
INTRODUCTION

Biomarker Discovery

Fundamental understanding of many biological processes has been greatly influenced by the completion of the human genome project and this initiated a new era for biological research. However, while genomic information is very important but it is not enough to fully understand the biological processes especially when they relate to disease. Therefore the focus was then shifted to the interactions and roles of other biomolecules such as proteins and metabolites in cells—that is, to new fields called proteomics and the small molecule complement of proteomics- metabolomics.(*1, 2*) Proteins and small molecules are very important constituents of biological systems. They can have diverse functions such as cytoskleletal building blocks, as enzymes which control biochemical reactions, or as antibodies that contribute to immune system or signaling molecules that provide communication between cells and organ systems. Their enormous versatility in structure, folding, and modification enable them to carry out very complex tasks within the cells and higher cellular associations.(*3*) Proteins and metabolites are also very rich sources of biomarkers for many different diseases. For example, overexpression of a number of serum marker proteins, such as α-fetoprotein for liver cancer(*4*), carcino-embryonic antigen (CEA) for colon cancer(*5*) and prostate specific antigen (PSA) for prostate cancer(*6*) are well established markers strongly related to tumor initiation and growth. Also, several growth factor proteins, such as epidermal growth factor receptor 2 (EGFR2), vascular enhanced growth factors (VEGF), platelet-derived growth factor (PDGF) and insulin-like growth factors (IGF) are also tumor related proteins that play important roles in tumor initiation.(*7*) It is estimated that

approximately 85% of breast cancer patients have significantly elevated levels of EGFR-2 protein and this elevation is strongly correlated with disease recurrence, metastasis or shortened survival.(*8*) On the metabolomics side, sarcosine -a small molecule- has recently been linked to prostate cancer.(*9*) Propionyl carnitine has been found as a biomarker for methylmalonic acidemia (MMA) and propionic acidemia (PA). (*10*). These studies have all shown that disease processes will ultimately result from proteins—proteomics and also from metabolites-metabolomics.

Protein Biomarkers

Contrary to the impressive and rapid progress in genomics with more than 800 organisms having been sequenced, including the human genome; proteomics and metabolomics research are still in its very early stages.(*11*) Proteomics by definition is the systematic determination of protein sequence, quantitation, modification state, interaction partners, activity, subcellular localization, and structure in a given cell type at a particular time. There are estimated 20,000 to 25,000 human genes. (*12*)However, the old “one gene, one protein” hypothesis is no longer valid, and today we know that one gene does not produce one protein and once proteins are made, many of them are modified by phosphate, carbohydrates, or lipid groups in different configurations, thus adding another level of complexity to the proteome. Similar to the human genome project the human proteome project was initiated by a group of scientists in 2005 by human proteome organization (HUPO).(*13*) This was followed by twelve other proteomics initiatives including the human liver proteome project, the human brain proteome project and the human kidney and urine proteome project. However the scientists must deal with approximately more than 10, 000, 000 proteins, which can then be further modified by many post-translational modifications. Because of the time and

effort and money it takes for a protein to be fully sequenced, identified and validated; such proteome project efforts are extremely challenging and therefore are not expected to give promising results and will not be feasible in the very near future- at least with the current technology that is used in proteomics. For that reason the very early hope of characterizing the whole human proteome failed too quickly and researchers in the proteomics field are more focused on trying to find molecular differences between one functional state of a biological system to another rather than trying to understand the systems biology as whole – which certainly will give more and more precise information- but this is very difficult to realize. It is noteworthy that differences between different cellular states are also reflected in changes in gene expression that also can be monitored at the genome and transcriptome level. For instance transcriptomic arrays and deoxyribonucleic acid (DNA) methylation studies have shown great potential for biomarker discovery.(*14, 15*) While the genome is fairly static, proteome is highly dynamic. Therefore the data suggested by genomics about diseases may not be completely true as it does not reflect the status of the system at any given time. Because of the common post-translational modifications such as phosphorylation, glycosylation and lipidation; the status of the cellular organism changes continuously. For these reasons the protein domain is likely the most affected part in disease, response and recovery. The main application of proteomics is therefore on the biomarker discovery. (*16, 17*) Proteomics itself cannot heal a person but it does have the potential to make a sizeable impact in medicine. The starting hypothesis in a proteomics-based biomarker study is that if there is a disease progression then the protein make-up of the diseased organism should change both in quality and in quantity

or sometimes in both. So if this information can be extracted and interpreted appropriately then it will be more useful for biomarker discovery and complemantary to the genomics or transcriptomics data. It is for that reason that many of the food and drug administration (FDA) approved drugs target the processes mediated by proteins and by protein-protein interactions.(*18*) It will be even more useful if this information can be obtained at the early stage of disease progression since the early diagnosis and treatment result in the best prognosis of many diseases. Over the past 20 years or so, thanks to the advances in different analytical technologies there has been tremendous increase in our understanding of how normal cells become diseased cells and which of the signaling pathways are more affected in disease initiation and progression.(*19*) However in searching for new tools for diagnostics, progress has been very slow in bringing the biomarkers to clinical practice. Biomarkers are becoming increasingly more and more important, and it is clear that patients would benefit by a greater availability of such effective molecular indicators that can be monitored noninvasively from readily accessible bodily fluids. This will also solve the problem that the pharmaceutical industry has been facing for many years. The current research and development (R&D) cost for developing a new therapeutic drug takes millions of dollars, and it takes an average of 12 years to get a new drug to market. (*20*)

P4 Medicine

Accurate diagnosis of diseases will also permit the development of more effective drugs and more effective therapies and will also enhance the success of clinical trials. Biomarkers also fit perfectly with the new vision of clinicians called P4 medicine. This is a new concept coined by biologist Leroy Hood, and shortly stands for Predictive, Preventive, Personalized, and Participatory Medicine.(*21*) Key to the success of P4

medicine is to detect disease at an earlier stage, when it is easier and less expensive to treat effectively. This is why biomarker research has been a central focus in many research labs across academia, government agencies, and the pharmaceutical industry. The definition of biomarker is an ongoing debate among scientists and clinicians. There are many different ways to define biomarkers based on molecular properties, applications, and methods. The National Institutes of Health (NIH) suggested an inclusive definition for biomarker as “a characteristic that is objectively measured and evaluated as an indicator of normal biologic processes, pathogenic processes, or pharmacologic responses to a therapeutic intervention.” (*22*) This is a very broad definition it does not exclude any particular molecule, therefore a biomarker can be DNA, protein, metabolite, mRNA (messenger ribonucleic acid), or lipid or even an ion. It is fair to say that full understanding will be possible with the combination of all the “omics” platforms and evaluation of the data altogether but this fact does not rule out the possibility of finding biomarkers with a single “omics” approach.

Methods for Protein Biomarker Discovery

Biomarker discovery methods vary a lot depending on the disease type, but generally they can be classified as mass spectrometry-based biomarker discovery and array- based biomarker discovery.

Mass Spectrometry Based Protein-Biomarker Discovery

Development of the “soft” desorption-ionization techniques namely, matrix-assisted laser desorption/ionization (MALDI) and electrospray ionization (ESI) revolutionized proteomics and biomarker discovery research by rendering the study of macromolecules in the gas phase feasible. (*23*) A schematic diagram for both of these ionization techniques are given in Figure 1-1.These innovative mass spectrometry

techniques have found widespread use in many different areas including genomics, transcriptomics, proteomics and metabolomics and used in all these “omics”-based biomarker discovery efforts as well. Mass spectrometry techniques are particularly useful for proteomics applications and have been a workhorse for peptide and protein identification. Therefore, the principal enabling technology of proteomic biomarker discovery is mass spectrometry (MS). As demonstrated in Figure 1-2 a recent web of science statistics clearly shows this fact.

All mass spectrometers, regardless of the type, ionization mode or performance characteristics produce mass spectra which plot the mass-to charge ratio of the ions (x-axis) observed versus detected ion abundance (y axis).(*24*) There are many different ways to realize MS based proteomics biomarker discovery but the methods are generally subcategorized as “bottom-up proteomics” and “top-down proteomics”.(*25*)The cartoon representation of both processes is shown in Figure 1-3.

In bottom-up approaches, the proteins can be first separated by gel electrophoresis or chromatography, in which the sample will contain separated proteins. Specific bands or fractions are first subjected to proteolytic cleavage and the peptide products are then further fragmentated and analyzed by MS. Alternatively, a complex protein mixture initially can be digested to the peptide level, and then separated by on-line chromatography coupled to electrospray mass spectrometry (LC-ESI–MS/MS) or MALDI (LC-MALDI MS/MS). The identity of the original protein is determined by comparison of the peptide mass spectra with theoretical peptide masses calculated from a proteomic or genomic database. Bottom-up proteomics is the most mature and the most widely used approach for protein identification and characterization.

Commercial instruments with control software and bioinformatics tools optimized for bottom-up applications are available from several vendors. The bottom-up strategy using multidimensional capillary LC–MS/MS has been the most successful method in identifying proteins in digests derived from very complex mixtures such as cell lysates. This method is also known as MudPIT (Multidimensional Protein Identification Technology) relies on bottom-up proteomics approaches and high performance separation(*26*).

In top-down proteomics, as opposed to the bottom up approach, intact protein ions or large protein fragments are directly subjected to gas-phase fragmentation for MS analysis. However top-down proteomics is a fairly new field in proteomics and its application to biomarker discovery is also very limited. The biggest drawback of top-down proteomics is the necessity for highly sophisticated and very expensive instrumentation which requires great expertise to operate and maintain. Therefore the top-down approach is still mainly used as a technique for analyzing purified proteins. In addition, automated hardware and software dedicated to top-down approaches are currently in development stages and few products have entered to the market so far. Hence, the top down approach is not competitive enough with bottom-up approaches for whole proteome analysis and biomarker discovery. In addition, the sensitivity of the mass spectrometers for proteins is much lower than for peptides, and the proteins might be processed and modified such that the combinatorial effect makes determining the masses of the numerous resulting isoforms impossible. On the other hand there are two major advantages of the top-down strategy: the potential access to the complete protein sequence and the ability to locate and characterize post translational modifications

(PTMs). In addition, the time-consuming protein digestion required for bottom-up methods is also eliminated.

Overall, whatever approach is undertaken for proteomics-based biomarker discovery, the success is totally dependent on the quality of the MS data and the quality of the MS data is highly dependent on how well the sample is prepared and how well it is fragmentated in the mass spectrometer. The classical method for breaking ions apart involves colliding them with a neutral gas such as helium or argon, a process known as collision -activated dissociation (CAD or CID). This is also the fundamental ion activation technique in which today`s proteomics methodologies are mostly built on. Newer methods use electrons instead of collisions. These methods are electron capture dissociation (ECD) and electron transfer dissociation (ETD). The fundamental difference between these two is actually very simple; the CAD method primarily breaks the amide bond whereas ECD and ETD mainly break the N-Cα bond. This is depicted in Figure 1-4. Recent data showed that when these two methods are applied for protein identification even though a great portion of the peptides identified overlaps, certain portions can be identified either by CAD only or ETD only method. So to get good proteome coverage and to get more confident peptide identification for more reliable biomarker discovery, implementation of both methods is definitely be advantageous (*27*).

The last and maybe the most important part of the biomarker identification process is the use of proper bioinformatics tools. After all the data has been generated by the mass spectrometer, data is then processed by many different databases which are available with the instruments or can be obtained from different commercial vendors

such as Mascot, Sequest and Probid. The basic drawback of the database searching for biomarker identification experiments is that it can only be carried out using the organisms that have had their genome sequenced so that all possible peptides are known in Silico. (*28*) The overall workflow of database searching is shown in Figure 1-5. Otherwise a manual data interpretation way which is called as de-novo sequencing should be applied. However considering the amount of data generated in a typical proteomics experiment, the success of the de-novo approach is very much limited and for larger scale identification studies is totally impossible.

Array-Based Protein-Biomarker Discovery

Microarrays can be defined as a functional element (DNA, RNA, antigen, antibody, aptamer, and small molecules) being attached to a solid substrate in an ordered manner at high density. Hundreds to thousands of these products can be immobilized on a very small area with a specialized robotic arraying tool. The immobilized products (i.e., the array) serve as interaction targets for a labeled probe.(*29*) This probe is generated by labeling it with a fluorescence dye, radioisotope, or chemiluminescence agent. A schematic diagram of the array based approaches is shown in Figure 1-6. The labeled probe then interacts with the sample and after washing and drying steps; a high-resolution image is created using a specialized image scanner. Software is then used to determine the intensity of each spot. The main steps of the growth and maturation of array platforms for proteomics are to a big extent similar and related to those of the genomics. The sequencing of the whole genome began with the development of the Sanger method nearly 30 years ago. This method enabled sequencing a few short DNA strands for the determination of whole chromosomes. Then the next important challenge was to develop software capable of managing all the data. Using an oligonucleotide

microarray containing a series of gene-specific oligonucleotides or cDNA sequences on a slide or a chip, one can probe the expression of thousands of genes at once. Even though the application of the array platforms for genomics was quite wide and successful it is very slowly becoming a complement to proteomics and its application to proteomic biomarker discovery is fairly new and different formats have recently begun to emerge. Since antibodies not DNA or RNA are used as the probes for screening the proteome it is very difficult to maintain the folded properties of proteins and this poses a potential problem in the fabrication of protein microarrays. Furthermore, relative to hybridization reactions, folded proteins have greater sequence dependence and are prone to nonspecific interactions. The complexity is additionally increased by the inability to draw an absolute correlation between abundance of mRNA and the level of its corresponding protein. This, in turn, depends on a number of factors such as post-translational modifications, proteolysis, and compartmentalization. Another reason is that there are no analogous tools available for protein analysis. There is no protein equivalent of polymerase chain reaction (PCR). It is currently not possible to induce polypeptide molecules to replicate themselves in a manner analogous to oligonucleotide replication through PCR. So unlike the DNA microarrays, the necessity for the sensitivity is far greater. Because even if a small amount of DNA piece is isolated it can be amplified through PCR, whereas a small amount of a polypeptide must be detected and analyzed without any amplification.(*30*)

Dynamic Range Problem

As outlined in details above, there are basically two important platforms for biomarker discovery namely mass spectrometry and microarrays. Each of them has its own challenges but for both approaches the challenge in protein biomarker discovery

can be condensed into two distinct categories. The first one is detection, identification and quantification of low abundance proteins from complex biological samples. The second one is the development of a high-throughput; low-cost mass spectrometry solution to validate promising protein markers identified in proteomics experiments. Unfortunately, the dynamic range of the biological mixtures is far beyond the dynamic range of the current instrumentation. Currently mass spectrometers are at a dynamic range of about 10^4 however; biological mixtures- including plasma, urine, cell lysates- contain proteins in a range of concentrations that, by some estimates, extend over 12 orders of magnitude as shown in Figure 1-7. This poses the greatest challenge for successful biomarker identification because while mass spectrometry (MS) has evolved as a tool to detect and identify femtomoles of peptides, the dynamic range of detection is still a limiting factor for comprehensive profiling of biological mixtures.(*31*) In the current status of the technology and the speed of the innovations in the instrumentation side, covering a dynamic range of 10^8 or 10^{10} will not be very likely in the near future. To put this problem into perspective a model calculation will be given here.(*32*) Serum has a total protein concentration of approximately 80 mg mL^{-1} or 1.6 mM for a 50 kDa protein. Most of the presently used tumor markers have cut-off values around 1–10 ng mL^{-1} (20–200 pM for a 50 kDa protein). If it is assumed that a given nano HPLC-MS method has a limit of detection of 1 fmol, then it will take 5–50 µL of serum to have 1 fmol of a putative cancer biomarker present to start with. However, 50 µL of serum contains 4 mg total protein, which is far too much to be loaded on a nanoLC column (capacity 5–10 pmol). It is thus indispensable to fractionate the sample in order to cover a wider dynamic range. Depletion of high-abundance proteins by affinity

chromatography is a widely used approach to reduce the total amount of protein in serum by a factor 10–20 reducing the initial protein load to approximately 0.2 mg or 4 nmol. It has to be mentioned that this depletion step does also remove non-target proteins due to adsorption to albumin or other high-abundance proteins. It appears, however, that the depletion step can be performed with good repeatability despite this shortcoming. Even after depletion there is still a discrepancy of about 1000-fold between the loading capacity of a nanoLC column and the amount of protein present. Further fractionation is thus required, for example, by strong cation-exchange HPLC (often done after trypsin digestion) or high temperature reversed-phase HPLC of intact proteins. Assuming that 50 fractions will be taken and that the amount of protein distributes evenly over each fraction (an assumption that is made to facilitate calculation), there will be approximately 80 pmol protein (or protein digest) per fraction leaving a 10-fold discrepancy between the loading capacity of a typical nano HPLC column and the amount present. It is obvious that further fractionation could easily overcome this gap but at the expense of extremely long analysis times per sample. If one considers that an LC run takes 1 h, then analyzing 50 fractions will take 50 h (approximately 2 days without considering any downtime of the instrument) and a further fractionation into 10 fractions would lead to a total analysis time of 500 h (approximately 21 days). It is very clear that this is not a very feasible or acceptable timeline for biomarker discovery research, where large numbers of samples have to be processed. On top of everything putative biomarkers for diseases are present at vanishingly small concentrations generally falling into ng/ml range. (*33*)

It is generally accepted that in most cases two MS instruments are required for unambiguous protein identification. The analytical performance of different instruments as illustrated in Figure 1-8 clearly shows that no single instrument has the capacity to simultaneously meet all the biological and analytical requirements of biomarker identification.(*34*) So if one totally relies on what mass spectrometry data can give, the rate of success in biomarker discovery will be less than the failure rates. The first problem is also related to the sensitivity of the mass spectrometry instruments. Even though it is highly dependent upon the analyte being analyzed, it is generally accepted that ionization yields are around 10 percent in electrospray ionization and around 5 percent in matrix assisted laser desorption ionization. So a very big portion of the analytes that is present in the original samples is never introduced into the mass spectrometer in the form of ions. The problem is also associated to the lack of mechanistic understanding of the ionization process both methods. In neither ESI nor MALDI no clear and solid understanding yet exists about the ionization mechanisms. There are detailed reviews on these topics but the physical chemistry associated with ionization is extremely complex, therefore it is very hard to draw a mechanistic understanding.(*35*) This has been an active field of research among mass spectrometrists, and many reports were published claiming big increases in ionization efficiency but most of them were successful only in certain cases and with limited analyte classes which are far from being generalized. The losses during the ion transfer process into the mass analyzer also contributes to the loss of sensitivity, and in essence a very tiny portion of the sample can be ionized, transferred through the ion optics, reach the detector, be detected and recorded as an ion signal. Recent technologies

such as ion funnels and off axis ion beam technologies have brought some improvements but they are still insufficient.(*36*)

Another difficulty is to establish which differences are the most important and likely to survive downstream pre-clinical validation. It is therefore necessary to conduct validation studies on identified proteomic differences. These candidate proteins are often selected based on the biological knowledge and the quality of the quantitative MS data. In this way the current status of biomarker discovery “looking for the needle in haystack status” should be transformed into a “looking for needle in the needlestack” approach. In conclusion it is fair to say that the improvement that will come from the instrumentation side will be quite limited and to meet the challenges of biomarker discovery new approaches are certainly needed.

Affinity Guided Approaches for Mass Spectrometry

While many technical and experimental difficulties still exist in the MS-based techniques, it is the most powerful discovery and identification tool and no other analytical technology has yet the capability to be an alternative making MS as a gold standard. Because of the limitations as explained in previous sections, most of the current efforts focus on more systematic and targeted approaches to use MS more effectively as a more sensitive, more selective and high throughput analytical tool.

Therefore affinity capture, enrichment and detection have become the new direction of the MS- based studies. Many different strategies have been employed for selective capture, enrichment followed by mass spectrometry analysis. In this context surface enhanced laser desorption mass spectrometry (SELDI) has emerged as the most successful method for affinity mass spectrometry applications.(*37*) While the actual method of preparation of the ProteinChip® surface(s) is proprietary, the approach

involves the covalent attachment of surface modification compounds to alter the surface chemistry of capillary chromatography columns. SELDI has been applied to proteomics, especially in cancer biomarker identification and disease diagnoses. (*38*) In the SELDI approach a small number of integrated surface chemistries are used to selectively bind various proteins from complex mixtures obtained from biological samples. The "fingerprint" MALDI mass spectra obtained from analysis of these samples can then be used to establish a database of responses for clinical diagnosis of disease states, i.e. an average "normal" response is defined on the basis of "fingerprint" MALDI mass spectra obtained from a large set of healthy patients and deviation in the fingerprint MALDI mass spectra for a given patient is taken as a diagnostic indicator of a disease state. However although very promising reports have been published in the literature, the SELDI results are also have poor diagnostic power and the success of SELDI as a clinically viable tool is highly debated. In addition to this patent protected technology, several other studies have demonstrated the efficacy of using an affinity capture tool combined to MS to improve selectivity and sensitivity. Both both proteins and DNA may be captured using beads via avidin-biotin interactions, immobilized metal affinity capture (IMAC), and antibody-antigen affinity interactions. In one of the earliest examples of affinity mass spectrometry, monoclonal antibody modified agarose beads were used to selectively capture the peptide containing the linear epitope of the antigen from the proteolytic digest of the antigen and then characterized the epitope by MS.(*39*) In practice the affinity capture structures may either be manipulated directly (e.g by placing surface chemically modified magnetic beads into a protein mixture and then depositing the withdrawn beads directly on the MALDI target) or loaded within a pipette tip and the

protein containing solution manipulated (e.g. by passing the protein solution through the affinity capture material and then eluting the captured protein. Both approaches are attractive but the choice highly depends on the molecular weight and hydrophobicity of the captured species. Affinity purification coupled to mass spectrometry has not only been used to capture analytes of interest from complex biological mixtures but also used as a very efficient tool for studying the interactions between different proteins. In this type of experimental setting, the protein of interest is first expressed in a cell line as a recombinant fusion protein and immobilized on a solid surface.(*40*) Interacting proteins can then be precipitated by applying a cellular lysate to the column. An obvious advantage of this method is that it is robust, easy to use and capable of retrieving even weakly interacting and low abundant proteins owing to the fact that large amounts of recombinant protein are present on the column. However, not all proteins can be easily overexpressed as a fusion protein. Sample complexity is largely dictated by the interactions established by the tagged protein, the number and nature of the purification steps and the stringency of the washes. Despite its limitations this method has successfully been applied for many different problems.(*41*)

Role of Nanotechnologies in Affinity- Based MS Applications

Nanotechnology is defined as the systematic study of a particular system at the nanoscale level at length scales between 1 and 100 nm. Considering that average bond lengths are in the picometer range; this is basically the limit of the metrics where molecules cannot be further manipulated at the molecular level. Therefore, nanotechnology opened up very unique opportunities not only for material research but also for biology, medicine and many other disciplines by manipulating individual atoms and molecules in a specific way that can fit a certain application. In the last decade

nanostructures have attracted great attention owing to their unique physical, chemical and structural properties. As discussed previously, MS technology is challenged by a number of limitations (dynamic range, PTMs, instrument sensitivity, biological complexity, etc). The field of nanotechnology has been recently associated with several MS based affinity applications.(*42*) While a diverse array of MS applications for nanostructures exist, they be can be condensed into three basic categories: (a) scaffold for biosensing (b) sample purification and enrichment tool (c) substrate for mass spectrometry analysis.

Nanoporous Materials

Changing the morphology of a surface from plain to a nanostructured form changes the sensing properties of that particular material. Surface enhanced laser desorption ionization (SELDI) was applied on a nanostructure surface (2-20 nm), and spectral features were completely different with different sized nanopores.(*43*) Similarly, mesoporous silica chips were used in proteome fractionation based on enhanced sieving properties of these nanostructure surfaces for low molecular weight peptides which were specifically isolated and fractionated from complex biological samples.(*44*) After fractionation, the response of mass spectrometry greatly improved by achieving better sensitivity in detecting low molecular weight peptides. Another nanostructured material, porous silicon which was first discovered by Bell laboratories in 1960`s, has been highly used for many MS applications in different formats. Unique fluorescence properties and the huge surface area of porous silicon (500-800 m^2/g) makes it an ideal candidate for MS applications. Porous silicon was used a scaffold for antibody arrays and obtained detection limits down to 1 picomolar for IgG and 20 picomolar for PSA in clinical samples.(*45*) As an alternative to classical sample preparation methods,

nanoporous silicon was used to trap trypsin protein and the sequence coverage for prostate specific antigen (PSA) and human glandular kallikrein 2 protein was achieved within 30 sec which usually takes up to 24 hrs using low sample amounts (fmol levels).(*46*) Porous silicon surfaces were also used as a source for ionization. In recent studies nanostructured porous silicon was used in two different formats called – desorption ionization on silicon (DIOS) and nanostructure initiator mass spectrometry (NIMS) which have proven to be useful for proteomics and metabolomics. The surface modification of porous silicon also allowed DIOS-MS to be used for sample capture and enrichment in LDI-MS analysis through the analyte-specific interaction by using immobilized ligands on the porous silicon for isolating the target molecules from the background in complexes.(*47*)

Nanoparticles as Substrates for MS

NPs were also tested for their applicability in MALDI-MS as substrates for ionization. The idea of using nanoparticles as a tool for ionization dates back to the early years of the soft-ionization mass spectrometry. In the seminal work which finally resulted in The 2002 Nobel Prize in Chemistry, a suspension of cobalt nanoparticles 30 nm in glycerol was used to analyze proteins and synthetic polymers by using a pulsed UV laser.(*48*) However because of the problems in handling glycerol and not being widely useful, this method has largely been omitted until the recent advancements in nanotechnology and MS. In contrast to traditional organic matrices, NPs allow a greater number of molecules to adsorb to their surfaces, thus more analytes can desorb and ionize from their surfaces per laser shot, theoretically and practically leading to excellent sensitivity. Nanomaterials having low thermal conductivity, high molar absorption coefficients and large surface areas and are favorable in MALDI-MS, mainly because

they efficiently absorb laser energy to induce desorption/ionization of greater number of analytes per unit area.(*49*) Some of these nanomaterials were reported to provide excellent sensitivity values in the range of zeptomole.(*50*) These sensitivity levels are very promising because as explained in previous sections above, many biomarker candidates exist in very rare amounts. Therefore, these sensitivity values (zeptomole) by pure MALDI-MS or ESI-MS are not yet possible in the absence of nanostructures. Moreover, in the case of MALDI-MS analyses the so called “sweet spot” effect causes irreproducible results. Nanostructures, on the other hand, overcome this problem to a great extent and improve shot to shot reproducibility. Moreover unlike MALDI matrices, NPs do not introduce any background ions, making metabolite analysis possible and greatly simplifying the spectra. NPs and their conjugates with recognition elements can, in some cases, are used as affinity probes for MALDI-MS to concentrate analytes of interest from complex sample matrixes. For example, carboxylated/oxidized diamond NPs having a nominal size of 100 nm have been employed to capture proteins from highly dilute and contaminated solutions; preconcentration of the proteins through hydrophilic interactions with the diamond NPs improved the sensitivity five-fold. (*51*) Antibody-modified Fe_3O_4 NPs have also been used to selectively capture multiple disease-associated antigens, including serum amyloid A, C-reactive protein, and serum amyloid P from human serum samples; the concentrated analytes were then mixed with sinapinic acid and myoglobin (internal standard) prior to MALDI-MS analysis. Relative to the signals obtained without employing this concentration strategy, the sensitivity for the analytes was improved 100-fold. (*52*) In a very recent work, a unique nanostructure was

developed that can ionize proteins as big as IgG (~150 kDa) and demonstrated that the interactions of proteins with other biomolecules can be monitored. (*53*)

Carbon Based Materials and Graphene

Elemental carbon in the sp^2 hybridization can form a variety of different structures. Graphite, nanodiamond, carbon nanotubes, fullerene, graphene and graphene oxide, which are different forms of carbon nanostructures that have been well studied in different applications.(*54*) The rationale behind using such kind of structures for affinity enrichment and matrix-free laser desorption ionization is that they provide high ionization efficiency with minimal background, are readily available in large quantities, are water soluble, have a high surface area and the surface chemistry is very straightforward.

As important examples, carbon nanotubes were used as a substrate for ionization as well as screening long chain fatty acids in patient samples (*55*). In another study, sputter coated nanostructured diamond like carbon on commercially available DVD disks were used this substrate for laser desorption ionization of peptides and femtomolar level sensitivity has been reported.(*56*) Graphene (G) and graphene oxide (GO), are other recently developed interesting materials which are used as substrates for ionization in the analysis of small peptides and small metabolites. Enriching DNA and proteins in solution also showed high recovery yields compared to conventional MALDI matrices. Graphene exhibited higher desorption ionization efficiencies with very low background ions.(*57*) Furthermore, it eliminated fragmentation and provided better tolerance to salts.(*58*)

Aptamers

In the last two decades, the potential of using oligonucleotides as molecular probes and recognition elements has expanded greatly as a result of the discovery of aptamers. They are single-stranded oligonucleotides (DNA or RNA), which have the ability to bind to other molecules with high affinity and specificity. They typically contain fewer than 100 bases and have a unique three-dimensional structure for target recognition through interactions such as van der Waals surface contacts, hydrogen bonding and base stacking.(*59*) They are evolved from random oligonucleotide pools by a process called Systematic Evolution of Ligands by EXponential enrichment (SELEX). Aptamers have been generated for a wide variety of targets, including small molecules, such as metal ions, organic dyes and amino acids, antibiotics, and peptides, as well as proteins of various sizes and functions, whole cells, viruses and virus infected cells and bacteria. (*60*)The selective interactions between aptamers and these diverse targets have been exploited for applications in a variety of disciplines, including biotechnology, medicine, pharmacology, cell biology, microbiology and chemistry. In each of these cases, the aptamer can be uniquely designed to meet specific goals, by taking advantage of the robust nature of these molecules. For example, aptamers have been effectively used for therapeutic applications such as targeted therapy, detection, and diagnostics. With the FDA-approved drug Mucagen now available, others, such as AS1411, (nucleolin aptamer in clinical trial), will contribute to cancer therapy. (*61*)

Aptamers versus Antibodies

Based on their target recognition capabilities, selective binding, and affinity, aptamers have been likened to antibodies. However, aptamers, by their unique features, have more flexibility in their development and range of applications. Also the

time needed for the generation of aptamers by the SELEX process is comparatively short. In addition, the use of animals for antibody production can lead to batch–to-batch variation. However, aptamers are chemically synthesized, which eliminates the possible batch-to-batch variations associated with antibodies. Furthermore, chemical synthesis of aptamers permits the biochemical manipulation required to incorporate various functional groups and specific moieties without compromising the function of most aptamers.(*62*) This phenomenon has been adopted for aptamer conjugation with drug molecules and nanomaterials and for the modification of nuclease resistant bases, such as locked nucleic acids and 2‘-O-methyl nucleotide analogues, to further enhance nuclease resistance when adopted for in vivo studies. Other attributes, such as long shelf life and controllable or cyclical denaturation and renaturation, have expanded the flexibility of aptamers in various experimental designs. Even with improved nuclease resistance, aptamers have low blood residence times compared to antibodies, as well as low toxicity or immunogenicity (if any), and these are important features when used for in vivo applications such as imaging.(*60*)

Cell-SELEX

As explained above aptamer have very similar attributes to antibodies and in many ways are superior affinity tools. Tan Lab has pioneered a strategy called Cell-SELEX, in which live cells are used as target to select aptamers for cell recognition and identification. This strategy is a particularly promising scheme for various diseases including cancer research and therapy. Specifically, by adopting cell-SELEX, useful probes can be developed to potentially differentiate tumor cells from normal cells, as well as differentiate between two different types of cancers and probably to characterize disease staging. Thus far, live cells of many different cancers such as T-Cell, B-Cell

leukemia, lung cancer, liver cancer, ovarian cancer, prostate cancer, colon cancer and glioblastoma have been used in this process, and, as a result, over 300 different aptamers have been generated for most cancers studied.(*59*) Apart from serving as a molecular recognition tool they are also very promising tools for cancer biomarker discovery for a number of reasons. First, prior knowledge of the target is unnecessary. The need to know the molecular composition of the cell surface does not play an important role in cell-SELEX. Instead, the different type of cells used in the selection is a critical parameter as the selected aptamers will be useful for the specific recognition of these cells. Second, aptamers can be generated for many targets. The cell membrane surface is a complex system which has a countless number of molecules, especially proteins. In cell-SELEX, each of these molecules is a potential target. At the end of a successful selection, aptamers are generated for many different targets. This feature is very important, as any one of these molecules may play one or more roles in the development of the cell or the disease they cause.

Cell-SELEX Derived Aptamers for Biomarker Discovery

Aptamers have very significant advantages in terms of biomarker discovery because cell-SELEX derived aptamers recognize proteins on the cell membrane which constitutes the most challenging subclass of the proteome. To date very few methods exist for their targeting, isolation and idenfitication. The recognition part has largely been accomplished using monoclonal antibodies, however, as explained above antibody production also has many limitations. Furthermore, membrane proteins are intrinsically very difficult to isolate and to identify as they are buried in a highly dense pack of lipid bilayers and membrane proteins are highly hydrophobic which poses a difficulty in MS based identification platforms.(*63*) In contrast to the technical difficulties to analyze

them, they are very important for disease diagnosis and therapeutics and they have been extensively targeted for drug design, and it accounts for about 70% of all known drug targets (e.g., HER2 and G-protein coupled receptors). Since selection is done blindly i.e without any bias towards a particular protein target the fished-out proteins will likely have important functions in disease diagnosis and therapatics.

Overview of the Dissertation

The research data presented in this dissertation demonstrate how aptamers with appropriate modifications, can be applied to the development of affinity based MS platforms in three different nanostructure based systems. Chapter 2 outlines the laser desorption ionization on silicon nanowell arrays and aptamer enhanced nanostructure initiator mass spectrometry for isolation of targets from biological mixtures. Chapter 3 discusses discovery of a new nanostructure based matrix graphene and graphene derivatives for aptamer-based MS. Chapter 4 explains how a ratioanally designed nanostructure -based mass spectrometry probe is developed and applied to aptamer-based mass spectrometry. Chapter 4 discusses the discovery of a new membrane protein biomarker for hepatocellular carcinoma. The chapters further assess the possible areas in which these aptamer based MS can be further exploited. The concluding chapter summarizes the overall significance of this research, and examines future directions of the research based on aptamer based MS strategies.

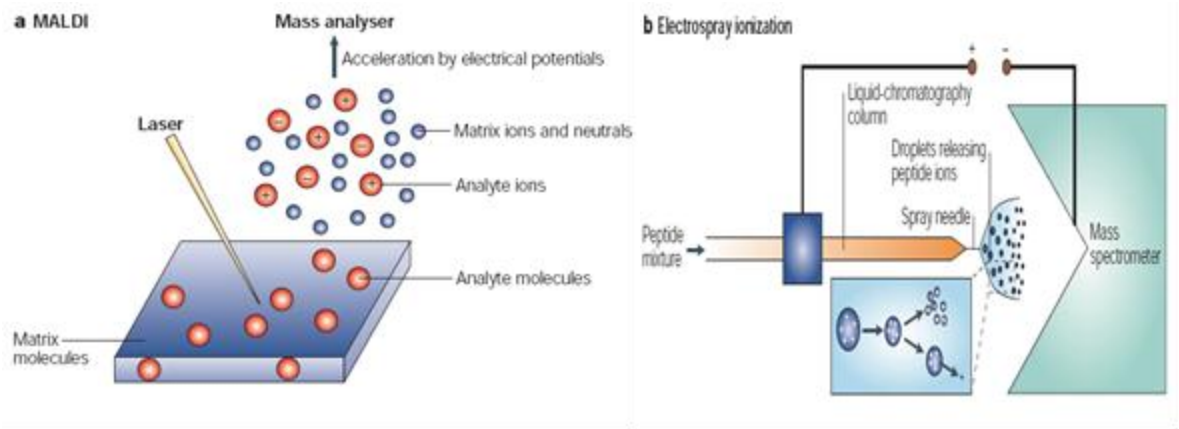

Figure 1-1. Schematic diagram of MALDI and ESI (*23*)

Figure 1-2. Number of publications between 2007-2012 found through the Web of Science database using the search terms biomarker AND mass spectrometry

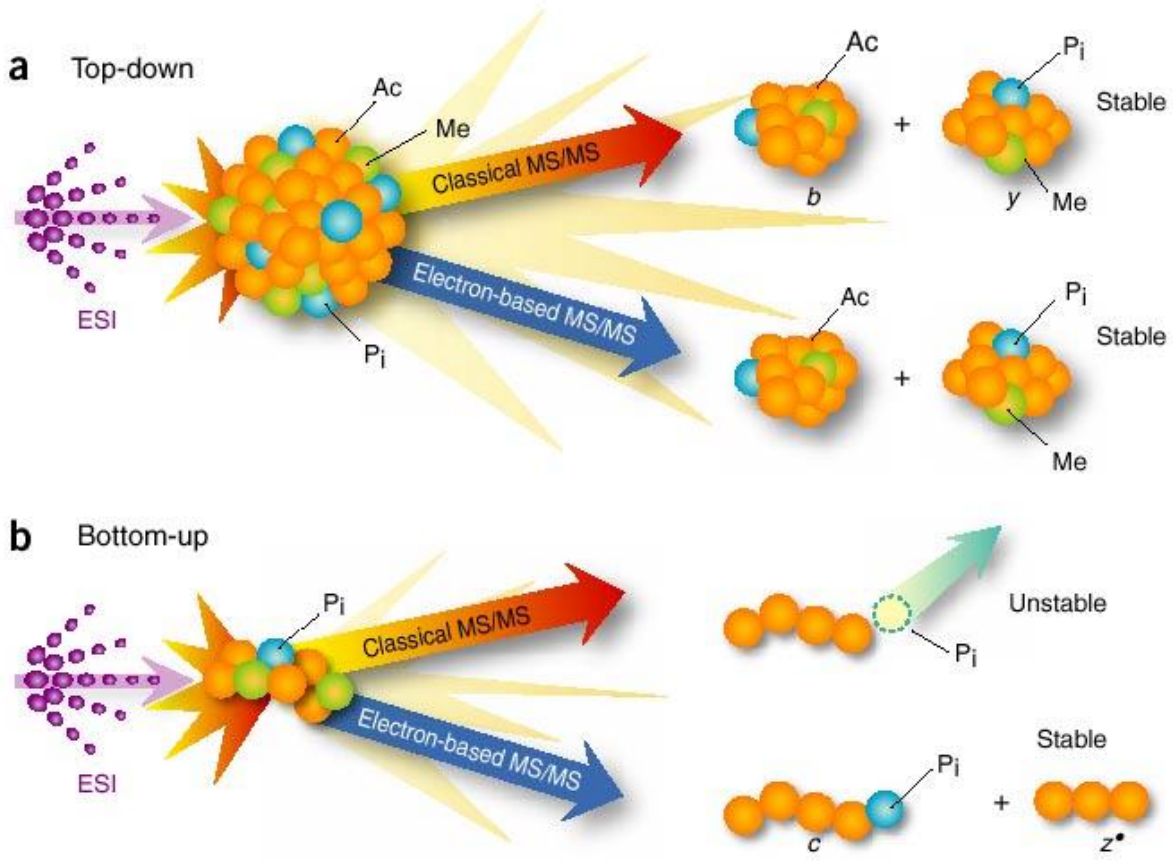

Figure 1-3. Schematic representation of Top-down versus Bottom-up proteomics (*64*)

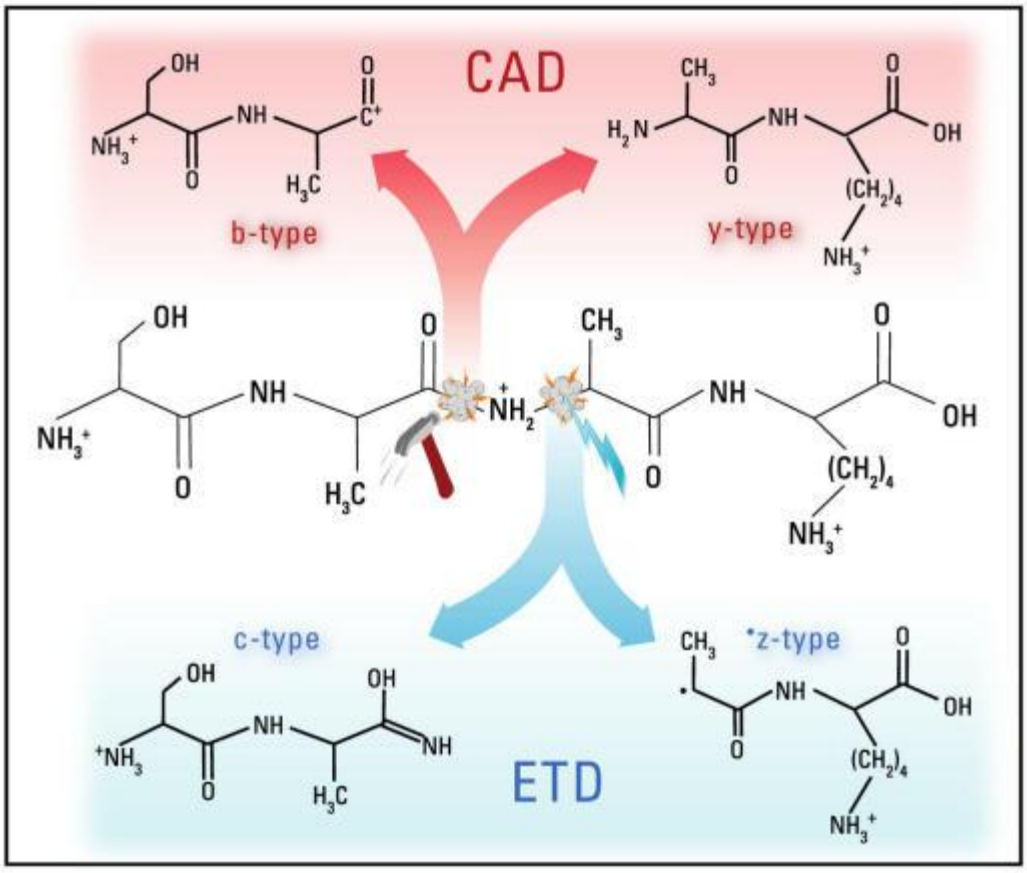

Figure 1-4. Fragment ion types produced following either CAD or ETD (*27*)

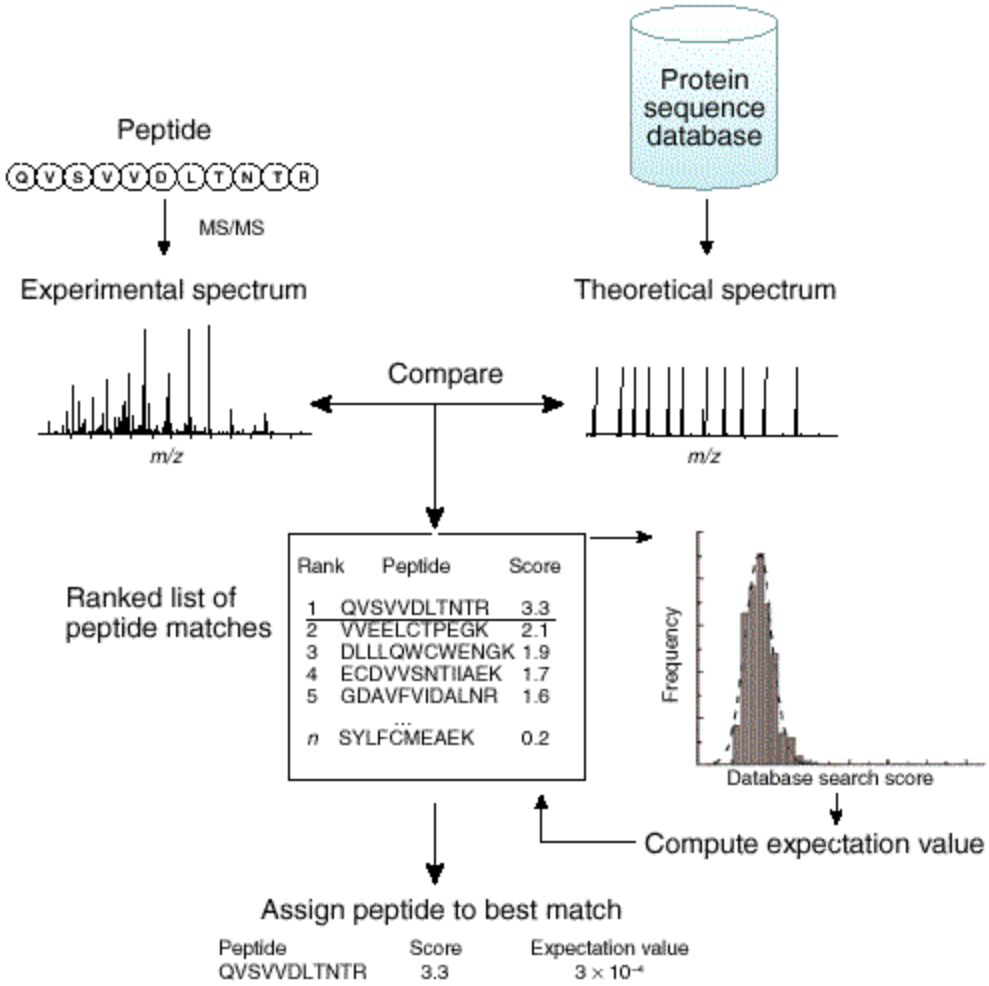

Figure 1-5. Database search in a typical MS based proteomics experiment (*28*)

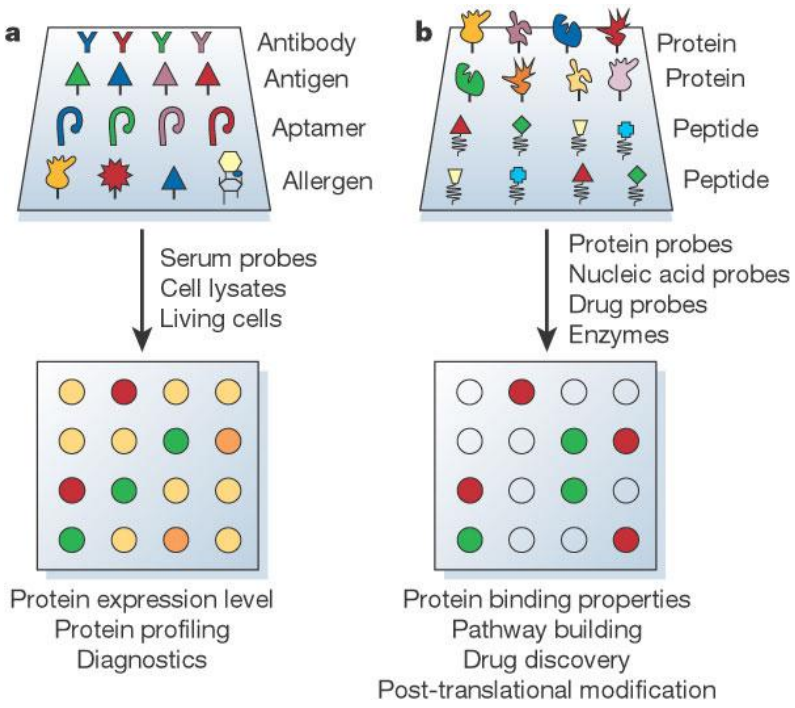

Figure 1-6. Array based proteomics (*65*)

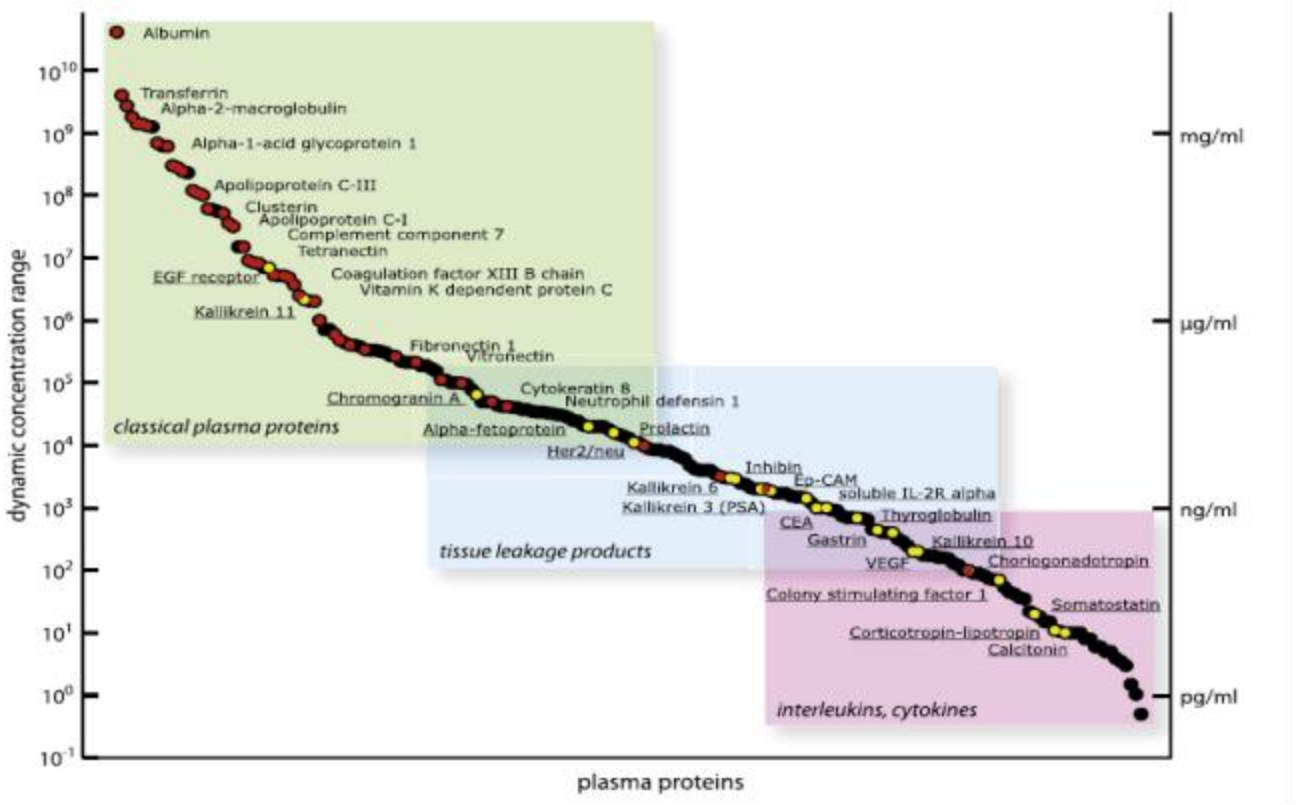

Figure 1-7. Levels of plasma proteins(*11*)

Table 1

Comparison of performance characteristics of commonly used mass spectrometers for proteomics

Instrument	Mass resolution	Mass accuracy (ppm)	Sensitivity	*m/z* range	Scan rate	Dynamic range	MS/MS capability	Ion source	Main applications
QIT	1000[a]	100–1000	Picomole	50–2000; 200–4000	Moderate	1E3	MS^{nd}	ESI	Protein identification of low complex samples; PTM identification
LTQ	2000[a]	100–500	Femtomole	50–2000; 200–4000	Fast	1E4	MS^{nd}	ESI	High throughput large scale protein identification from complex peptide mixtures by on-line LC–MS^n; PTM identification
Q-q-Q	1000	100–1000	Attomole to femtomole	10–4000	Moderate	6E6	MS/MS	ESI	Quantification in selective reaction monitoring (SRM) mode; PTM detection in precursor ion and neutral loss scanning modes
Q-q-LIT	2000[a]	100–500	Femtomole	5–2800	Fast	4E6	MS^{nd}	ESI	Quantification in SRM mode; PTM detection in precursor ion and neutral loss scanning modes
TOF	10 000–20 000	10–20[b]; <5[c]	Femtomole	No upper limit	Fast	1E4	n/a[e]	MALDI	Protein identification from in-gel digestion of gel separated protein band by peptide mass fingerprinting
TOF–TOF	10 000–20 000	10–20[b]; <5[c]	Femtomole	No upper limit	Fast	1E4	MS/MS	MALDI	Protein identification from in-gel digestion of gel separated protein band by peptide mass fingerprinting or sequence tagging via CID MS/MS
Q-q-TOF	10 000–20 000	10–20[b]; <5[c]	Femtomole	No upper limit	Moderate to fast	1E4	MS/MS	MALDI; ESI	Protein identification from complex peptide mixtures; intact protein analysis; PTM identification
FTICR	50 000–750 000	<2	Femtomole	50–2000; 200–4000	Slow	1E3	MS^{nd}	ESI; MALDI	Top-down proteomics; high mass accuracy PTM characterization
LTQ–Orbitrap	30 000–100 000	<5	Femtomole	50–2000; 200–4000	Moderate to fast	4E3	MS^{nd}	ESI; MALDI	Top-down proteomics; high mass accuracy PTM characterization; protein identification from complex peptide mixtures; quantification

[a] Mass resolution achieved at normal scan rate; higher resolution achievable at slower scan rate.
[b] With external calibration.
[c] With internal calibration.
[d] $n > 2$, up to 13.
[e] Fragmentation achievable by post-source-decay.

Figure 1-8. Instruments used for protein identification (*34*)

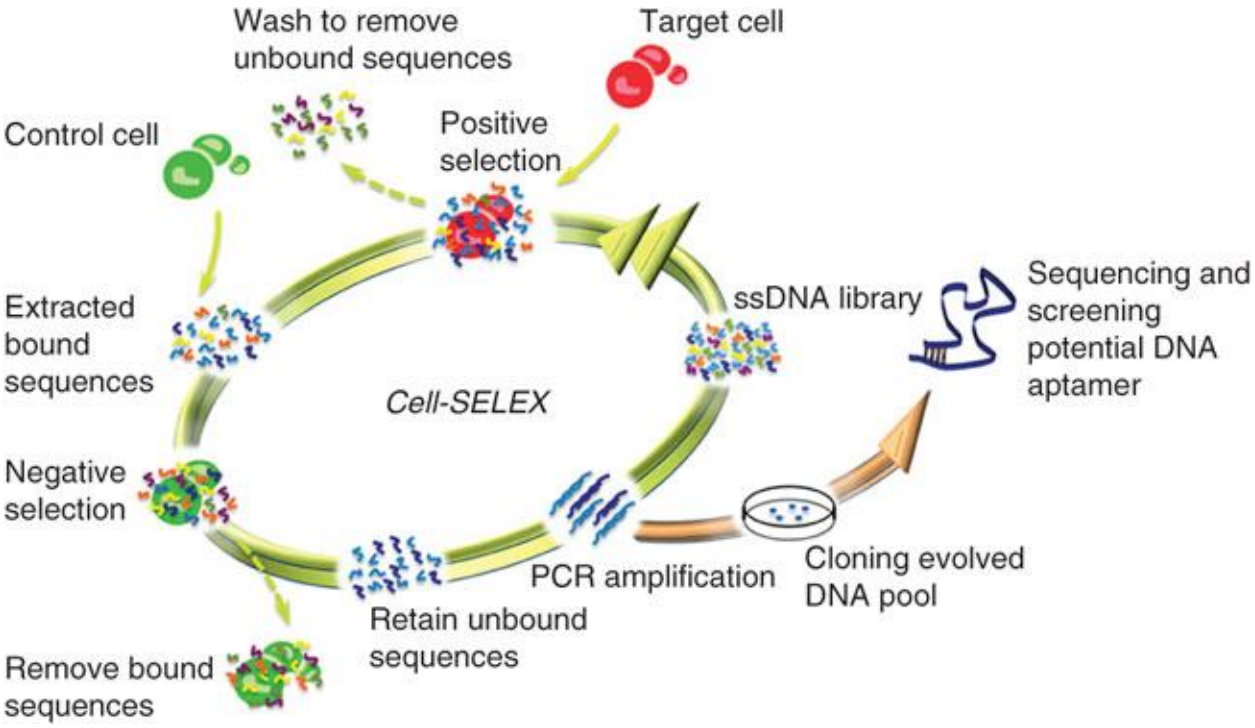

Figure 1-9. Schematics of cell-SELEX(*59*)

CHAPTER 2
LASER DESORPTION IONIZATION ON SILICON NANOSTRUCTURES

Matrix-assisted laser desorption/ionization (MALDI) has been utilized in the study of large biomolecules, such as peptides, proteins, carbohydrates and DNA.(*66*) The broad success of MALDI-MS is related to the ability of the matrix to incorporate and transfer energy to an analyte, thereby ionizing it in a very soft manner. However, MALDI is complicated because the presence of the matrix often causes heterogeneous cocrystallization of the matrix and analyte, resulting in significant background ion intensity in the low-mass range (<500 m/z).(*67*)

As a complementary alternative, Siuzdak and co-workers have developed desorption/ionization on silicon (DIOS) using nanoporous silicon substrates for the detection of small peptides and antiviral drugs without any mass interference due to matrix ions. In DIOS-MS, the analytes in solution are directly deposited on a nanoporous silicon surface without a chemical matrix. Compared to MALDI, this approach provides simplified sample preparation, more uniform surfaces, and less background noise at masses below 600 Da. Although the DIOS mechanism is not fully understood, porous silicon was found to be an effective medium for desorbing compounds and generating intact ions in the gas phase. It is suggested that porous silicon effectively absorbs and transfers the energy from the UV irradiation laser to the adsorbed analytes, while also protecting these molecules from fragmentation caused by direct laser exposure.(*68*)

Most existing DIOS platforms are prepared by electrochemical anodization of crystalline silicon necessitating the use of toxic HF solution. In addition, it is difficult to obtain reproducible surfaces with the same nanostructures, because pore size and pore

density are not well controlled by chemical etching.(*69*) To overcome this issue, Vertes et.al reported the use of silicon microcolumn arrays (*70*) and silicon nanopost arrays used as alternative DIOS substrates and showed that structure specific fragmentation can be also be induced.(*71*) In another study He et al. have used electron beam lithography (EBL) and nanosphere lithography to investigate the impact of the surface morphology of porous silicon on analyte desorption and ionization. (*72*) Electron beam lithography allows accurate fabrication of sub-100 nm features, but the serial nature of the technique makes it very slow. In the nanosphere technique, the self-assembly can be very time consuming, and long-range order is still not achieved.

Self-ordered porous alumina substrates have also been used as useful platforms for laser desorption/ionization MS. Because Wada et al. found that surface electroconductivity was one of the requirements for a porous alumina chip to be effective for laser-induced desorption/ionization, the surface was coated with gold or platinum.(*73*) Masuda et al. suggested that the porous alumina layer beneath the surface metal probably acted as a thermal insulator.(*74*)

In this chapter, the fabrication of porous silicon by a non-lithographic method using a self-ordered porous alumina membrane and its application for laser desorption ionization mass spectrometry is discussed. The self-ordered pore pattern of the alumina membrane is transferred into the silicon substrate via the plasma-etching method, resulting in rapid, low cost and reproducible fabrication without the use of toxic chemicals. Pore size and porosity are comparable to that of the alumina mask and the pore depth can be controlled in the range of 10 nm to 50 nm by changing the etch time. The porous silicon platforms with 10 nm, 30 nm and 50 nm-depth nanowells were used

for laser desorption/ionization (LDI) MS detection of biomolecules. To the best of our knowledge laser desorption ionization at this depth regime has not been reported before and the submicrometer porosity limit to induce ionization is yet unclear. The utility of nanowell arrays under atmospheric pressure and vacuum regimes were studied.

Experimental Methods

Materials

Aluminum foil (99.99%) was obtained from Alfa Aesar. Single-side polished P/Boron type silicon wafers, having 100 orientation, low resistivity (0.01-0.02 Ω cm), 525 ± 25 μm thicknesses and 100 mm diameter were obtained from Silicon Valley Microelectronics, Inc. (Santa Clara, CA). Phosphoric acid, sulfuric acid, chromium trioxide, oxalic acid and hydrogen peroxide were obtained from Fisher Scientific. Triton X-100, adenosine, Pro-Leu-Gly tripeptide and [*Des-Arg*^{9}]-bradykinin were obtained from Sigma-Aldrich. Stock solutions (500 pmol/μL) of these analytes were prepared by dissolving each compound in 1:1 acetonitrile:aqueous 0.1 % trifluoroacetic acid solution. Bovine serum albumin (BSA) was obtained from Sigma-Aldrich. In-Solution tryptic digestion and guanidination Kit was obtained from Pierce and digestion of 10 μg of BSA was carried out using manufacturer's instructions. A carnitine metabolite cocktail containing carnitine, butyrylcarnitine, octanoylcarnitine decanoylcarnitine, myristoylcarnitine, palmitoylcarnitine, stearoylcarnitine (5 ppm each) and red blood cell extracts were provided by Dr.Peggy Borum (University of Florida) as a kind gift and used without any further treatment. Reference standard solution of fentanyl (1.0 mg/mL in methanol) was obtained from Restek and used with further dilution in methanol.

Preparation of the Porous Alumina Mask

The alumina mask was an in house-prepared nanopore alumina film. The electrochemical anodization method used to prepare these films has been described previously.(*75*) The same procedure was followed for preparation of the alumina masks.

Fabrication of the nanowell arrays on silicon substrates.Silicon wafers were cleaned in a piranha solution (3:1 (v/v) 98% H_2SO_4: 30% H_2O_2) for 30 min. The silicon substrates were rinsed with deionized water, followed by drying under a stream of nitrogen. The alumina mask was mounted on top of the silicon wafer with the barrier-layer side of the mask facing up using a drop of Triton X-100 solution as an adhesive. The masked substrate was then inserted into the vacuum chamber of a reactive-ion etching apparatus (Samco® model RIE-1C). Ar plasma was used to etch the substrate surface through the mask with the following etching parameters (13.56 MHz, 100 W, 10 Pa, 12 sccm Ar flow). The etch time was varied (5, 10, 15, 20, and 25 mins, respectively) in order to determine the etch rate of silicon under these conditions. The alumina mask was removed by the use of sonication in water for 10 min. The silicon substrates were rinsed with nanopure water and ethanol followed by drying with a stream of nitrogen gas. Porous silicon substrates were stored in ethanol and they were re-dried by N_2 flow just prior to mass spectrometry experiments.

Fabrication of desorption/Ionization on Silicon (DIOS) Surfaces

To provide a benchmark for comparison, standard DIOS surfaces have been prepared. Briefly, low resistivity (0.01-0.02 Ω cm) silicon wafers were sputter-coated with 30-Å with a Desk II Cold Sputter instrument (Denton Vacuum, LLC) and chemically etched using the HOME method with a solution of 1:1:2 EtOH/HF (49%)/H_2O_2 (30%) for 30 s.

Characterization of Porous Surfaces

Tapping mode Atomic Force Microscopy (AFM) was used to examine the morphology and depth of the nanowell-array on silicon substrates. In order to investigate the etch rate, three porous silicon samples were prepared at each etch time. Average depth of wells (at least 450 nanowells) for each etching time was obtained from three different positions of each sample. AFM experiments were performed using a Multimode AFM with a NanoScope IIIa controller (Digital Instruments, Santa Barbara, CA) and MPP-11200 Si tips (Veeco, manufacture suggested tip radius is r < 10 nm). Height images were obtained in the tapping mode under dry N2 gas. The nanowell depth was assessed using the profile analysis made by the WSxM image analysis package (Nanotec Electronica, Madrid, Spain). A Hitachi S4000 FE-SEM was used to obtain the pore diameter and the thickness of the alumina mask. Both the top view and the cross section of the alumina membrane were investigated. All samples were coated with an Au/Pd film by a Desk II Cold Sputter instrument (Denton Vacuum, LLC).

Synthesis of DNA Aptamers

The following aptamer selected against thrombin 5 ′-GGTTGGTGTGGTTGG-3′ was used in the experiments. Cocaine aptamer 5′- GAC AAG GAA AAT CCT TCA ATG AAG TGG GTC 3` was used as a negative control. Both of the aptamers were coupled with a 5′-fluorous modifier and FTIC flurophore dye. An ABI 3400 DNA/RNA synthesizer (Applied Biosystems, Foster City, CA) was used for the synthesis of all DNA sequences. A ProStar HPLC instrument (Varian, Walnut Creek, CA) with a C18 column (Econosil, 5u, 250 × 4.6 mm) from Alltech (Deerfield, IL) was used to purify all aptamers. A Cary Bio-300 UV spectrometer (Varian, Walnut Creek, CA) was used to measure absorbances to quantify the manufactured sequences. All oligonucleotides were

synthesized by solid-state phosphoramidite chemistry at a 1 μmol scale. The completed sequences were then deprotected in AMA (ammonium hydroxide/40% aqueous methylamine 1:1) at 65 °C for 20 min and further purified with reverse phase HPLC on a C-18 column.

Slide Scanning and Data Analysis

After being spun dry, the fluorescence signals were recorded with a microarray scanner (Agilent) or epifluorescent microscope (Leica) equipped with FTIC filter cube. The gain of the photomultiplier tube (PMT) was set to a fixed value while comparing different spots.

Formation of Fluorous-Derivatized Glass Slides

Glass slides were first cleaned by immersion into piranha solution (3:1 mixture of concentrated sulfuric acid H_2SO_4 with hydrogen peroxide H_2O_2 for 1 h. This was followed by washing with copious amounts of water. The slides were then immersed into a solution of 60% ethanol containing NaOH (10 g/100 mL). The slides were washed twice in distilled water and then submerged in 95% ethanol. Cleaned slides were immersed three times in a solution of RF_8-ethyl-$SiCl_3$ (10% solution 100 mL in methanol) and then dried for a few minutes; the process was repeated two more times. The slides were then washed twice by immersion in MilliQ-filtered water and baked at 120°C then dried in a dessicator at room temperature.

Formation of Fluorous-Based Aptamer Arrays on Glass Slides

Fluorous-tagged aptamers were dissolved in a buffer resembling physiological conditions which contains 25 mM Tris-HCl at pH 7.4, 150 mM NaCl, 5 mM KCl, 1mM $MgCl_2$, 1mM $CaCl_2$. A volume of 1 μl of each aptamer solution dissolved in binding buffer was spotted manually with a manual pipettor on the the fluorous glass slide as

just explained and kept in a humifying chamber overnight for incubation. After that slides were washed with SSC (saline-sodium citrate) buffer and deionized water respectively by simply pipetting 1 µl of each up and down. Subsequent slide processing steps were performed in dark to prevent bleaching of the fluorophores. After 30 mins of incubation time slides were washed with water and dried for subsequent analysis.

NIMS Surface Preparation

Low resistivity (0.01–0.02 Ω-cm) P-type (Boron) silicon from Silicon Quest was etched with 25% hydrofluoric acid in ethanol (these and other solvents were obtained from Fisher Scientific), using extreme caution and employing a Bio-Rad Power Pack 1000 with 48 mA/cm^2 (2.5 x2.5-cm chip) for 30 min. The etched surface was rinsed with methanol, dried with a jet of nitrogen. The initiator bis (heptadecafluoro-1, 1, 2, 2-tetrahydrooctyl) tetramethyldisiloxane, purchased from Gelest, was added to the surface for 2 hours and then blown off with nitrogen. For aptamer enhanced NIMS analyses, fluorous tag carrying cocaine aptamer was spotted onto the NIMS chip and incubated overnight in a humidifying chamber. After that, the slides were washed with 100 µl water and 100 µl binding buffer. 1 µl of cocaine spiked plasma sample spotted onto aptamer modified NIMS chips and incubated for 30 min to ensure complete binding at room temperature. After this step the NIMS chips were washed with 100 µl of water 3 times and dried for mass spectrometry analyses.

Mass Spectrometry

Mass spectra at atmospheric pressure were acquired using an Agilent 6210 MSD time-of-flight (TOF) mass spectrometer configured for ESI (Agilent Technologies Inc., Santa Clara, CA, USA). Laser desorption/ionization experiments were conducted by installing an external MassTech atmospheric pressure/matrix assisted laser desorption

ionization pulse dynamic focusing (AP/MALDI PDF) ion source. The results were analyzed using Analyst® software. Mass spectrometry experiments in the vacuum regime were conducted using either an ABI 4700 MALDI TOF/TOF or ABI/SCIEX 5800 MALDI TOF/TOF (Applied Biosystems, Framingham, MA) equipped with an Nd:YAG laser (355 nm, 3-7 ns pulses) which was operated in the reflector, positive ion mode with an acceleration voltage of 20 kV. The laser was operated at a fixed pulse rate at 200 Hz. The laser-firing pattern was set to “uniform.” Both the sample plate and the laser were aligned before spectral acquisition. Spectra were smoothed by “noise filter” and baseline corrected with Data Explorer 4.0.

Results and Discussion

Characterization of the Alumina Mask

Figure 2-1 shows representative SEM images of the mask prepared for etching. The pores were formed in a hexagonally packed array. Image J software (Wayne Rasband, NIH, USA) was used to characterize the morphology of the alumina membrane: pore diameter (80 ± 5 nm); pore density ((9.3 ± 0.3) × 109 pores/cm^2); porosity (48 ± 2 %). These films have two distinct surfaces. Figure 2-1 shows the surface that faced the solution during the anodization, and that faced the Al substrate during the anodization. The latter surface is often called the “barrier layer,” because it initially has a film coating which must be removed during processing. In Figure 2-1 the cross section of the film indicates that the thickness was 2.3 µm and that the pores were cylindrical.

Fabrication and Morphology of Porous Silicon Substrates

In Figure 2-2, AFM images show the surface characteristics of the silicon nanowell-array: density (6.0×109 nanowells/cm^2), diameter (93±7 nm), and porosity

(44%). According to surface characteristics from AFM images, the pore pattern of the alumina mask was successively transferred into silicon substrates. The pore size, pore density and porosity of porous silicon are compatible to those of alumina mask. The pore diameter showed a narrow distribution. Moreover, as shown in Figure 2-3, as the etching time was increased the depth of nanowells increased linearly while the array pattern remained unchanged.

Mass Spectrometry Analyses

Porous silicon substrates were prepared by etching for 5 min (depth = 10 nm) and 15 min (depth = 30 nm) and 25 min (50 nm). Silicon nanowells were spotted with 0.2 uL of 5 pmol/uL solutions of adenosine, Pro-Leu-Gly tripeptide and bradykinin, and the samples were dried in room temperature for 30 mins prior to analyses. For atmospheric pressure laser desorption versus vacuum laser desorption comparison experiments, 0.2 uL of 500 pmol/uL solutions of the respective analytes were used. A schematic of the entire process is shown in Figure 2-4. The mass spectra of adenosine acquired on 10 nm, 30 nm, 50 nm nanowell surfaces and DIOS surface are shown in Figure 2-5 indicates that an increase in etching time provides a significant improvement in the ion signal. Analyses with the 10 nm-deep pores were repeated with concentrations from 1 pmol to 500 pmol and with various laser attenuations, but no significant improvement was observed. In a recent report on the thermochemistry of adenosine, it was shown that a significant amount of energy has to be imparted to induce protonation.(*76*) The authors reported the proton affinity of adenosine as 979 ± 1 kJ/mol in the gas-phase by using nano-ESI-MS. In the light of these findings, we can hypothesize that for the surface etched to a depth of 10 nm, the surface induced heating does not provide sufficient energy to desorb the molecule from the surface and ionize it. However, when

the etching time was increased and the same experiment was conducted using 30 nm and 50 nm deep nanowells and DIOS surface, significant ion signals for protonated adenosine $[M+H]^+$ before (268.1054) and adenine after (136.0594) loss of the ribose group were observed. Similar behavior was observed on DIOS surfaces as well. After this experiment, analyses on the nanowell surfaces were extended to two different compounds: Pro-Leu-Gly ($[M+H]^+$= 285.1921) and [Des-Arg^9]-bradykinin (($[M+H]^+$= 904.4691). Similar to adenosine, 0.2 uL of 5 pmol/uL of Pro-Leu-Gly and [Des-Arg^9]-bradykinin were spotted on the nanowells and the attenuation of the laser was fixed. The mass spectra are shown in Figures 2-6 and 2-7.

The mass spectra for the two compounds clearly show that the ion signals significantly increase with increasing pore depth and electrochemically etched DIOS surface gave higher intensities in all analyses. DIOS surfaces are well characterized previously and have surface features of 200 nm deep. This result led us to think about the events associated with laser desorption/ionization and the effect of increased nanostructuring on the ion signals. Northen et al.reported that the surface area is the key factor.(*77*) They demonstrated that the submicrometer surface porosity, irrespective of the substrate material, is the most important effect for desorption/ionization. In the most similar report to our work it was demonstrated that silicon wafers roughened with sandpaper can act as a surface for laser desorption.(*73*) An increase in surface porosity enhances ion signals via multiple effects: The surface is resupplied with analyte after a laser pulse, and a local environment for the laser-induced field is provided to facilitate physical separation of preformed analyte ions from their counterions. Also, the heat capacity and heat conductivity are decreased when rapid heating of the surface occurs,

resulting in effective sublimation of analytes by laser irradiation as well as effective absorption of the laser light. Recently Hsu et al. showed that laser desorption ionization can occur even on metals.(*78*) They showed that although ion signals greatly improve with surface roughness ionization can occur even on a commercial non-porous aluminum film. Our results are in good agreement with these previous findings. In addition to unique energy absorbing properties of porous surfaces, nanostructuring also helps to create a thin layer when analytes are spotted and thereby the interaction between the surface and analyte is facilitated resulting in more efficient ionization. This fact has been shown very recently.(*79*)

Significant dimer and trimer signals are observed in Figures 2-6 and 2-7. Since the ionization event occurs at atmospheric pressure, it is possible that ion-ion reactions occur after the desorption event, and that dimerization and trimerization are favored. Desorption ionization on porous silicon is mostly carried out in MALDI instruments operating under vacuum regime and only a few reports exist about atmospheric pressure DIOS and to date no comparision yet exists. Since the concentrations of the analyte solutions are low, this is probably not due to the concentration effect. To investigate this factor, a vacuum MALDI instrument was used both to check the effectiveness of the surfaces in vacuum conditions and to make a comparison between atmospheric pressure and vacuum MALDI regimes. Comparison of atmospheric pressure and vacuum spectra, shown in Figure 2-8, Figure 2-9 and Figure 2-10, indicates that a significant difference exists between atmospheric pressure and vacuum regimes. Because the dimer and trimer signals did not appear in vacuum regime, these peaks were due in part to atmospheric pressure conditions.

Application of the Nanowell Arrays for Complex Biological Mixture Analysis

After investigating the ionization efficiencies with increasing pore depth, we applied our nanowell array surfaces for real biological sample analyses. Carnitines serve as important biomarkers for metabolic disorders and there is a growing interest in the analysis of carnitines in complex biological samples.*(80)* Because of the much larger signal-to-noise ratios, the nanowells with 50 nm pores were used for these measurements. For this purpose, 0.2 µL of the standard carnitine metabolite cocktail (contaning 5 ppm of each) was spotted on our surfaces. Theoretical masses of the carnitines are given in Table 2.1 We can clearly see in Figure 2-11 that carnitine standard can be successfully analyzed with a very clear background and no interfering peak which is the major drawback of the MALDI for metabolomics. We then analyzed 0.2 uL of 5 pmol/uL tryptic digest of bovine serum albumin on 50 nm deep nanowells and many of the tryptic peptides were observed and it is worthnoting that no peak was observed at the low mass range as shown in Figure 2-12

To further demonstrate the analytical applicability of nanowell arrays we spiked varying concentrations of the illicit drug fentanyl $[M+H]^+$= 307.2220 (ranging from 10 ng/mL to 1.5 µg/mL) into red blood cell extract and by applied it onto our surfaces using Z-touch method and then analyzed. Figure 2-13 shows spiked fentanyl in red blood cell extract (200 ng/mL) and the corresponding calibration curve. As can be seen in this data, the nanowell surfaces show good linearity for the analysis of fentanyl in complex biological mixtures.

Unifying NIMS and Aptamer Assisted Capturing

Use of flurous chemistry for affinity mass spectrometry applications is a new approach that has been proven successful in recent years.(*81, 82*) The most notable

example is named nanostructure initiator mass spectrometry (NIMS) which relies on fabrication of a nanostructured porous silicon surface and modifying this surface with a flurous compound termed as “initiator”.(*83*) This resulted in a very sensitive platform for the analysis of metabolites, peptides and even single cells. The same “fluorous chemistry” is not only useful for NIMS but has also been applied as a new noncovalent immbolization strategy to create sugar microarrays, to study histone deacetylases and also for assembling nanoparticles for DNA capture.(*84-86*)The main advantage of fluorous surfaces is that they limit nonspecific interactions to a great extent, but still allow the facile noncovalent attachment of flurous modified compounds. So we wanted to tether aptamers onto NIMS surfaces to create a mass spectrometry platform that will build upon the selectivity of the aptamers and sensitivity of NIMS. We also incorporated a spacer between the fluorous anchoring group and the aptamer to bring the aptamer away from the slide surface so that aptamers can interact with their targets similar to solution-phase environment. The general structure of the fluorous-tagged aptamers substrates used for immobilization onto NIMS surfaces is shown in Figure 2-14.

As can be seen from the Figure 2-15 that aptamers can stick onto flourous glass surfaces and even after washing they do not get washed away. However the interactions were not very strong and we observed spiky spots. This might be ascribed to the improper orientation of the aptamers to bind their targets. Even though fluorous-fluorous interactions are very selective and binding onto fluorous surfaces occur only by a fluorous group, strength of fluorous interactions are not comparable to that of covalent bonds. Initial work using fluorous chemistry field were done by small molecules like carbohydrates, peptides so there is no existing literature report about immobilization of

bigger molecules such as proteins or oligonucleotide onto fluorous surfaces through fluorous linkers.(*87, 88*) Failure to get good immobilization onto fluorous glass led us to think about alternative ways about this immobilization strategy. The first option is to change the surface and the second option is to introduce multiple fluorous linkers on the aptamers`structure. Recent data has shown that multiple fluorus tags significantly improve fluorous based immobilization.(*89*) We therefore introduced multiple fluorous tag to the aptamer structure to improve the immobilization. The succesfull incorporation of double and triple fluorus tags into aptamer structure was monitored by using HPLC. The peak position at which the fluouros aptamers are eluted from the column shifted on the order of single, double and triple fluorous linker carrying aptamers. The results are depicted in Figure 2-16 and Figure 2-17 and Figure 2-18. After showing that aptamers can be attached onto fluorous tags, the next step was to use in them in combination with NIMS. We have spotted triple fluorus tag carrying cocaine aptamer onto NIMS surfaces as explained in the experimental part. After washing steps we treated the aptamer modified NIMS surface with plasma samples containing 10 µM cocaine. However the mass spectra as shown in Figure 2-19 were dominated with too many background ions in sharp contrast to literature findings about NIMS. The results and the source for background ions were initially unclear for us and we attributed this to unsuccessful capture or inproper washing conditions. We performed initial experiments using an atmospheric pressure MALDI instrument. As opposed to vacuum MALDI instruments, the source region and ion transfer capillary is held at atmospheric pressure conditions and also kept at fairly high temperatures (>200 °C). The initiator bis (heptadecafluoro-1, 1, 2, 2-tetrahydrooctyl) tetramethyldisiloxane has a boiling

temperature of 306 °C. Therefore we think that at this temperature, volatile initiator molecules escape from the nanoporous silicon surface which leads to ionization of initiator and decomposition products therefore no significant signal can be observed.

We repeated the experiments as just discussed using 5800 ABI/SCIEX MALDI-TOF/TOF instrument which operates under vacuum. As can be seen in Figure 2-20 results greatly improved and we can clearly see the enrichment and clean-up effect of aptamers in capturing target species from cocaine spiked plasma samples.

The applicability of nanowell silicon substrates for desorption/ionization on silicon mass spectrometry has been demonstrated. The pore pattern of an alumina mask has been successively transferred onto silicon substrates by means of Ar-ion-plasma etch. This method has several advantages: (1) elimination of toxic HF; (2) reproducibility (uniform pore size, pore density, and porosity); and (3) low-cost and fast production. The nanowell depth is linearly related to etch time. The etch rate was determined to be 2.0 nm/min with about 2 μm thick AAO mask. The pore depth requirement for inducing laser desorption ionization has not been well addressed before and our results show that very little porosity (10 nm) is sufficient to induce ion formation and the ion signals significantly improve with the change of the pore depth. We also showed that a reasonable level of sensitivity has been achieved with 50 nm deep nanowells. Comparison of nanowell arrays and DIOS surfaces show that ionization is more favored with nanostructures having deeper pores however even with a slightly nanostructured surface, ionization takes place (10 nm deep nanowells.)

The mechanism of ion formation on nanowell arrays is still not clear but we attribute the ion formation to unique thermal and optical properties of silicon. We are in

the process of systematically investigating the effects of pore size, pore depth and pore density by changing the AAO mask and by controlling the aspect ratio of the nanowells using different substrates. Our initial findings suggest that nanowell arrays are suitable substrates for laser desorption ionization of biomolecules and can be used for the analysis of small molecules, metabolites and peptides. We also showed that fluorous chemistry can be used for immobilization of aptamers onto fluorous surfaces which could be potentially used as a new chemistry for making protein and DNA microarray surfaces. We also demonstrated that sensitivity and matrix free features of the NIMS method is compromised when experiments are conducted under atmospheric pressure conditions. Finally aptamer-enhanced nanostructure initiator mass spectrometry has been demonstrated as a proof of concept experiment.

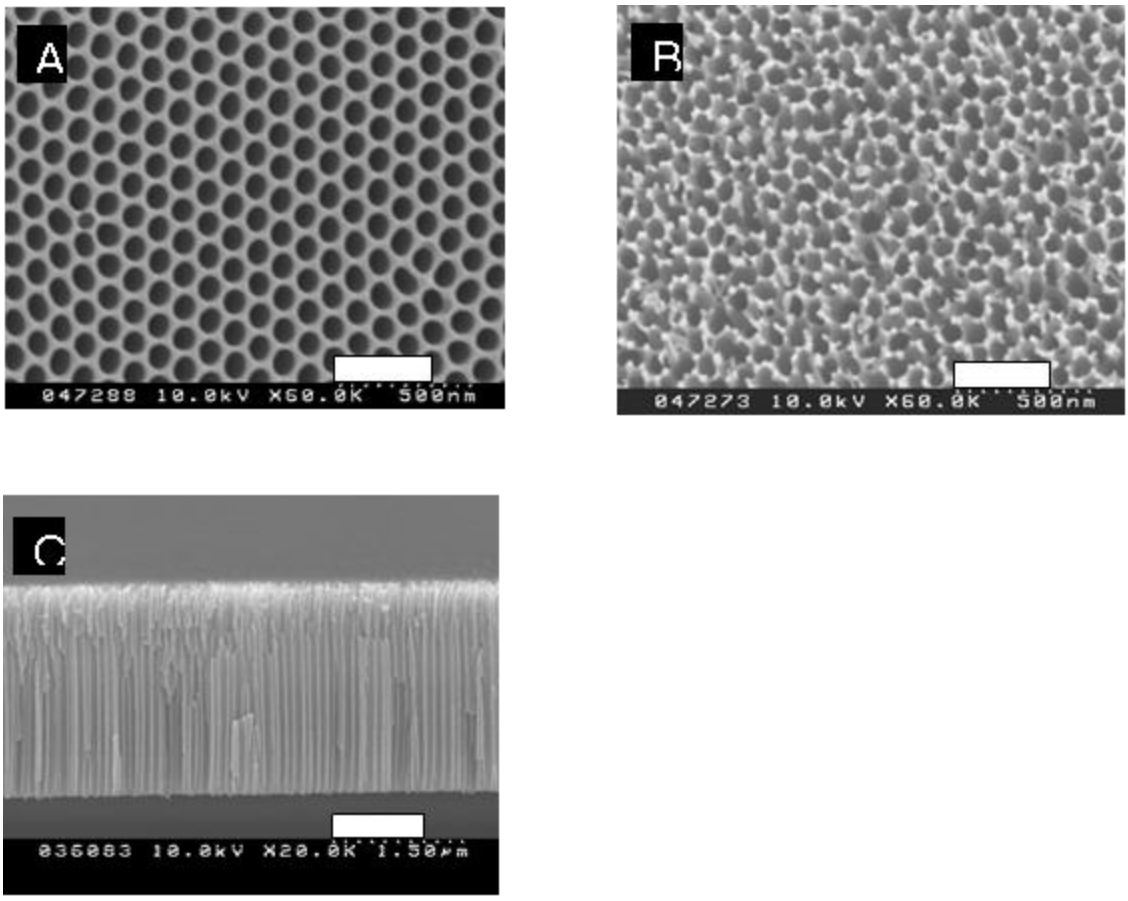

Figure 2-1. Scanning electron micrographs of the alumina mask: Top view of (A) outer surface and (B) barrier layer surface, and (C) cross section.

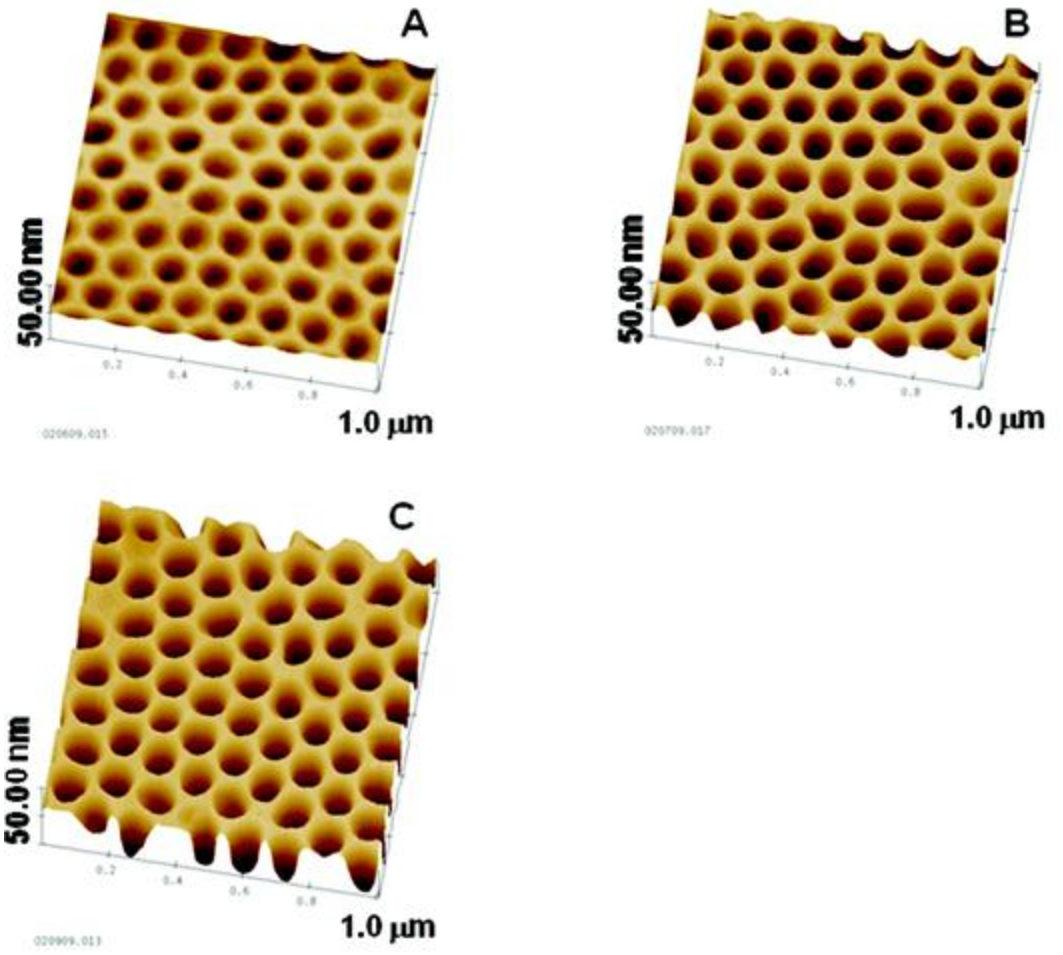

Figure 2-2. Tapping mode AFM images of nanowell arrays on silicon substrates prepared by means of Ar-ion plasma etching for: (A) 5 mins, (B) 15 mins, and (C) 25 mins.

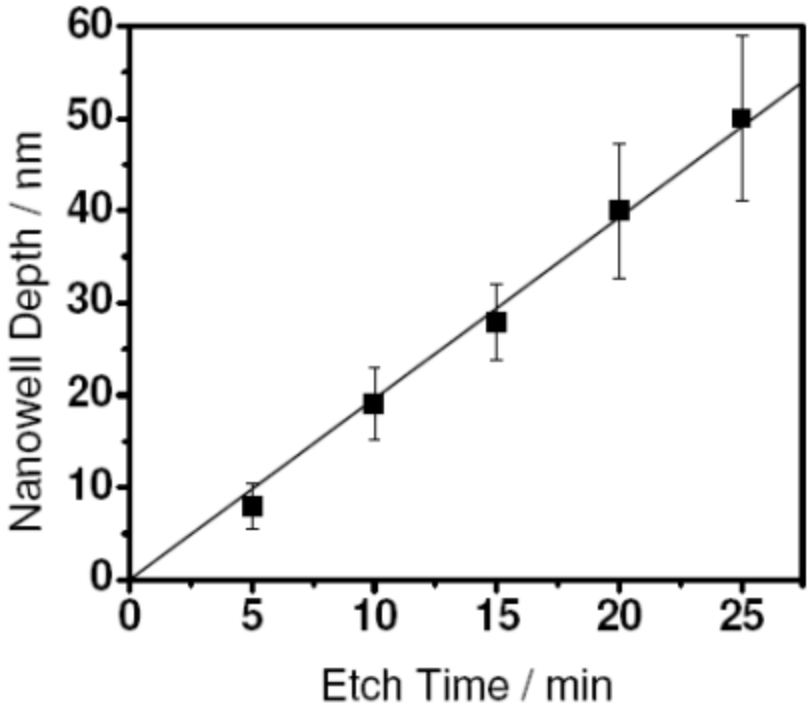

Figure 2-3. Nanowell depth versus etch time

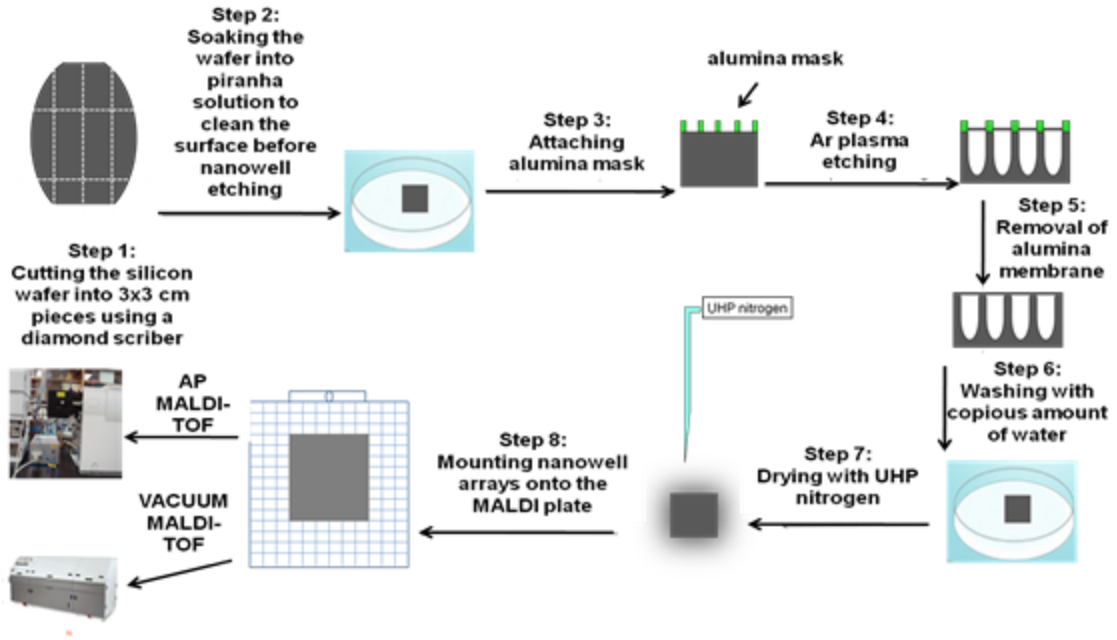

Figure 2-4. Workflow for the preparation of nanowell arrays and MS analysis.

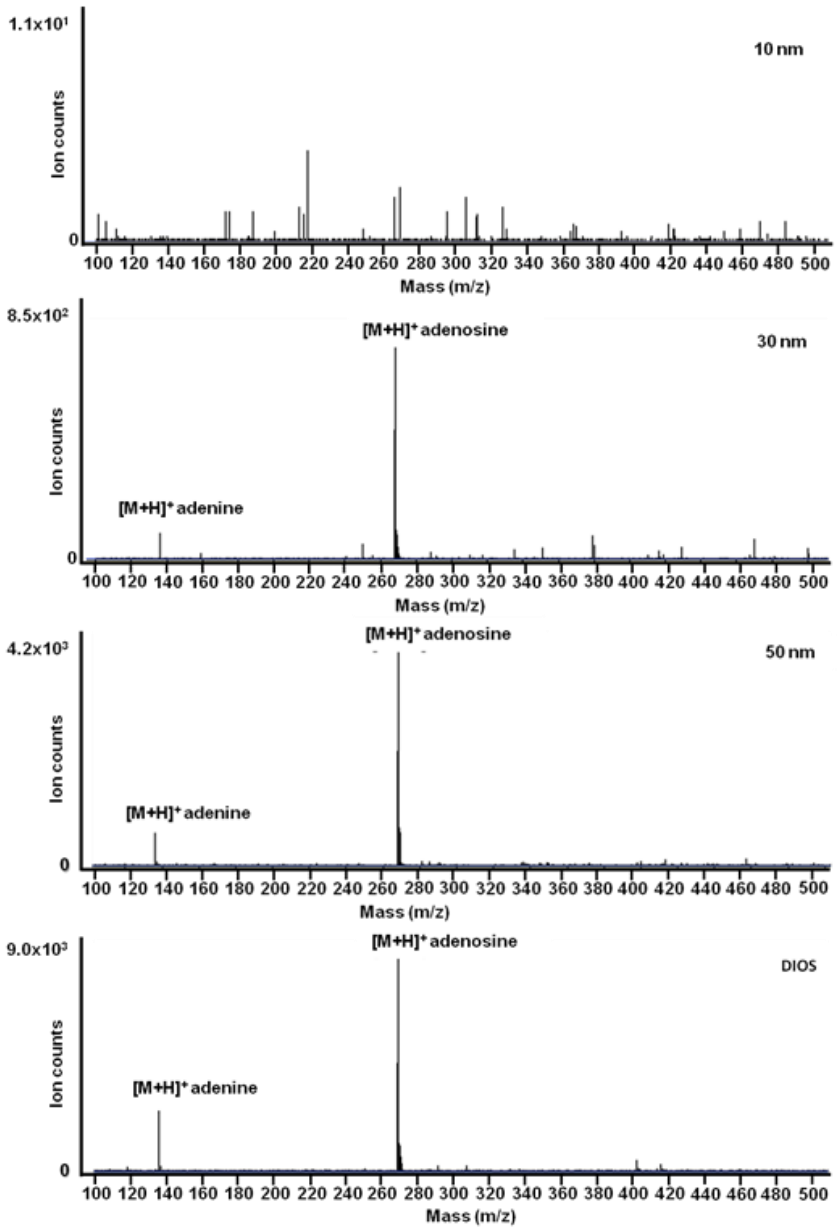

Figure 2-5. Mass spectra of adenosine acquired on 10 nm, 30 nm, 50 nm-deep nanowells and a DIOS surface

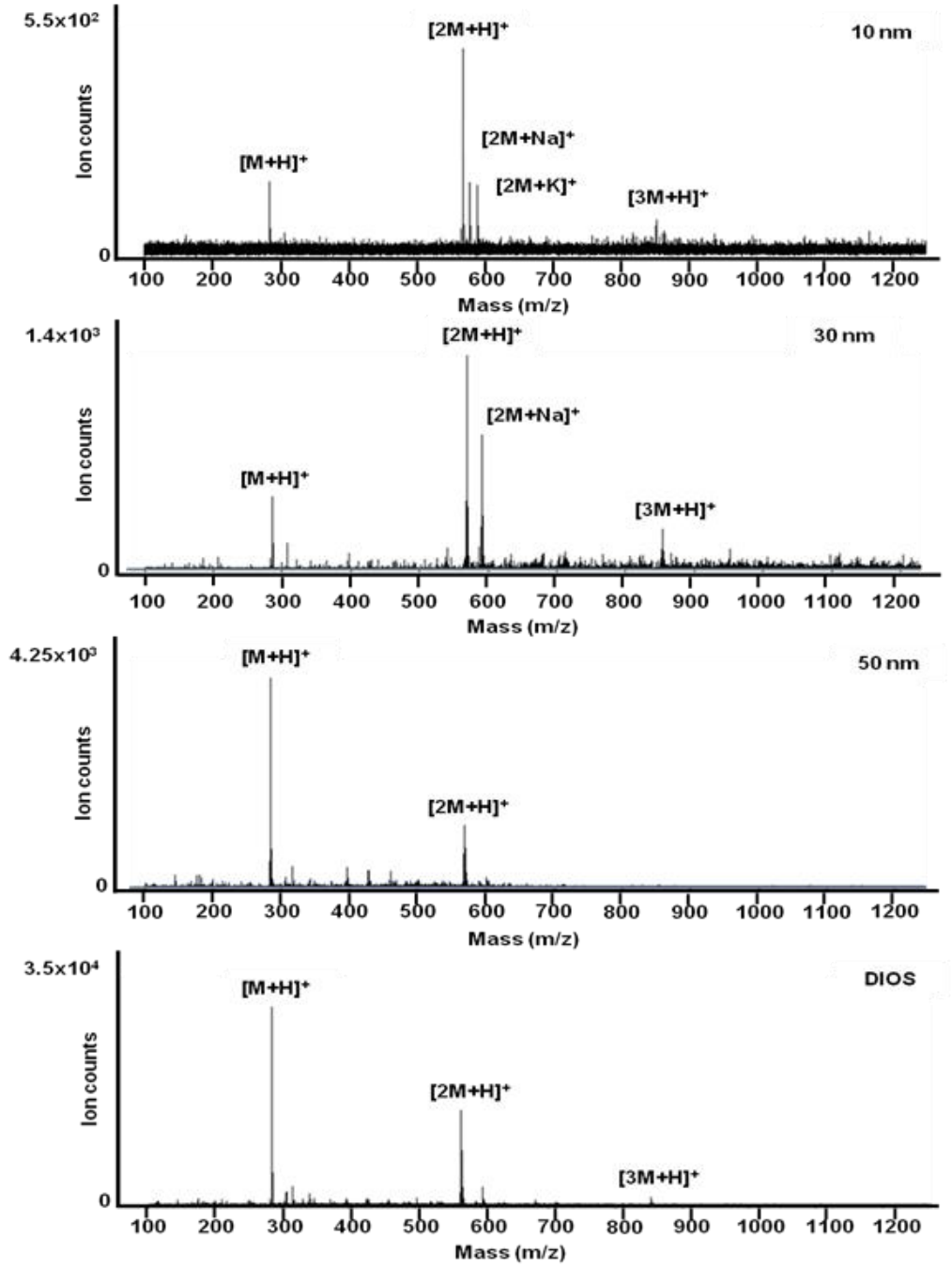

Figure 2-6. Mass spectra of adenosine acquired on 10 nm, 30 nm, 50 nm-deep nanowells and a DIOS surface

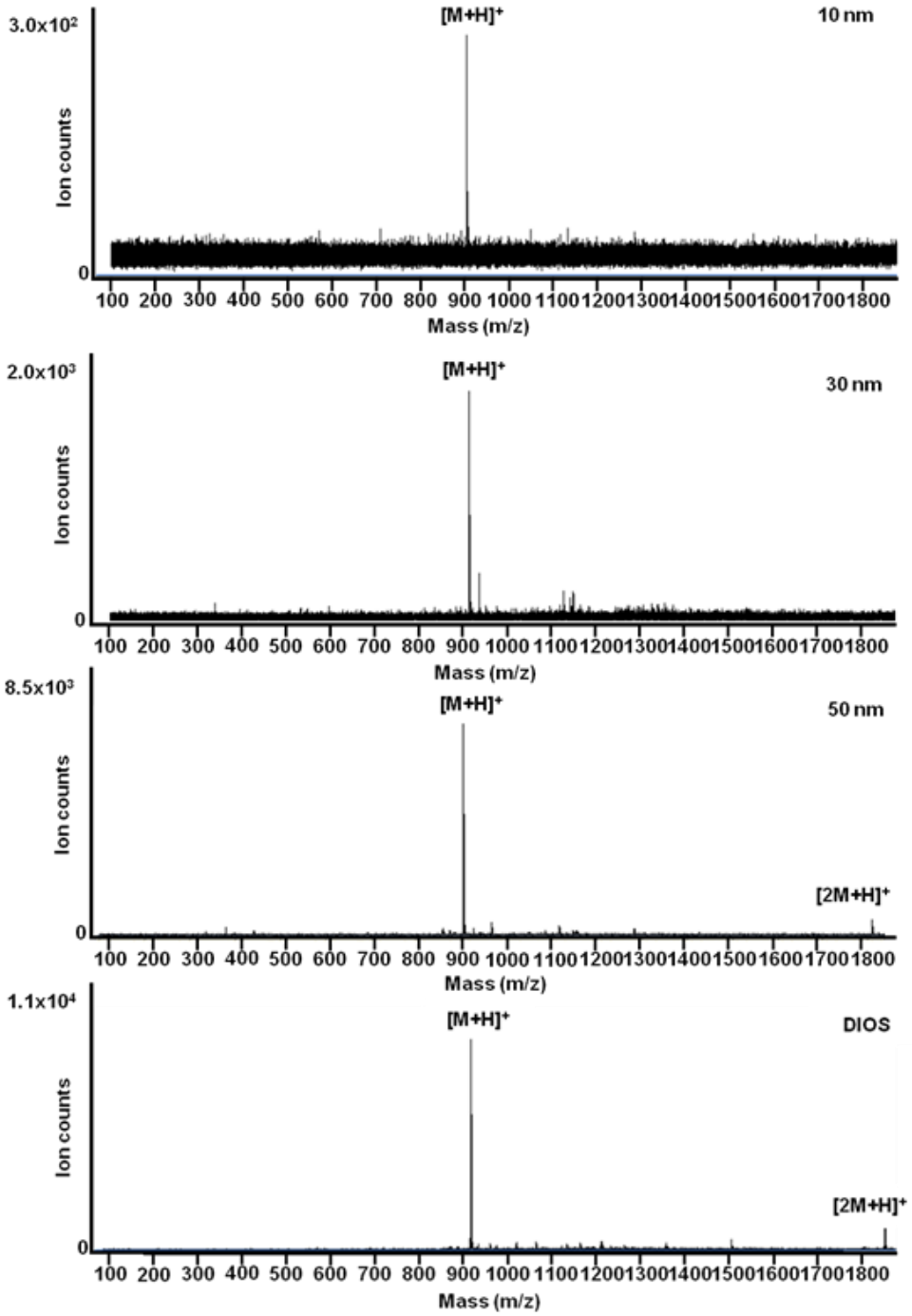

Figure 2-7. Mass spectra of adenosine acquired on 10 nm, 30 nm, 50 nm-deep nanowells and a DIOS surface

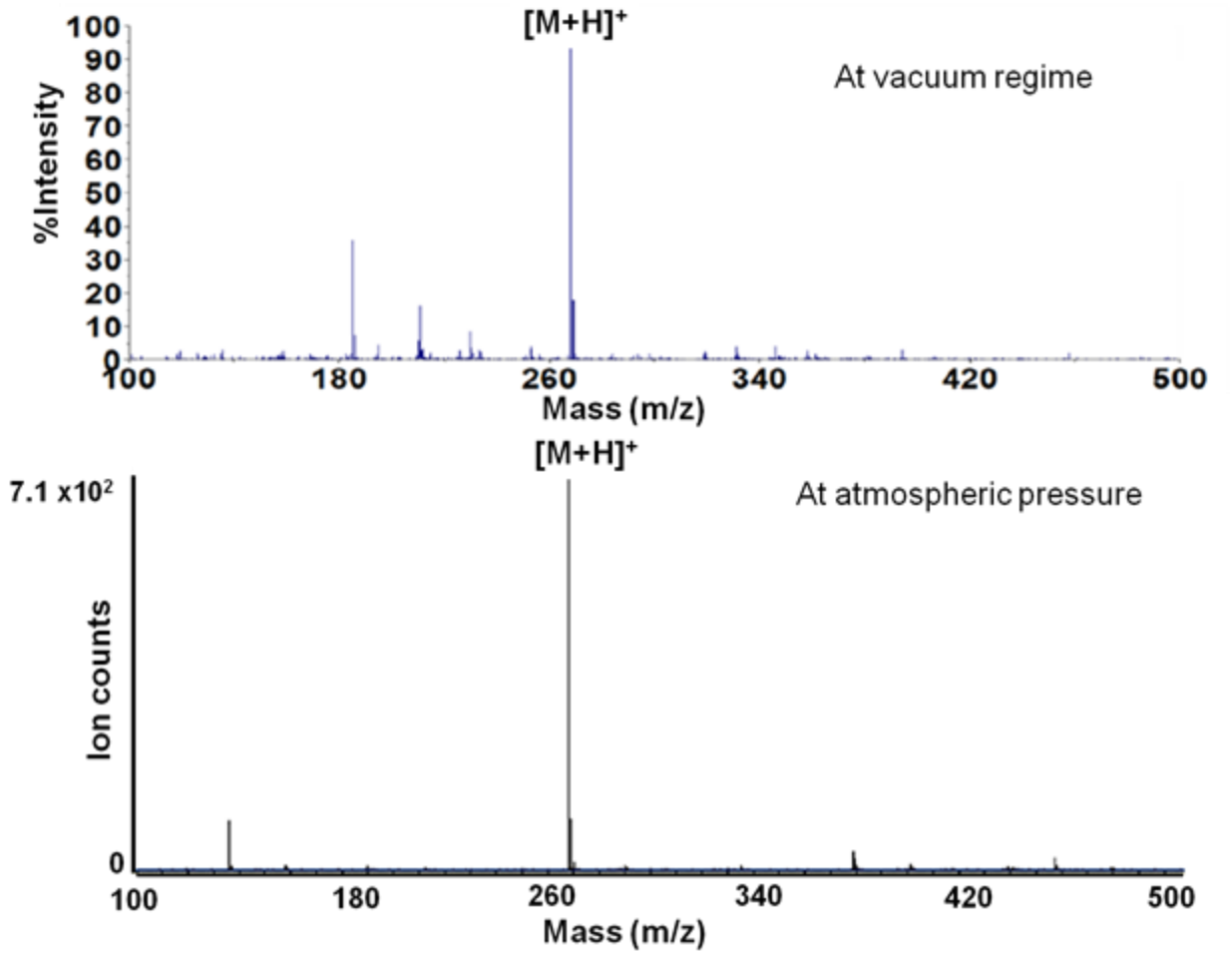

Figure 2-8. Comparison of atmospheric pressure and vacuum regime laser desorption ionization on 30 nm-deep nanowell arrays for adenosine.

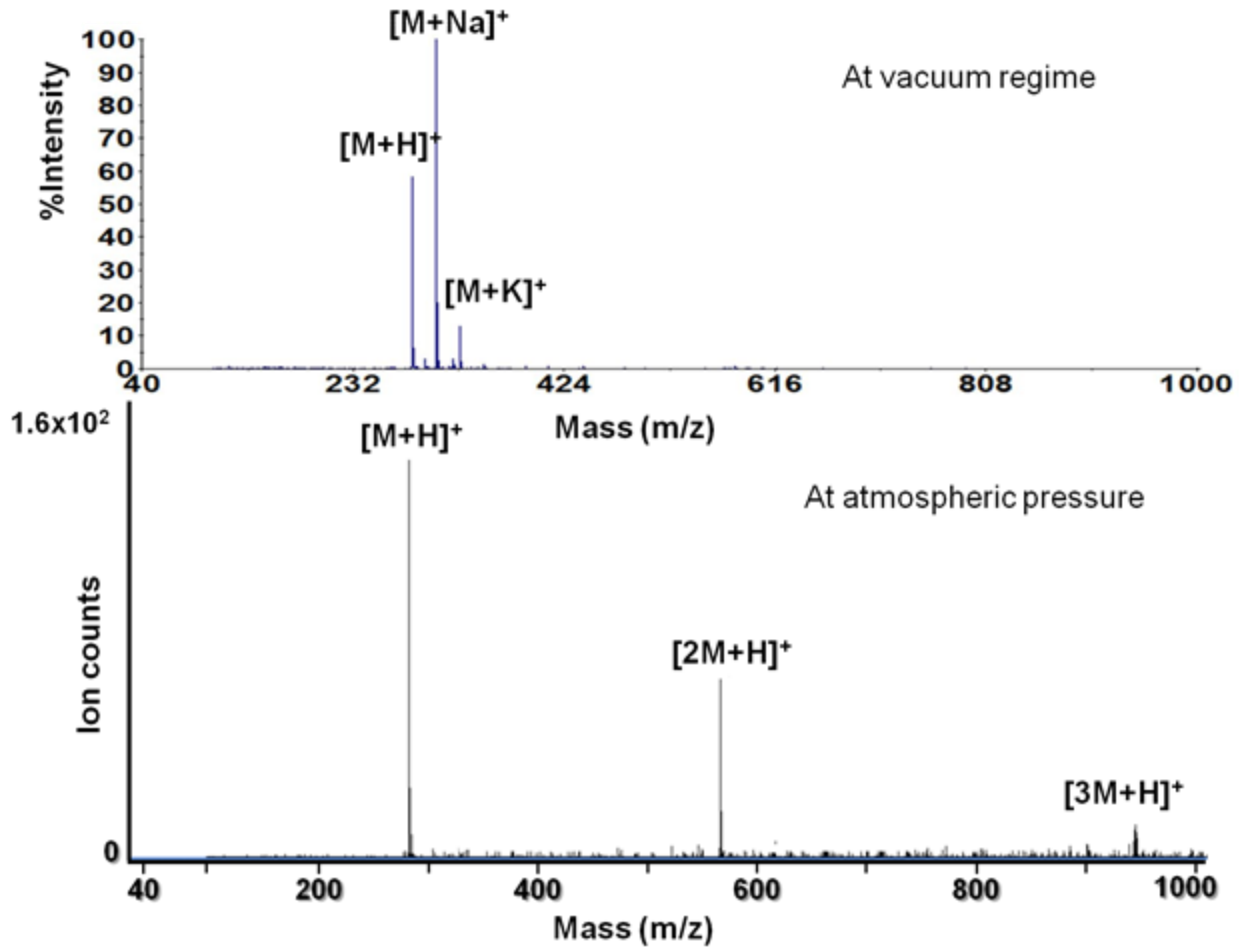

Figure 2-9. Comparison of atmospheric pressure and vacuum regime laser desorption ionization on 30 nm-deep nanowell arrays for Pro-Leu-Gly.

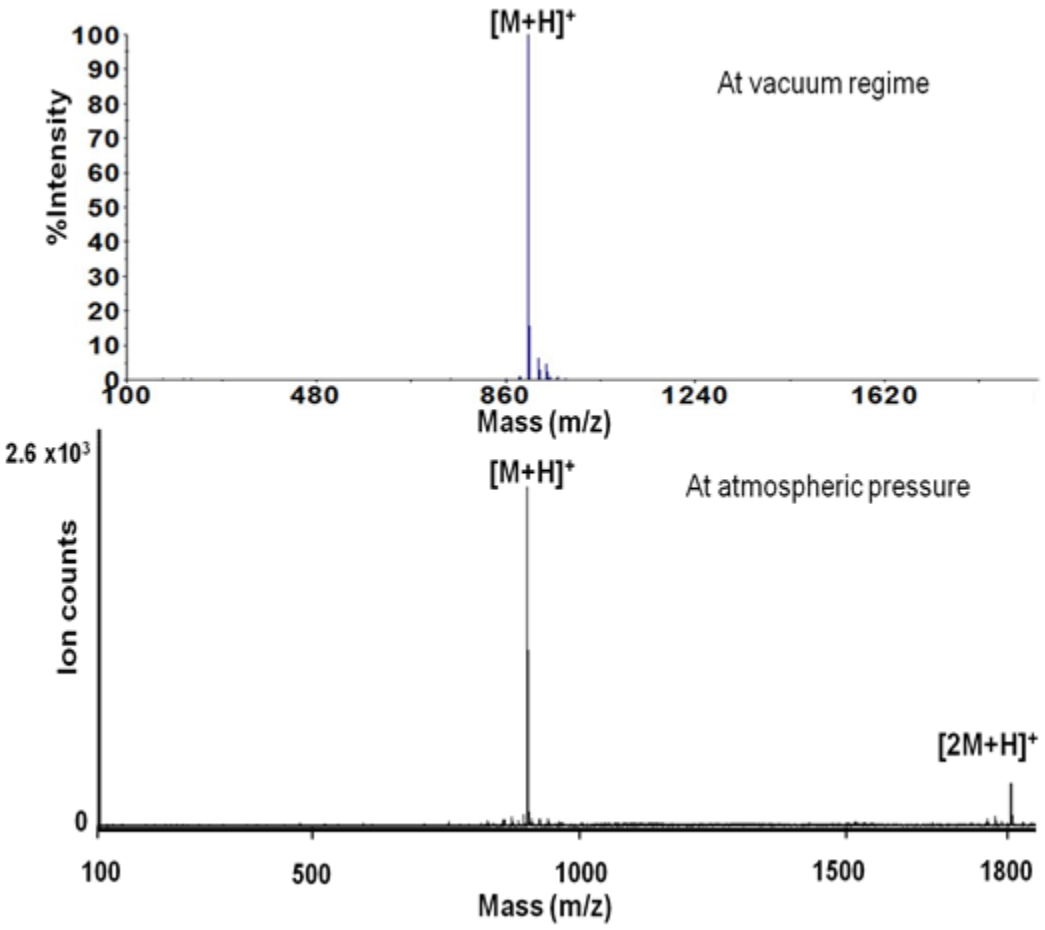

Figure 2-10. Comparison of atmospheric pressure and vacuum regime laser desorption ionization on 30 nm-deep nanowell arrays for [Des-Arg^9]-bradykinin

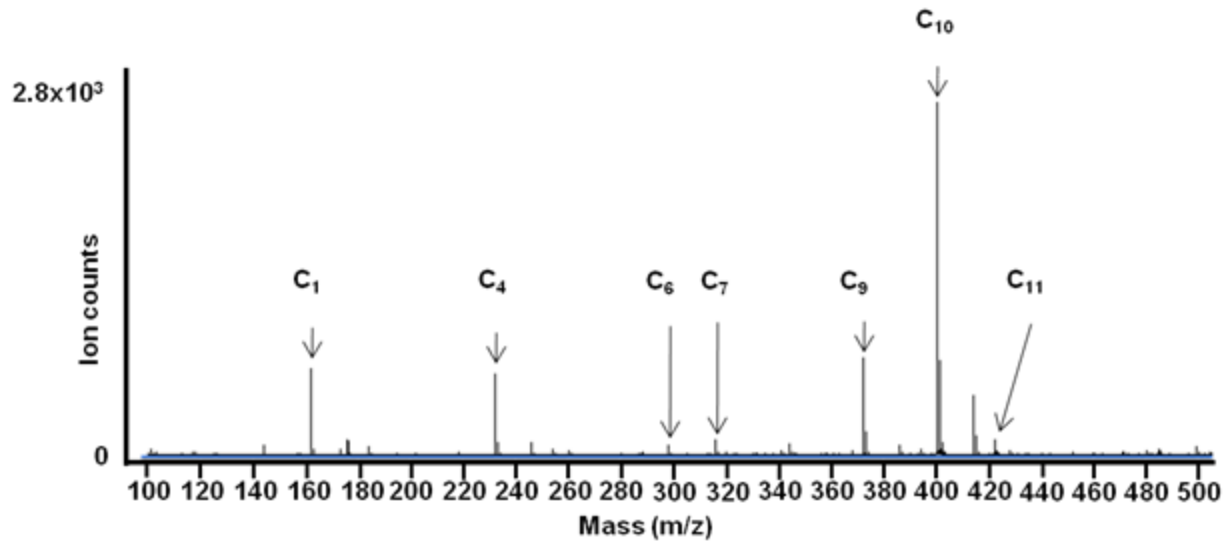

Figure 2-11. Analysis of carnitine standard solution on 50 nm deep nanowell array.

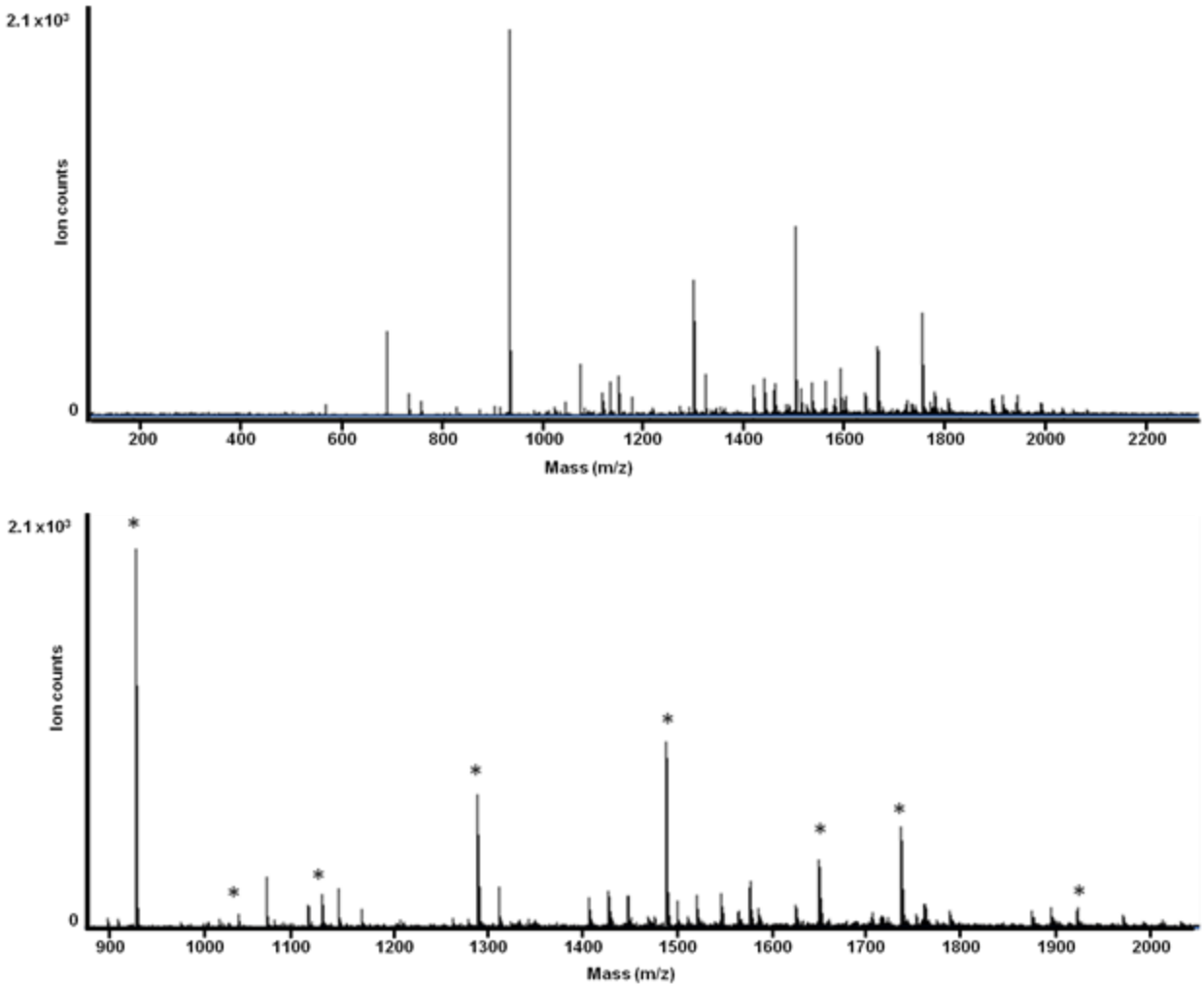

Figure 2-12. Analysis of tryptic digest of BSA on a 50 nm deep nanowell array. Peaks labeled with (*) denote tryptic peptides.

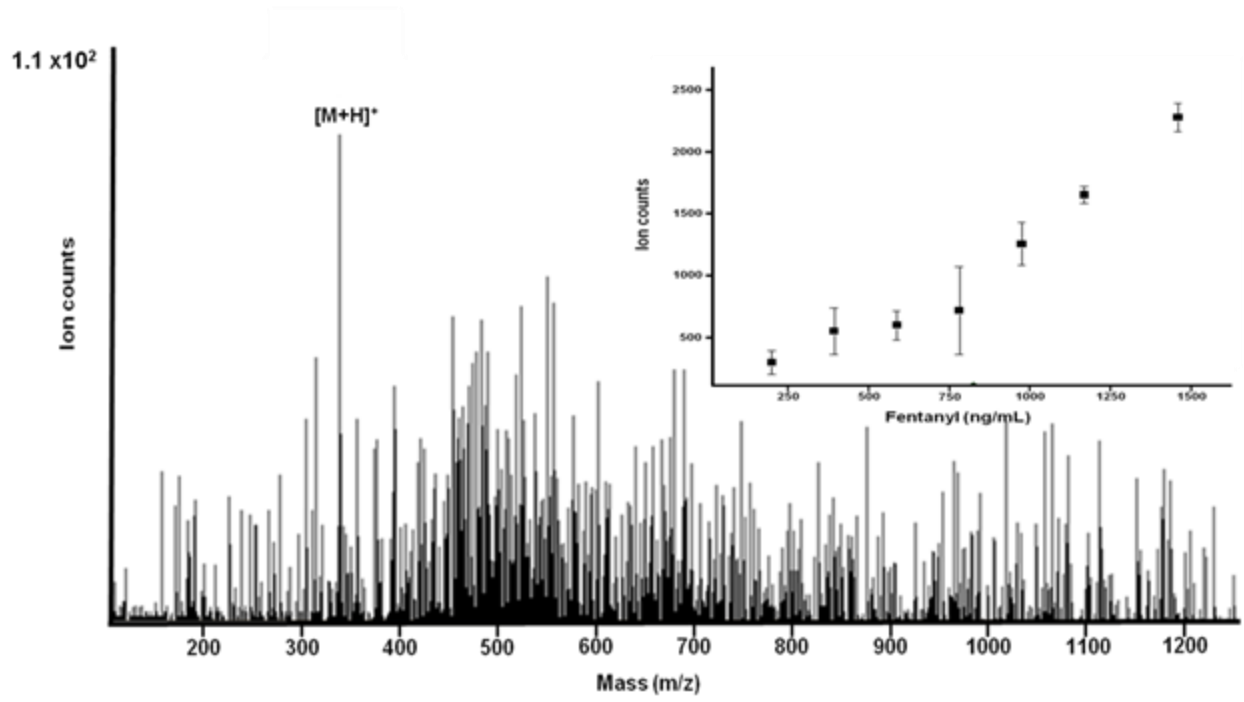

Figure 2-13. Mass spectrum of fentanyl in a red blood cell extract (200 ng/mL) obtained on a 50-nm deep nanowell array.

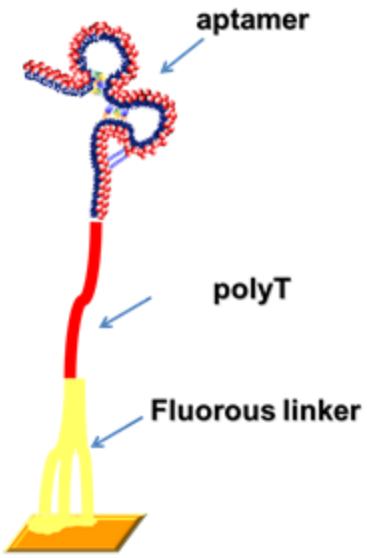

Figure 2-14. Schematic representation fluorous aptamers.

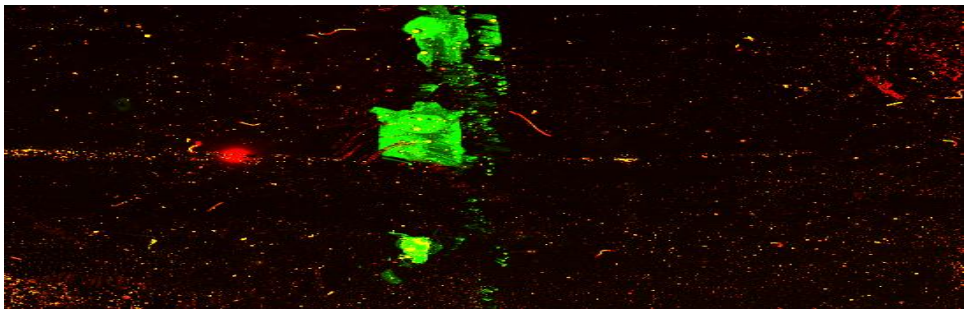

Figure 2-15. Immobilization of single fluorous tag carrying aptamers.

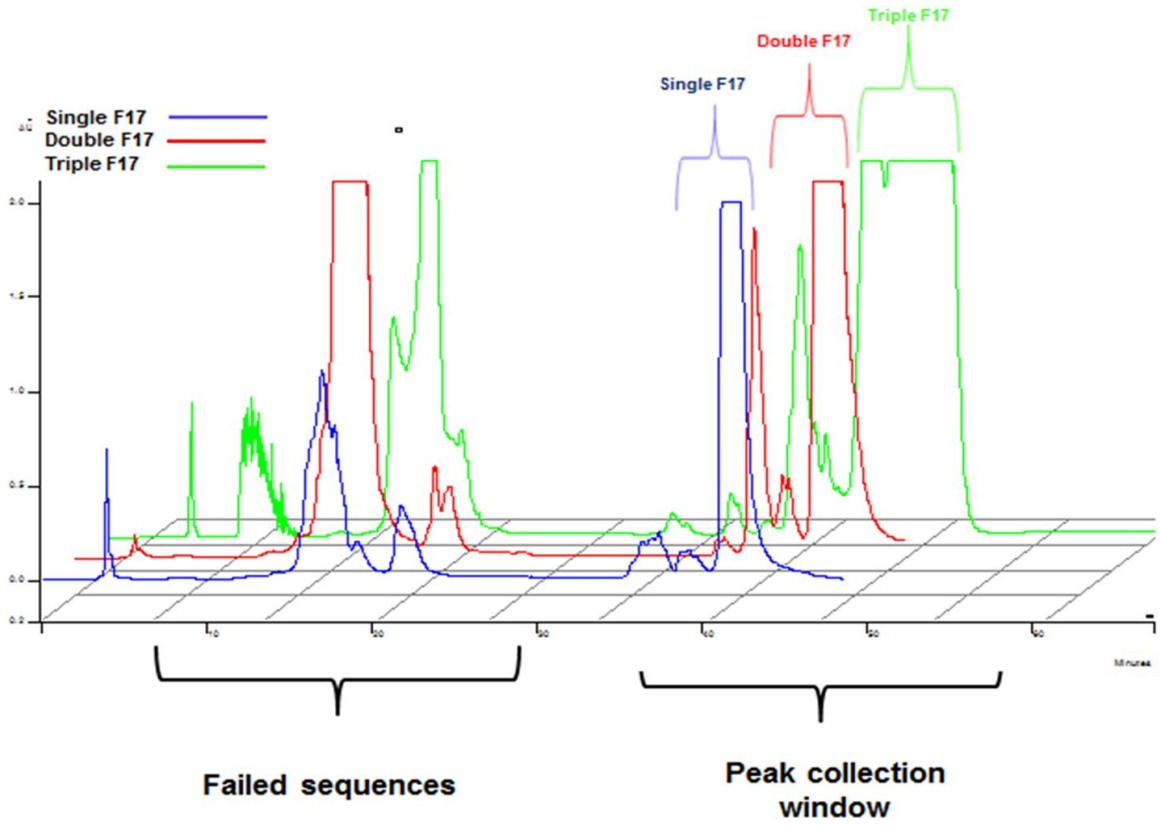

Figure 2-16. Seperation of single, double and triple fluorous tag containing aptamers

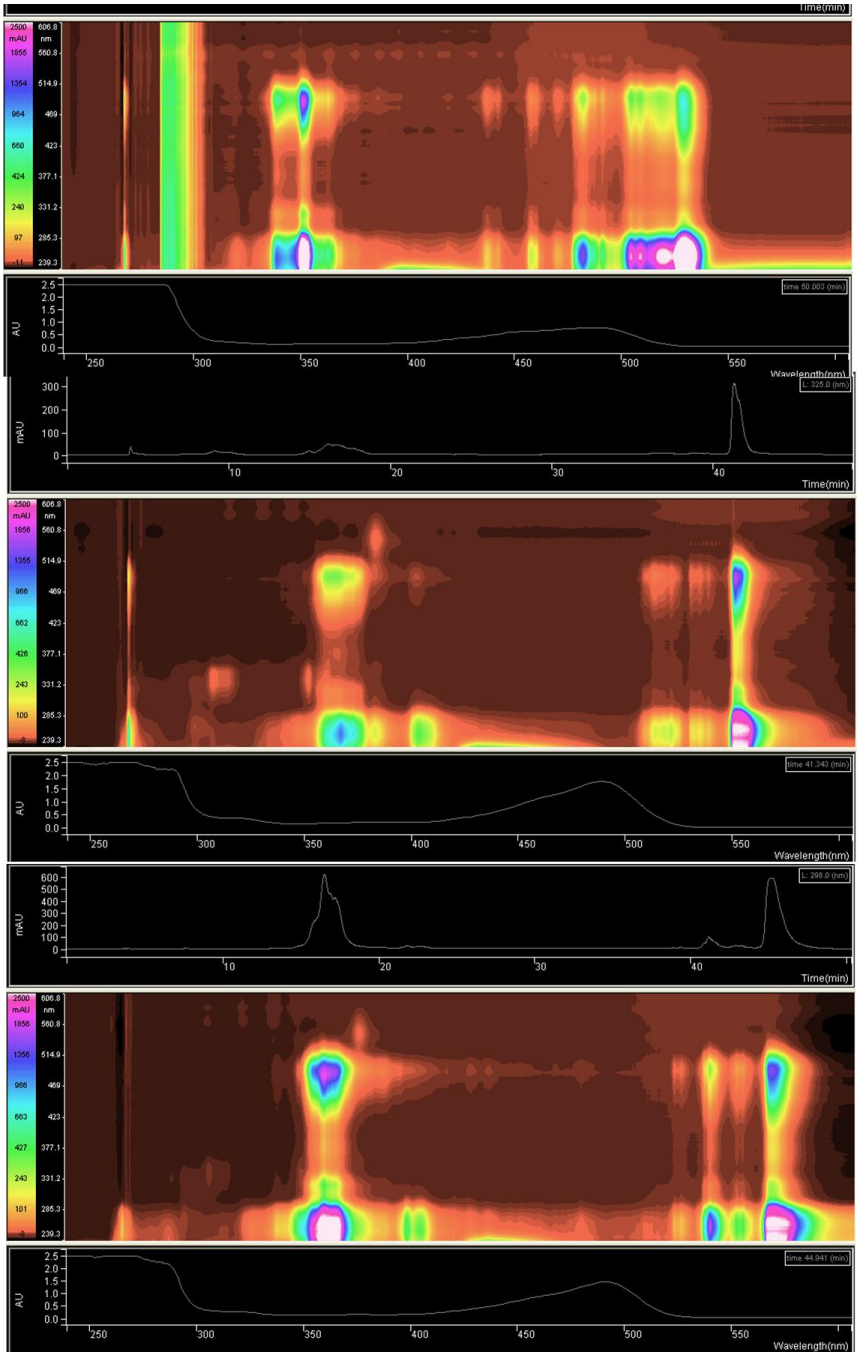

Figure 2-17. Separation of single, double and triple fluorous tag containing aptamers

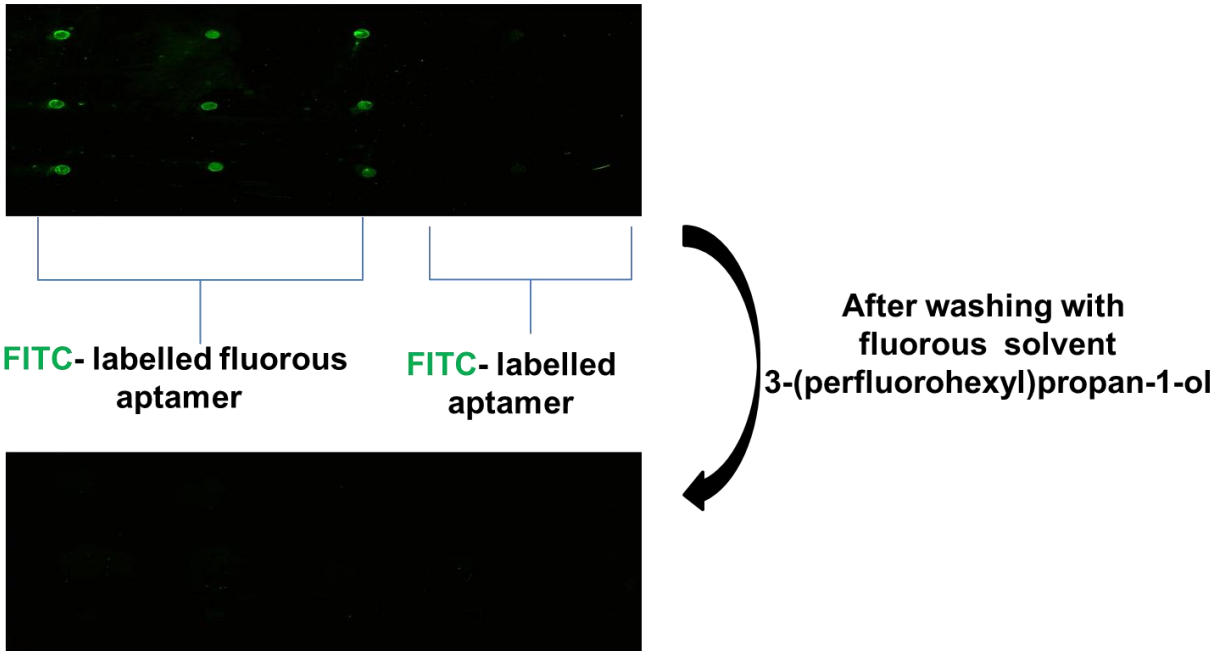

Figure 2-18. Immobiliization of triple flurous tag carrying aptamers onto glass slides

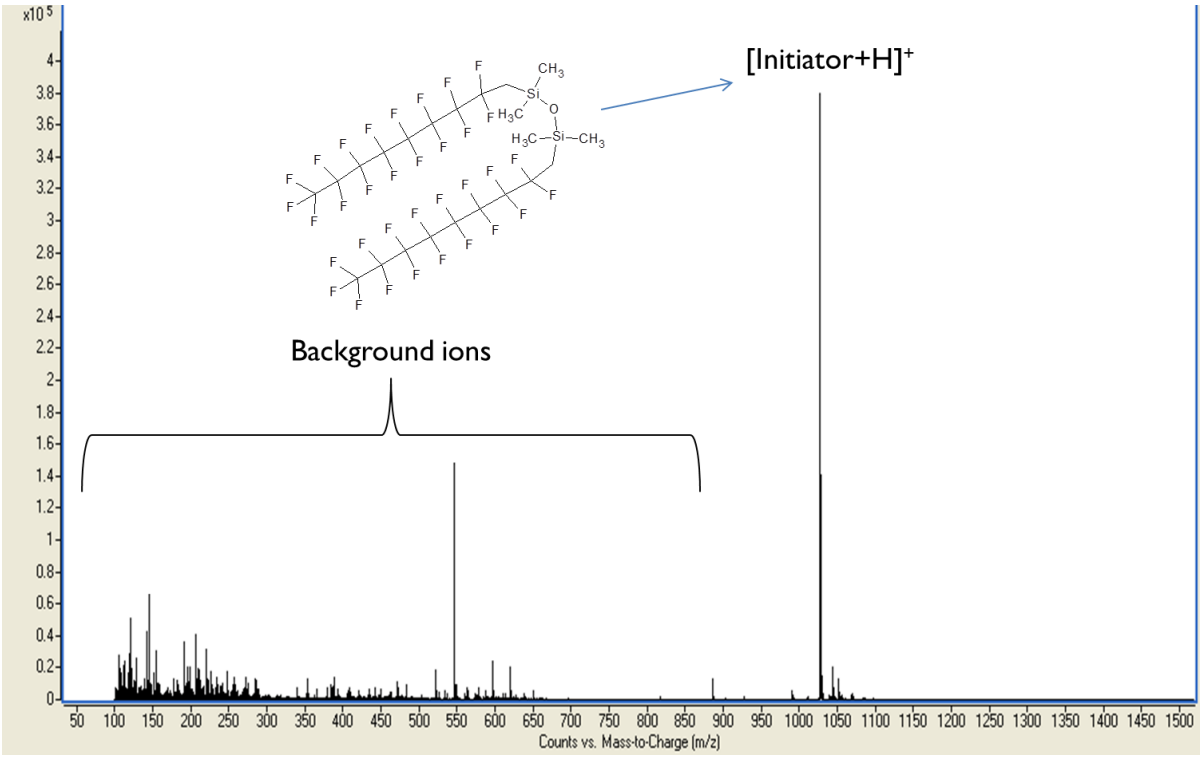

Figure 2-19. Aptamer enhanced NIMS under atmospheric pressure

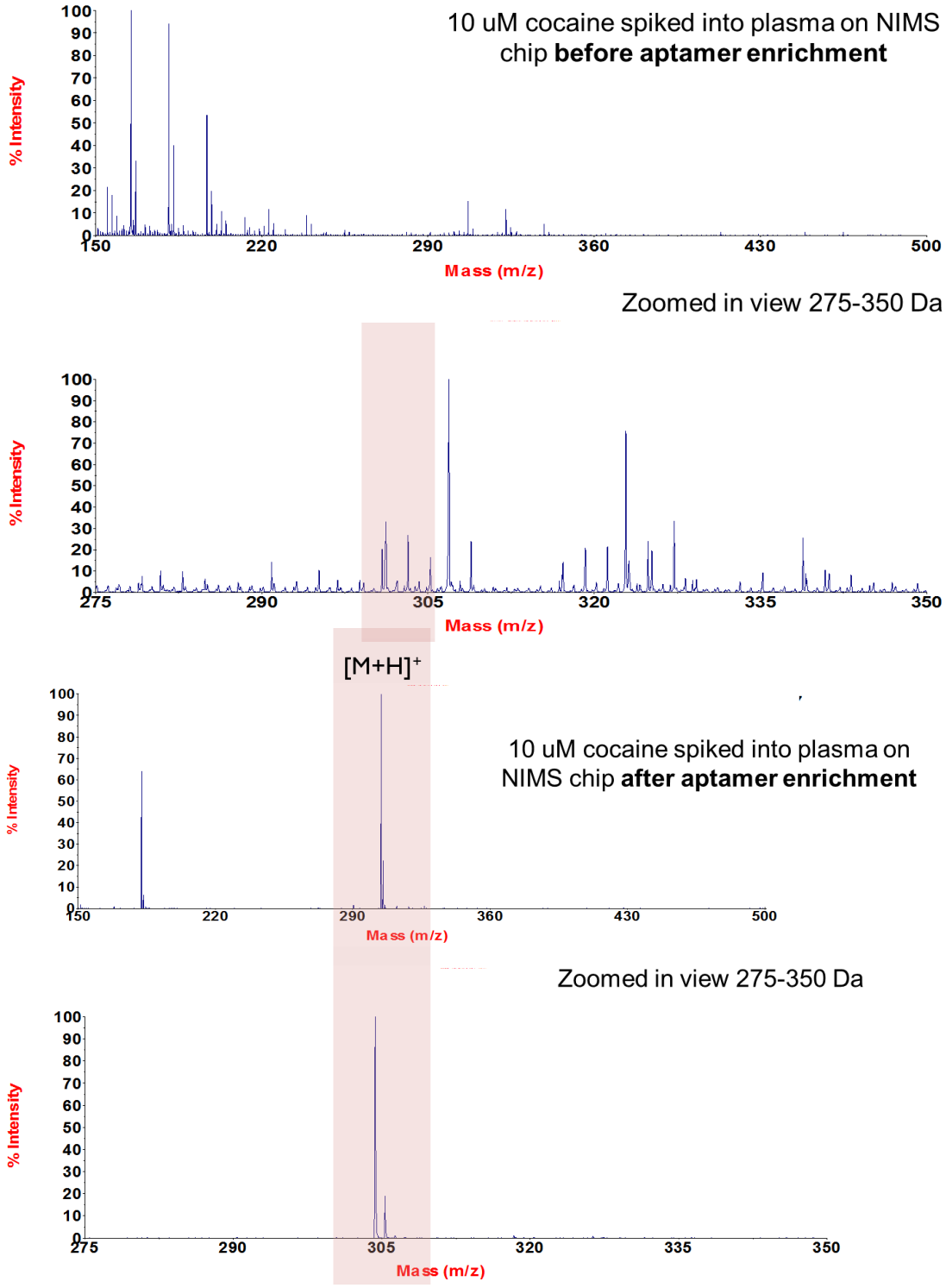

Figure 2-20. Aptamer enhanced NIMS under vacuum

Table 2-1. Name of the carnitines analyzed and their respective molecular weights

Name of the Carnitine	Molecular weight (m/z)
Carnitine (C1)	162.1125
Butyrylcarnitine (C4)	232.1543
Octanoylcarnitine(C5)	288.2169
Decanoylcarnitine(C6)	316.2482
Myristoylcarnitine(C9)	372.3108
Palmitoylcarnitine(C10)	400.3421
Stearoylcarnitine(C11)	428.3734
Decanoylcarnitine(C6)	316.2482

CHAPTER 3
A DUAL PLATFORM FOR SELECTIVE ANALYTE ENRICHMENT AND IONIZATION IN MASS SPECTROMETRY USING APTAMER-CONJUGATED GRAPHENE OXIDE

Development of “soft” desorption-ionization techniques namely, matrix-assisted laser desorption/ionization (MALDI) and electrospray ionization (ESI) revolutionized biological research by rendering the study of biomolecules feasible. These innovative mass spectrometry techniques have found widespread use in many different areas including genomics, transcriptomics, proteomics and metabolomics. However, despite the power of mass spectrometry, identification of species of interest among a vast number of other molecules for subsequent functional characterization still remains as one of the most challenging tasks. To address this problem extraction and fractionation methods are often applied. However since they lack of specificity, the best option would be the use of affinity reagents tethered on a substrate which mass spectrometry readout can be obtained. So far different kinds of affinity reagents have been applied in different formats such as mass spectrometric immunoassay (MSIA) (*90*), nanoprobe affinity mass spectrometry (*91*) and surface enhanced laser desorption/ionization (SELDI). Aptamers are single-stranded oligonucleotides that bind target molecules with very high affinity similar to antibodies. They are generated by an iterative process called “systematic evolution of ligands by exponential enrichment” (SELEX) and selected against various targets including metal ions, metabolites, proteins and even whole cells. Aptamers have very distinct advantages over antibodies that they can be produced without the need of an animal source, can be chemically modified with various functional groups, smaller size, non-toxic, non-immunogenic and have faster tissue penetration, all these unique properties make them ideal candidates among other affinity reagents. Aptamer modified nanomaterials as detection platforms for targeted

analyte capture have been previously used in mass spectrometry. Recently GO joined the bandwagon as a substrate for analyte detection owing to its unique electronic, thermal and mechanical properties and so has been reported as an excellent substrate for mass spectrometery (MS). In this chapter, aptamer modified GO as a selective enrichment and matrix-free detection platform for affinity mass spectrometry is discussed.

Experimental

Mass Spectrometry

Mass spectra under atmospheric pressure conditions were acquired using an Agilent 6210 MSD time-of-flight (TOF) mass spectrometer configured for ESI (Agilent Technologies Inc., Santa Clara, CA). Laser-desorption/ionization experiments were conducted by installing an external MassTech atmospheric pressure/matrix assisted laser desorption ionization pulse dynamic focusing (AP/MALDI PDF) ion source. The results were analyzed using Analyst software. All mass spectra in the vacuum regime were acquired using a MALDI-TOF/TOF mass spectrometer (ABI/SCIEX 5800, Applied Biosystems, Foster City, CA). A Nd:YAG laser at 355 nm was used. The spectra were recorded in reflection mode in either positive or negative mode using an accelerating voltage of 25 kV, a 62% grid voltage, and a 100 ns delay extraction. Typically, 30-80 laser shots were collected per spectrum. Applied Biosystems calibration mixture 1 was used to calibrate the mass spectrometer. Data analysis and was performed using Data Explorer software.

Transmission Electron Microscopy

GO was treated by ultrasonication for 24 hours before any surface modification, to ensure small size and homogeneous dispersibility. TEM images were taken with a JEOL TEM 2010F transmission electron microscope on a copper grid.

PEGylation of Graphene Oxide

Before starting the modification, the GO solution (1mg/mL) was sonicated for approximately 24 hours. Then 100 µL of GO solution (1mg/mL) was treated with 0.0022 M EDC and 0.0015 M NHS in PBS (pH =7.4) buffer. After the activation of carboxyl groups, the solution was treated with 130.6 µM HS-PEG-NH_2. After 1h incubation, the solution is centrifuged and washed room temperature for 4 times at 14000 rpm and for 4 minutes to discard the supernatants, which consist of the unbound PEGs to the surface of GO, each time 450 µL of PBS is added for each washing step and the last solution is prepared with 100µL of PBS (pH = 7.4).

Aptamer Synthesis

The cocaine and adenosine aptamers have been used in aptamer assisted extraction experiments. (Adenosine, 5′-ACC TGG GGG AGT ATT GCG GAG GAA GGT-3′; Cocaine, 5′-GGG AGA CAA GGA AAA TCC TTC AAT GAA GTG GGT CGA CA-3′ respectively.) All of the aptamers were coupled with 5′-thiol modifier for graphene oxide modification and also the same aptamers are synthesized and labeled with fluorescein at the 3′-end by using 3′-(6-fluorescein) CPG to detect the modification on graphene oxide surface. An ABI 3400 DNA/RNA synthesizer (Applied Biosystems, Foster City, CA) was used for the synthesis of all DNA sequences. A ProStar HPLC (Varian, Walnut Creek, CA) with a C18 column (Econosil, 5 ím, 250 4.6 mm) from Alltech (Deerfield, IL) was used to purify all fabricated DNA. A Cary Bio-300 UV

spectrometer (Varian, Walnut Creek, CA) was used to measure absorbance to quantify the concentrations of the obtained sequences. All oligonucleotides were synthesized by solid-state phosphoramidite chemistry at a 1-µmol scale. The completed sequences were then deprotected in AMA (ammonium hydroxide/40% aqueous methylamine 1:1) at 65 °C for 20 min and further purified with reversed-phase HPLC on a C_{18} column.

Aptamer Conjugation to PEGylated Graphene Oxide

The 5' end of the aptamers was modified with disulfide functional group during the aptamer synthesis process. So before the reaction with the thiol groups at the tips of the PEGs that are attached to the surface of GO, the disulfide bonds at the 5' end of the aptamers should be cleaved to give thiol groups. For this purpose, 100 µM disulfide modified aptamers were treated with 5 mM of TCEP in 50 mM Tris/HCl (pH=7.5) buffer for 1 hour at room temperature. Then the desired thiol modified aptamers are collected in small portions by eluting the TCEP mixture through a NAP-5 column. The concentrations of these portions are calculated by taking their UV absorption spectra. The 100 µL of the PEGylated GO that is obtained at the first step is incubated with 1 µM of thiol modified aptamers that is obtained in the third step, in 200 µL of PBS (pH= 7.4) buffer for 2 hours. After this incubation the unbound aptamers were removed by excessive centrifuging and washing steps.

Aptamer Assisted Target Extraction

Universal Coagulation Reference Plasma (UCRP) was obtained from Thermo Scientific 500 µL of the plasma sample was spiked with 500 µL of 20 µM of cocaine and 500 µL 20 µM adenosine separately in two different eppendorf tubes. They are then vortexed to ensure complete mixing. In all experiments 100 µL of GO (1 mg/ml in water) was first centrifuged at 4000 rpm for 15 mins and supernatant was taken out and then

GO was redispersed in 100 uL of the binding buffer (20 mM Tris-HCl, 140 mM NaCl, and 2 mM $MgCl_2$, pH: 7.5). For target extraction experiments 50 µL of GO (with or without aptamer modification) was mixed with the 50 µL of target spiked plasma and gently mixed for 30 mins by occasional vortexing at every 10 mins. After that mixture was vortexed at 4000 rpm for 15 mins GO pelletted, supernatant was taken out and GO and washed with 100 µL of binding buffer followed by 100 µL of washing with water. Finally the GO was centrifuged at 14000 rpm for 10 mins, supernatant was taken out and resulting GO was redispersed in 10 µL of H_20 (in %0.1 TFA) and 2 µL of that GO suspension was pipetted onto the sample plate. It was left at room temperature for 20 min until dryness and laser desorption ionization experiments were carried out.

Synthesis of Au, Cu, Pt, and Au/Cu/Pt Alloy and CdTe Derivatives of GO

Au-GO synthesis

DNA-1: 5′ AATGTGCTCCCCCAGCGCGCTT-FITC-3 ′ and DNA-2: 3′-TTACACGAGGGGGT-5 were mixed together at the same concentration (1µM) to obtain double stranded DNA(dsDNA) via hybridization in 10 mM HEPES buffer (50mM $NaNO_3$, pH 7.5) for 30 min. Then, graphene oxide (GO) (final concentration of graphene oxide was 20 µg/mL in DNA solution), was added for adsorption of dsDNA on the GO. After 30 min incubation, the mixture was centrifuged and excess DNA in the supernatant was decanted. The gold precursor, $HAuCl_4.3H_2O$, was used with sodium citrate to form Au NPs on dsDNA-GO. $HAuCl_4.3H_2O$ solution was put in dsDNA-GO mixture with final concentration of 100 µM Au^{+3} and the mixture was stirred for 5 minute. The freshly prepared reducing agent solution 500 µM (sodium citrate) was added in a dropwise manner for 30 min with vigorous stirring. Purification was the same as described above.

Cu-GO and Pt-GO synthesis

The protocol given above was followed except $CuSO_4$ and $PtCl_4$ were separately reduced on dsDNA-GO using sodium L-ascorbate as reductant. The final concentrations of metal ions (Cu^{+2} or Pt^{+4}) and reducing agent in mixtures were adjusted to 100 µM and 500 µM, respectively.

Au/Cu/Pt- alloy GO

The 100 µM each metal ion, Au^{+3}, Cu^{+2} and Pt^{+4}, solutions were simultaneously added into the dsDNA-GO mixture stated above with vigorous stirring. After 10 minute incubation, reducing agent 500 µM (sodium L-ascorbate) was added dropwise to mixture for 30 minute stirring.

CdTe- GO synthesis

For a typical CdTe synthesis, 400 ml $CdCl_2$ -GSH stock solution was mixed with 0.8 ml of freshly prepared NaHTe solution in a 0.7 ml eppendorf tube and then DNA solution containing 120 nmol nucleotides was added on GO.

Synthesis of Benzylpyridinium Salt (BP) and SY Experiments

12 mL of pyridine was mixed with benzyl chloride at a molar ratio 20:1 (pyridine/benzyl chloride), refluxed at 60 °C for 6 h. The BP was collected by removal of excess pyridine with rotary evaporation under vacuum and used to prepare 1 mM methanolic solution.

GO-metal conjugates were washed with copius amounts of water and ethanol and 1 µL of each GO-metal conjugate (1 mg/ ml for each) was spotted onto MALDI plate and dried. After that 1 µL of the BP ion was spotted onto GO-metal conjugates and analyzed by using the same instrumental conditions by only varying the laser fluence.

LDI-MS Analysis of Proteins on CdTe-GO

Bradykinin acetate, Insulin beta chain, bovine serum albumin were used as the model compounds. After spotting 1 µL of CdTe (1 mg/ml) and drying on the MALDI plate, 1 µL of each (10 pmol/ µL) compound was spotted onto CdTe-GO dried under ambient conditions, subjected to LDI-MS analysis under the same experimental conditions.

Results and Discussion

Testing GO as Matrix for LDI

The first step of the experiments in this part was to show that graphene can be used as a matrix for small molecule analysis. Carbon nanotubes and diamond like carbon films have been previously used for LDI analysis. To demonstrate that graphene oxide (GO) can be used as matrix for laser desorption ionization, a series of small molecules including glucose, caffeine, glutathione were analyzed using GO as an efficient energy absorbing molecule. The mass spectra are shown in through Figures 3-1 to 3-3. It can clearly be seen that GO serves as an excellent substrate for LDI of small molecules. To eliminate the possibility of self-ionization we also spotted the same compounds on stainless steel plate and analyzed. The spectra show no discernible signal associated to these compounds. The results were also compared to the MALDI analyses. When LDI on GO is compared with MALDI, significant amount of background peaks are seen in MALDI spectra.

Characterization of Aptamer Modified GO

The results of FTIR spectroscopy is shown in Figure 3-4. It can be seen that the aptamer modification occurred by covalent binding via the disulfide bond formation between the thiol groups of the corresponding aptamer and PEG that is previously

attached to the surface of the GO with amide bonds. Before aptamer or PEG modification FTIR spectrum of Graphene Oxide has a carboxyl (C=O) stretching peak at around 1728 cm^{-1}, but after the modification the peak is shifted to 1649 cm^{-1}, which is representing the amide carbonyl-stretching mode (amide I vibrational stretch). Also at around 1557 cm^{-1} the N-H bending and C-N stretching vibrational frequencies can be seen (amide II vibrational mode). Since graphene oxide has lots of reactive epoxy groups, its exposure to amine groups can lead to a ring-opening reaction of the reactive three-membered epoxide ring, forming new C-N bonds. The ring-opening reaction of the epoxy group due to nucleophilic attack from amine groups has been well established. After the modification, the increase of the peak intensity at around 1557 cm^{-1} and the decrease of the peak intensity of the epoxy mode is actually showing that the amine groups are not just attaching to the carboxylic groups of GO but also epoxide groups. All of these amide vibrational peaks are the proof for the amide bond formation during the PEGylation of Graphene Oxide.(*92*) Other vibrational modes are C-O (epoxy) and C-O (alkoxy) can be seen at 1203 cm^{-1} and 1051 cm^{-1} respectively. Also differing from the FTIR spectrum of the GO only, the S-S disulfide vibrational mode appeared at 535 cm^{-1} in the FTIR spectrum of the GO that is modified with the aptamer through the disulfide bond formation. This is also the proof of the aptamer modification by covalent binding via the disulfide bond formation.

Aptamer Assisted LDI on GO

Next we immobilized thiol-functionalized cocaine and adenosine aptamers onto GO by activation of carboxyl (-COOH) rich groups using EDC / NHS chemistry and introducing a bifunctional PEG as a spacer molecule, which provides stability in physiological media like serum and blood. Furthermore, the PEG linker also provides

freedom to aptamers to obtain a 3D conformation to recognize their targets.(*93*)The bifunctional PEG linker carries amine (-NH_2) groups on one side to bind to the carboxyl on the GO surface and thiol (SH) groups to help anchor the SH-functionalized aptamers through disulfide bond formation. Schematics of the whole process can be seen in Figure 3-5. Next, aptamer conjugated GO was applied for selective enrichment and detection of cocaine spiked in human plasma along with respective control experiments. Figure 3-6 (a) shows the MS analysis of cocaine spiked plasma samples analyzed directly onto GO without any enrichment step (no aptamer modification) where it served only as a matrix. The cocaine peaks can be detected among huge background ions with an average S/N ratio of 15. Figure 3-6(b) also shows the analysis of cocaine spiked plasma extracted and ionized with unmodified GO. As can be seen, even in the presence of unmodified GO, enrichment of the sample was observed to some extent along with a reduction in background ions. This can be due to the structure of cocaine bearing an aromatic ring which aids in π-π interactions with GO. In another control experiment, GO with physically adsorbed cocaine aptamer was used for target extraction, where, following washing steps, no or scantily extracted cocaine with an S/N ratio of 5 was obtained. (Figure 3-6 (c)). On contrary, GO was shown to physically adsorb DNA in high yields. We assume that surface coverage of GO by physically adsorbed aptamers prevent the loading of cocaine by means of nonspecific interactions (in case with π-π interactions or aptamers upon target capture comes off the GO surface following washing steps due to the absence of any chemical functionalization. However, upon chemical modification of GO with the cocaine aptamer an efficient capture of target analyte was achived with an average S/N ratio of 52. Figure 3-6(d).

The S/N ratio is shown in Figure 3-7. To further demonstrate the analytical utitily of our approach we applied the same concept to adenosine aptamer. As can clearly be seen in Figure 3-8, we observed a very similar trend. This result proves that even if some extraction can be achived with pristine GO, aptamer conjugation yields significantly better extraction efficiency with an increase in S/N increase as shown in Figure 3-9.

Formation of Au, Cu, Pt, and Au/Cu/Pt Alloy and CdTe on GO

In the previous section we have shown that GO can be a very efficient material for small molecule analysis and by proper chemical modification it can also be tuned as a selective capture and ionization matrix by aptamers. However the mass range at which GO can perform well is limited to compounds that are below 1000 Da in molecular weight. It is obvious that it will be very useful for metabolomics applications but its use for protein analysis will be limited. Therefore we sought to develop a GO based hybrid material which could also be used for the analysis of proteins. To accomplish this, uniformly sized Au, Cu, Pt nanoparticles and Au/Cu/Pt alloy structures and GO- CdTe structures were produced by reduction of cationic metal ions (Au^{+3}, Cu^{+2}, Pt^{+4} , CdTe) bound to and accumulated on the main groove of dsDNA with reducing agents. The reaction temperature, reaction time, stirring rate, concentration of each metal ion (100 µM) and reductant (500 µM) were kept constant to synthesize each metal nanoparticle graphene oxide (MNP-GO) hybrid structures. The TEM images of Au-GO and Cu-GO and Au-Cu-Pt-GO and CdTe-GO samples given in Figure 3-10, show well-ordered nanoparticle distributions. The long reaction time and the increase of concentration of metal ions may cause the large particles from aggregative growth of small particles. In other words, when the reaction time is extended and highly concentrated metal ion solutions are used, small nucleated particles randomly coalesce with each other or with

generated particles before separate growth process and start aggregative growth in dimer, trimers form under stirring. Using considerably concentrated metal ions solutions limits the free space between metal ions and hinders to nucleate and form single dispersed nanoparticles because there is a favorably strong Van der waals interaction between metal nanoparticles inducing agglomeration. There is no formation of MNPs during the 30 min reaction time at room temperature in the absence of dsDNA. TEM image of pristine GO is included for comparison. The dsDNA provides a homogeneous distribution of Au nanoparticles on the GO surface, but previous studies without dsDNA using different techniques and experimental conditions resulted in nanoparticles on the randomly pre-existing functional groups on GO surface.

Survival Yield Calculations

After the synthesis of various GO-metal heteroconjugates benzylpyridinium salts (BP) was employed as a model analyte to determine survival yield to estimate how well the generated intact molecular ions survive avoiding fragmentation under the given condition and how efficiently the analytes are desorbed from the given substrate, respectively.(*94-96*) A typical fragmentation pattern of BP salt is given in Figure 3-11. It is well known that high survival yield is favored for the development of good LDI systems. In our system, survival yield were calculated from the mass spectra of BP obtained with different graphene derivatives, by dividing the peak intensity of the parent ion by the total mass peak intensities of the fragment and parent ions, and by summing the absolute intensities of the fragment and parent ions, respectively. According to our results we found that CdTe-GO gave the best results with a survival yield of 80% whereas GO-Cu giving the worst results as shown in Figure 3-12 and Figure 3-13.

Analysis of Proteins Using CdTe-GO

Motivated by the high survival yield of CdTe-GO heterostructures we next sought to apply this for the analysis of proteins. While we used cocaine and adenosine as the model compounds to demonstrate the aptamer based affinity mass spectrometry aptamer targeting proteins are becoming more available and finding a new platform to analyze proteins in the dual format (capture and ionization on the same substrate) will be highly innovative will be very useful for not only metabolomics applications but also proteomics. The results are shown in Figure 3-14 to 3-16. As can easily be seen from these data that CdTe incorporation into GO significantly improves the ionization efficiency of GO. CdTe is an important example of quantum dot (QDs). These materials are nanometer-sized crystals made of metallic or mostly of semiconductor materials. QDs have found widespread use in the bioimaging field as highly bright fluorescent materials. Their applications in disease diagnostics, proteomics, genomics, drug delivery, and even drug candidates screening are increasing to a great extent.(*97*) Very recently QDs were proposed as matrices for laser desorption ionization experiments. (*98*) In a similar study to our work HgTe was used to detect high molecular weight protein complexes. (*99*) So our results are very consistent with the literature. However mechanistic studies of the ionization process were not performed in the context of this dissertation so it is yet to be determined.

Our results show that GO, when combined with aptamer-based affinity capture provides an efficient platform for selective enrichment of target analytes and getting direct mass spectrometric readout even from very complex media with improved signal to noise ratios. Since a huge repertoire of aptamers exist for different targets including proteins, metabolites, and cell surface markers, we believe that the above introduced

methodology may also enable multiplexing when screening different biological samples. We also investigated the structural factors of alternating by synthesizing different GO hybrids on the LDI-MS efficiency of small molecules. Based on the results, we found that by changing the metal identity rather than GO it is possible to obtain more effective substrates which can then be used for aptamer immobilization and for better performance in protein analysis. The present study is meaningful and serves as an important basis for the development of efficient LDI-MS analysis platform by using graphene. Future studies will include development LDI-MS platforms based on graphene optimized for specific samples, for example, oligosaccharides, hydrophobic molecules, and phosphopeptides and also for cell-SELEX derived aptamers to capture their targets from cellular samples. Investigation of the ionization mechanism on GO based substrates is another exciting area which might open-up new venues and provide some guideline for developing rationally designed nanostructure based materials.

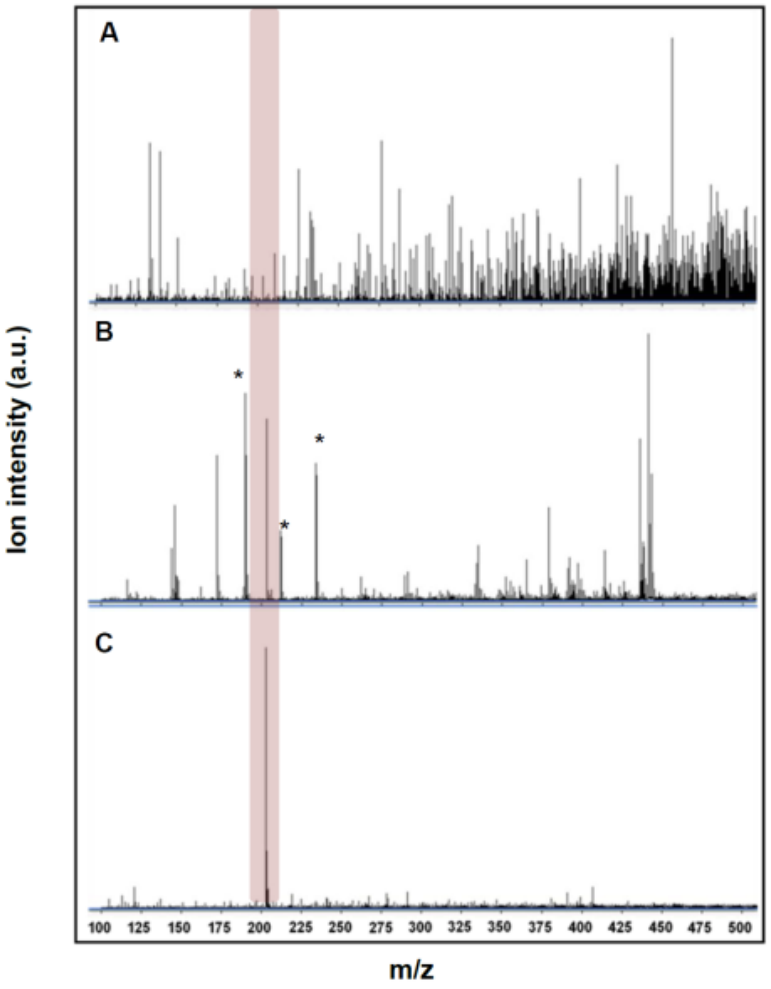

Figure 3-1. Analysis of glucose on GO A) No matrix B) HCCA matrix C) GO

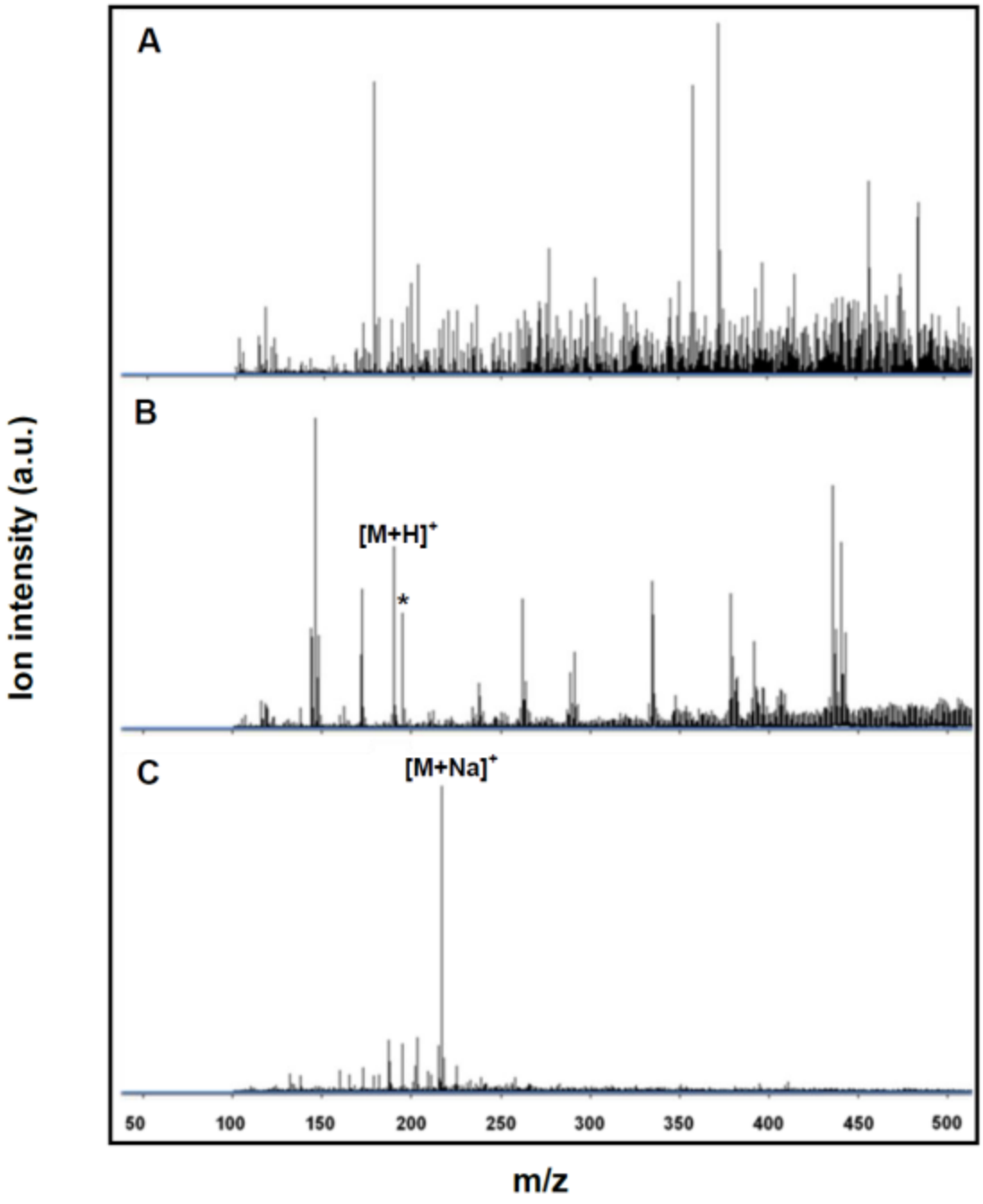

Figure 3-2. Analysis of caffeine on GO A) No matrix B) HCCA matrix C) GO

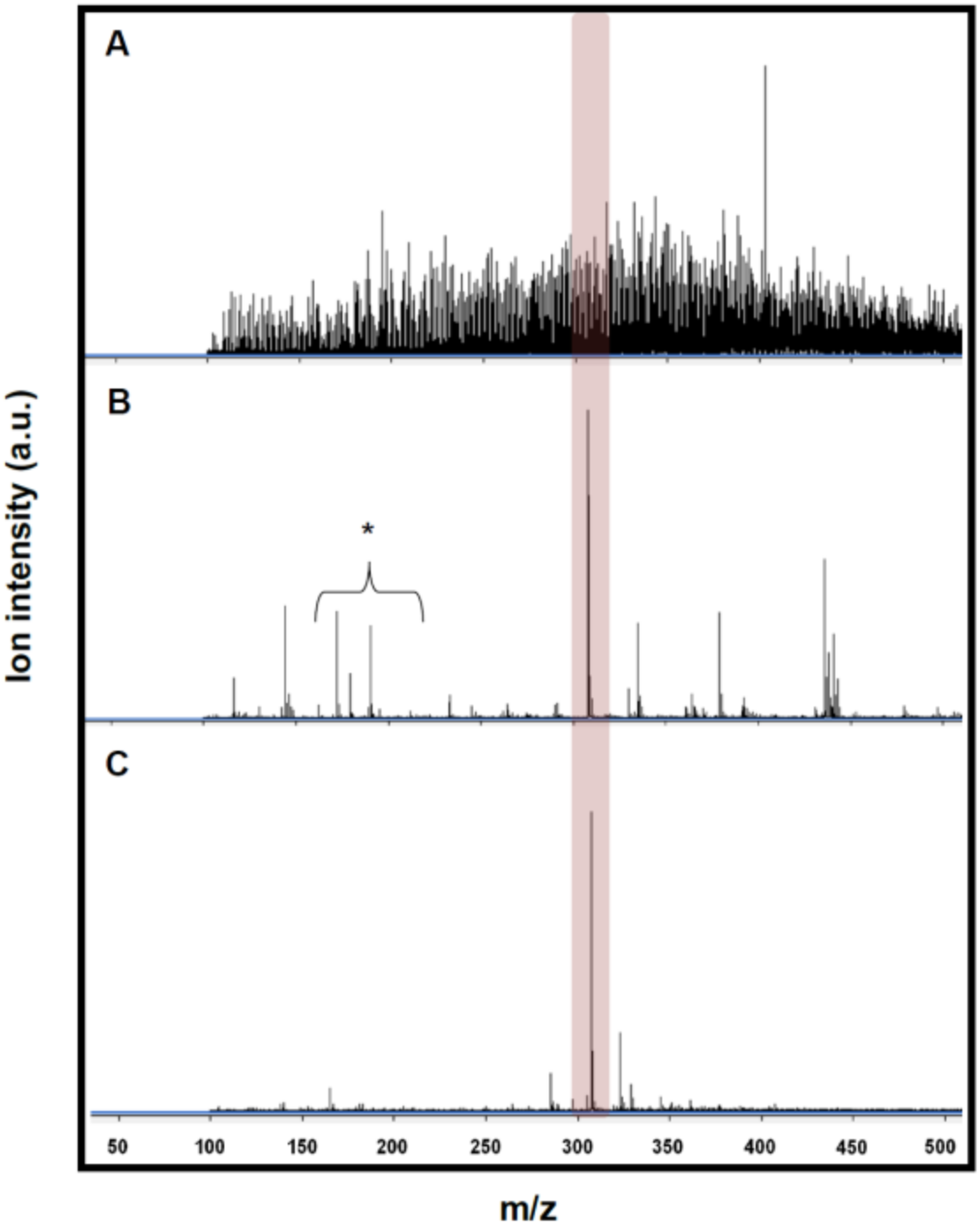

Figure 3-3. Analysis of glutathione on GO A) No matrix B) HCCA matrix C) GO

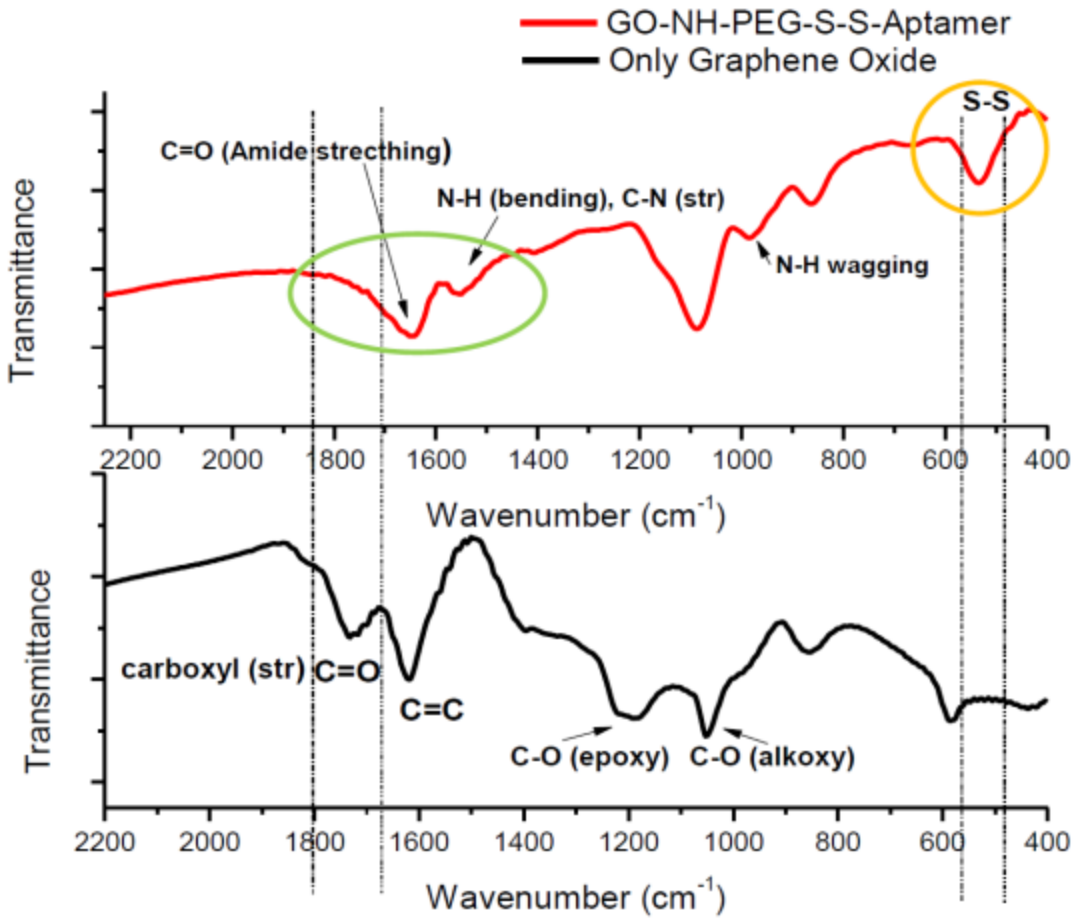

Figure 3-4. FTIR analysis of aptamer conjugated GO

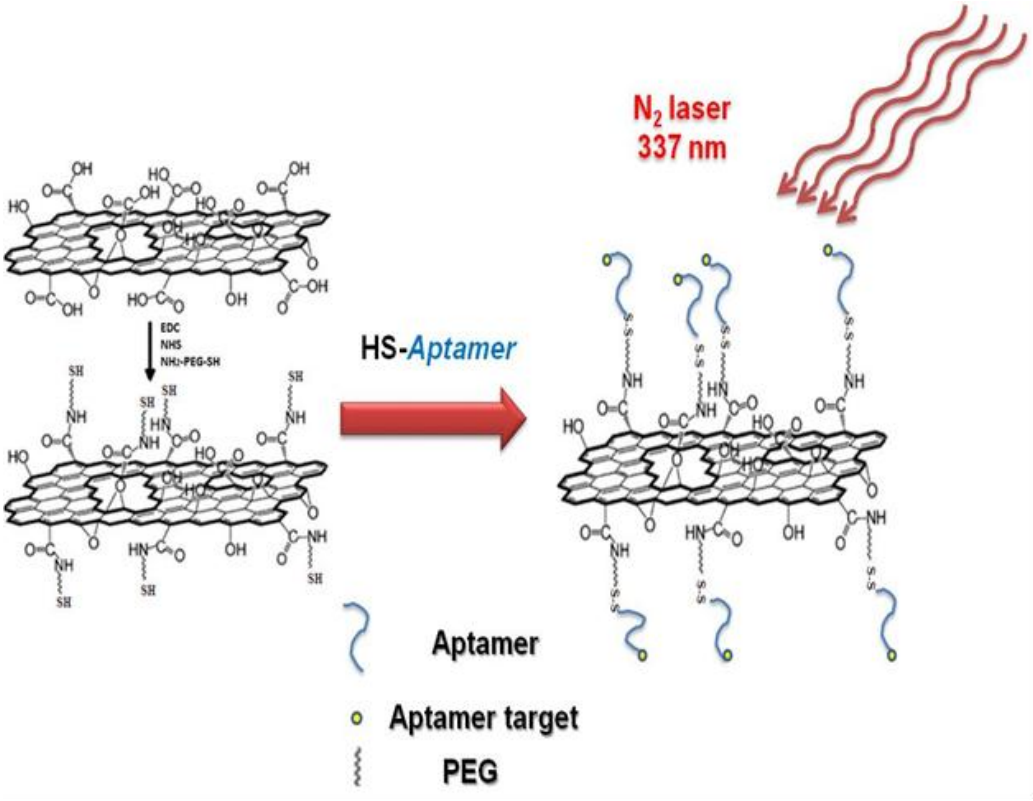

Figure 3-5. Schematics of aptamer assisted LDI on GO

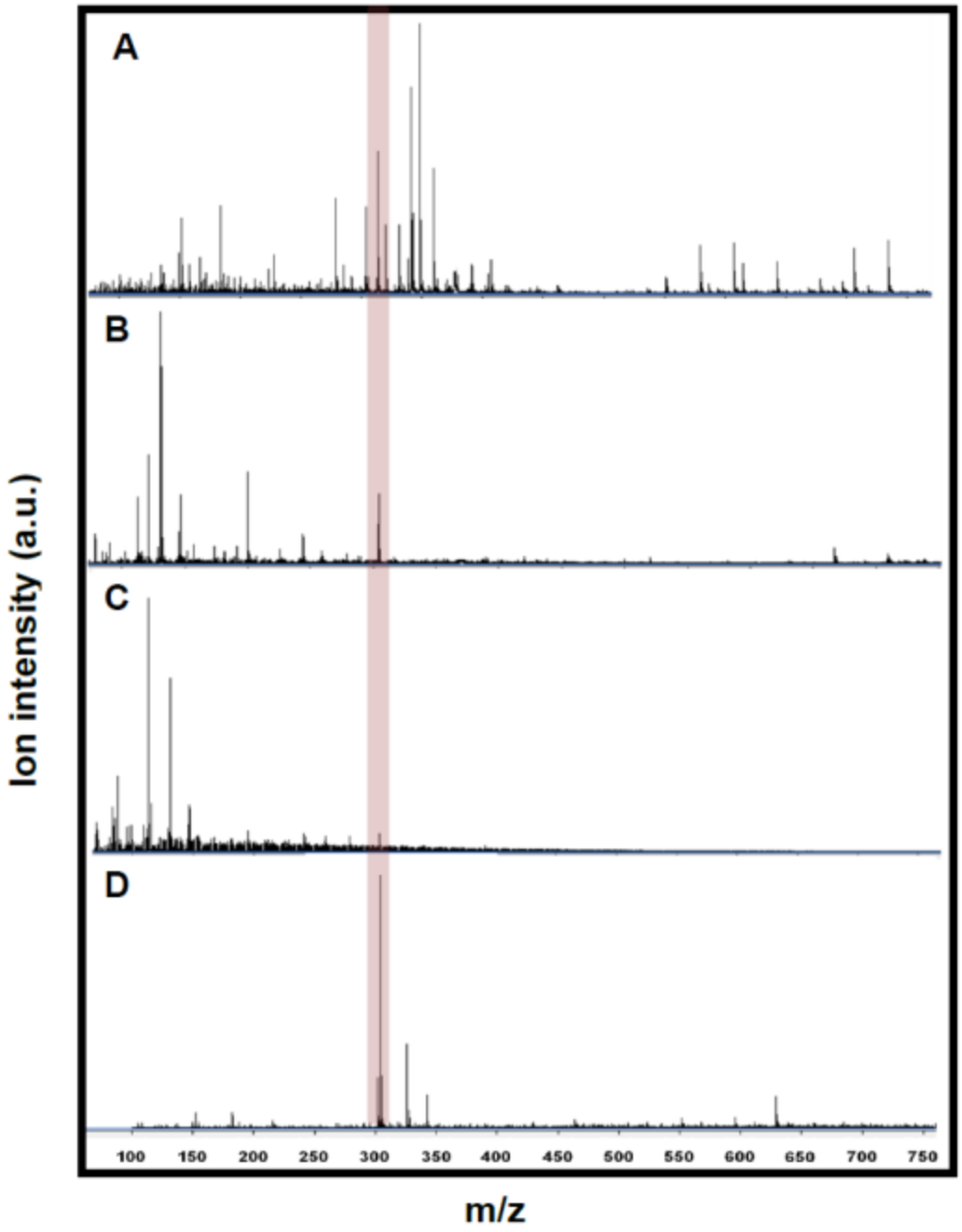

Figure 3-6. Analysis of aptamer assisted capture of cocaine on GO A)Plasma B) plasma enrichned by GO (no aptamer) C) Plasma analysis by physically adsorbed aptamer on GO) D) Plasma enriched by chemically modified aptamer on GO

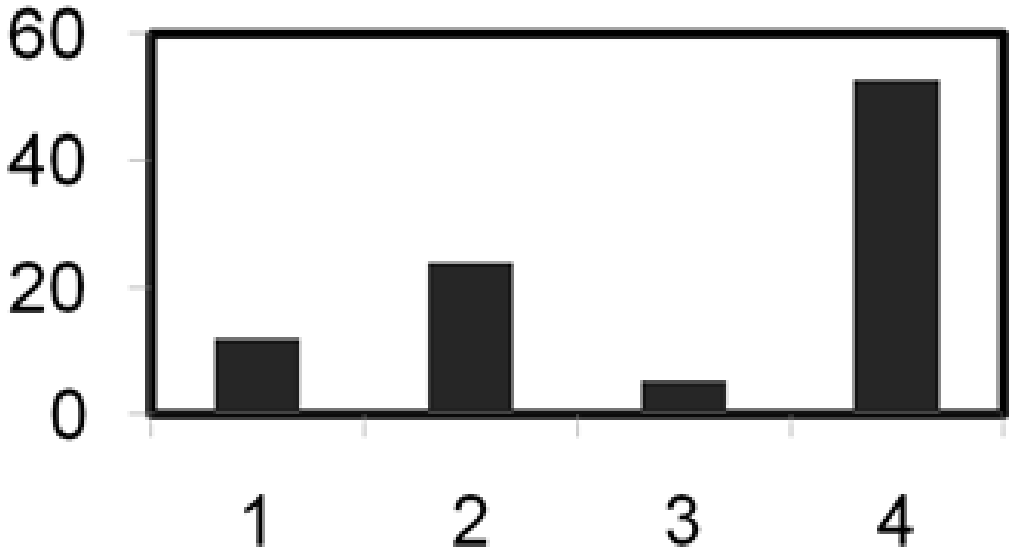

Figure 3-7. S/N ratios aptamer assisted capture of cocaine on GO (1) spiked into plasma (2) extracted with GO (3) extracted with noncovalently aptamer-modified GO and (4) extracted with covalently aptamer-modified GO.

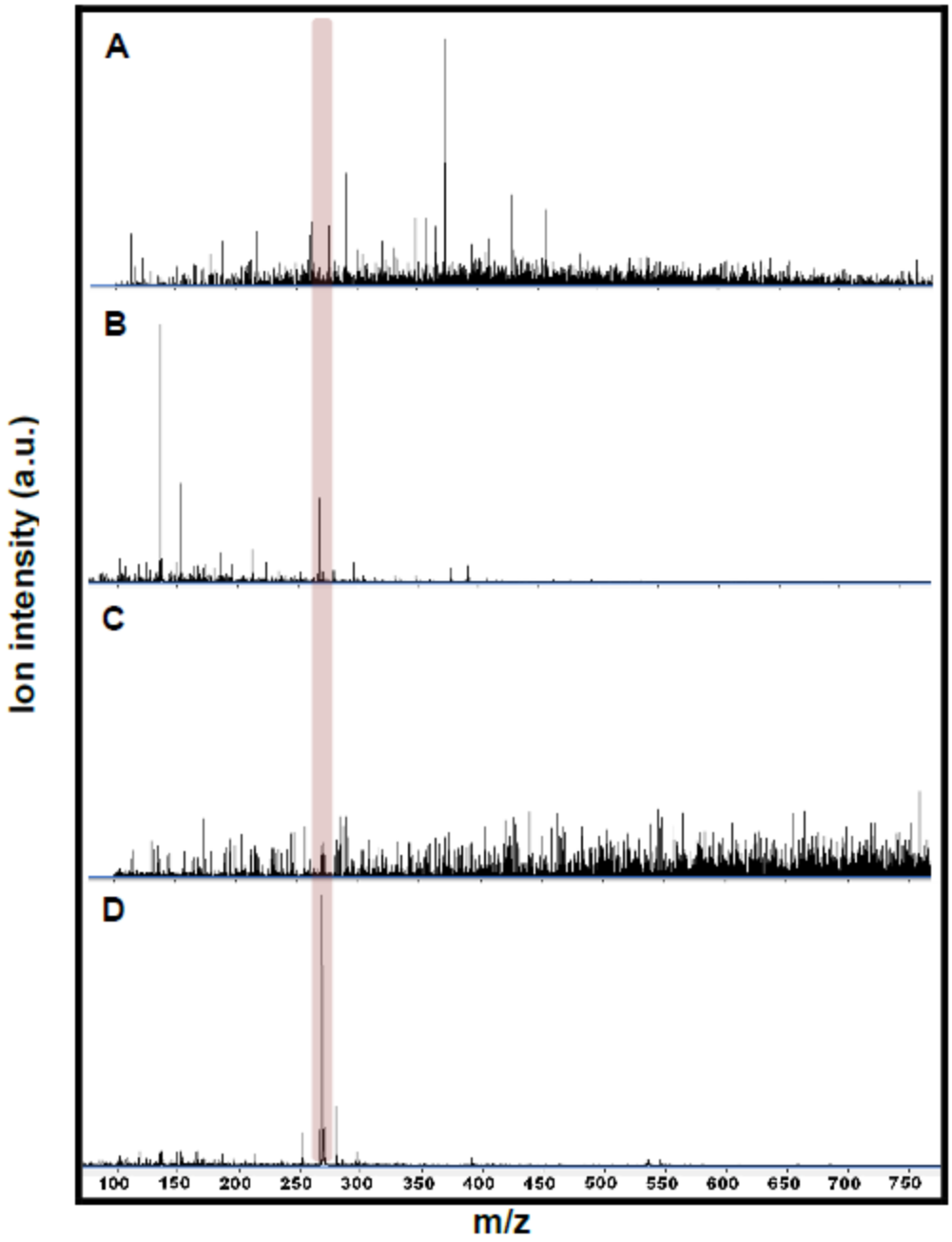

Figure 3-8. Analysis of aptamer assisted capture of adenosine on GO A) Plasma B) plasma enriched by GO (no aptamer) C) Plasma analysis by physically adsorbed aptamer on GO) D) Plasma enriched by chemically modified aptamer on GO

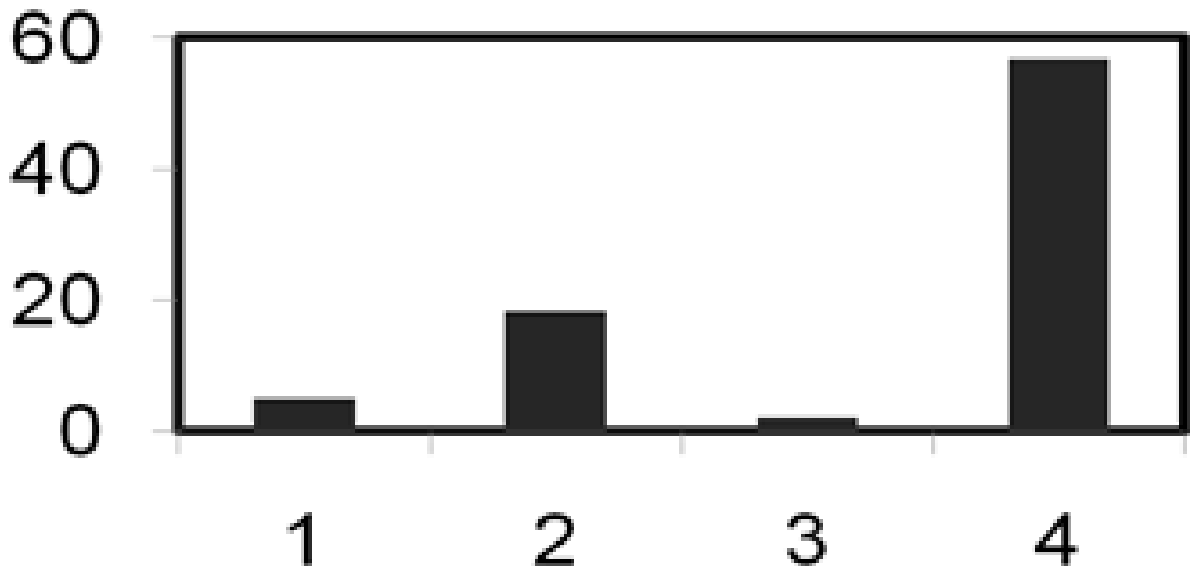

Figure 3-9. S/N ratios aptamer assisted capture of adenosine on GO 1) spiked into plasma, (2) extracted with GO, (3) extracted with noncovalently aptamer-modified GO, and (4) extracted with covalently aptamer-modified GO.

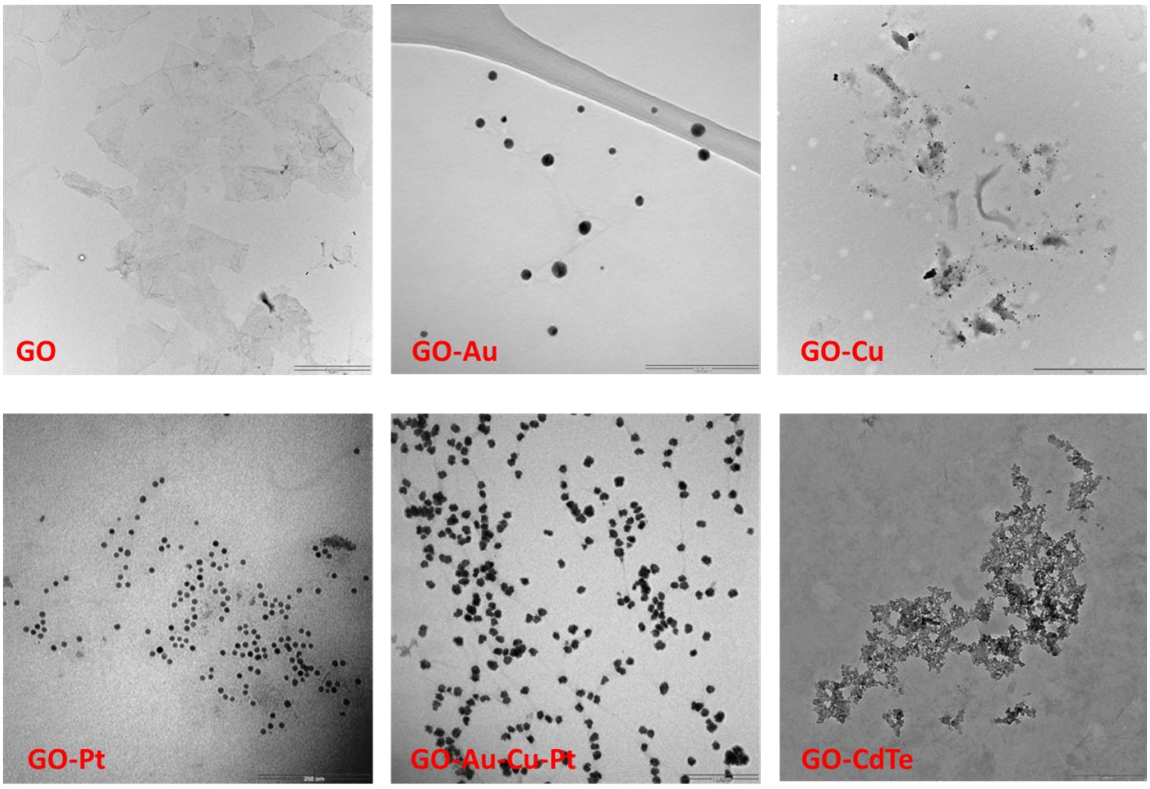

Figure 3-10. TEM images of (A) GO (B) Au-GO,(C) Cu-GO (D) Pt-GO E) Au-Cu-Pt-GO f) CdTe-GO

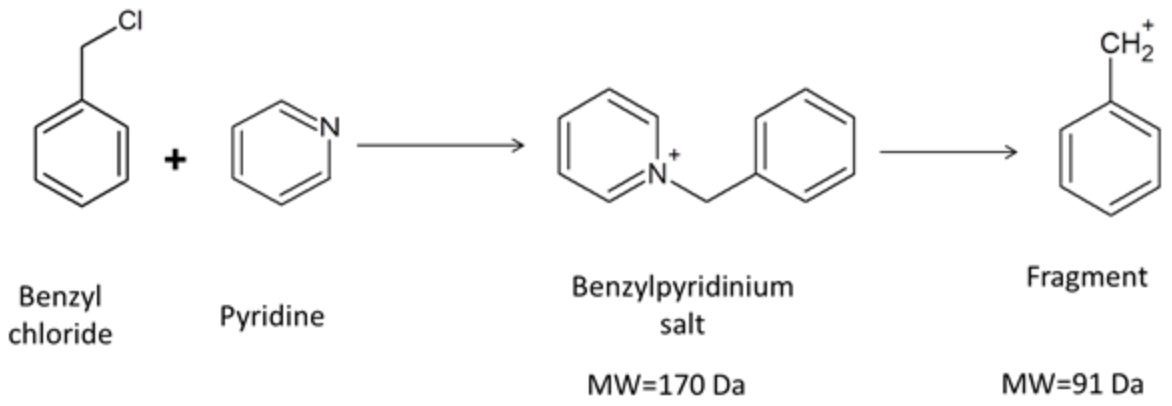

$$SURVIVAL\ YIELD = \frac{I(M)^+}{I(M)^+ + I(F)^+}$$

Figure 3-11. Fragmentation of BP ions

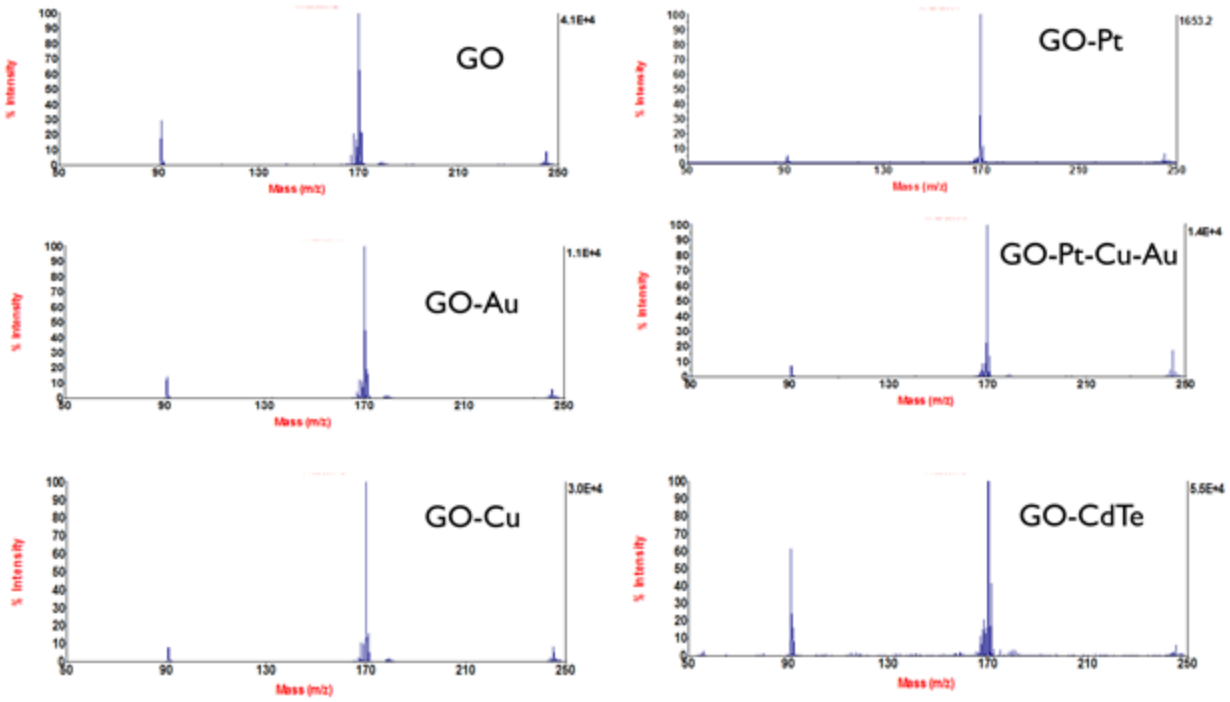

Figure 3-12. Fragmentation of BP ions on different GO derivatives

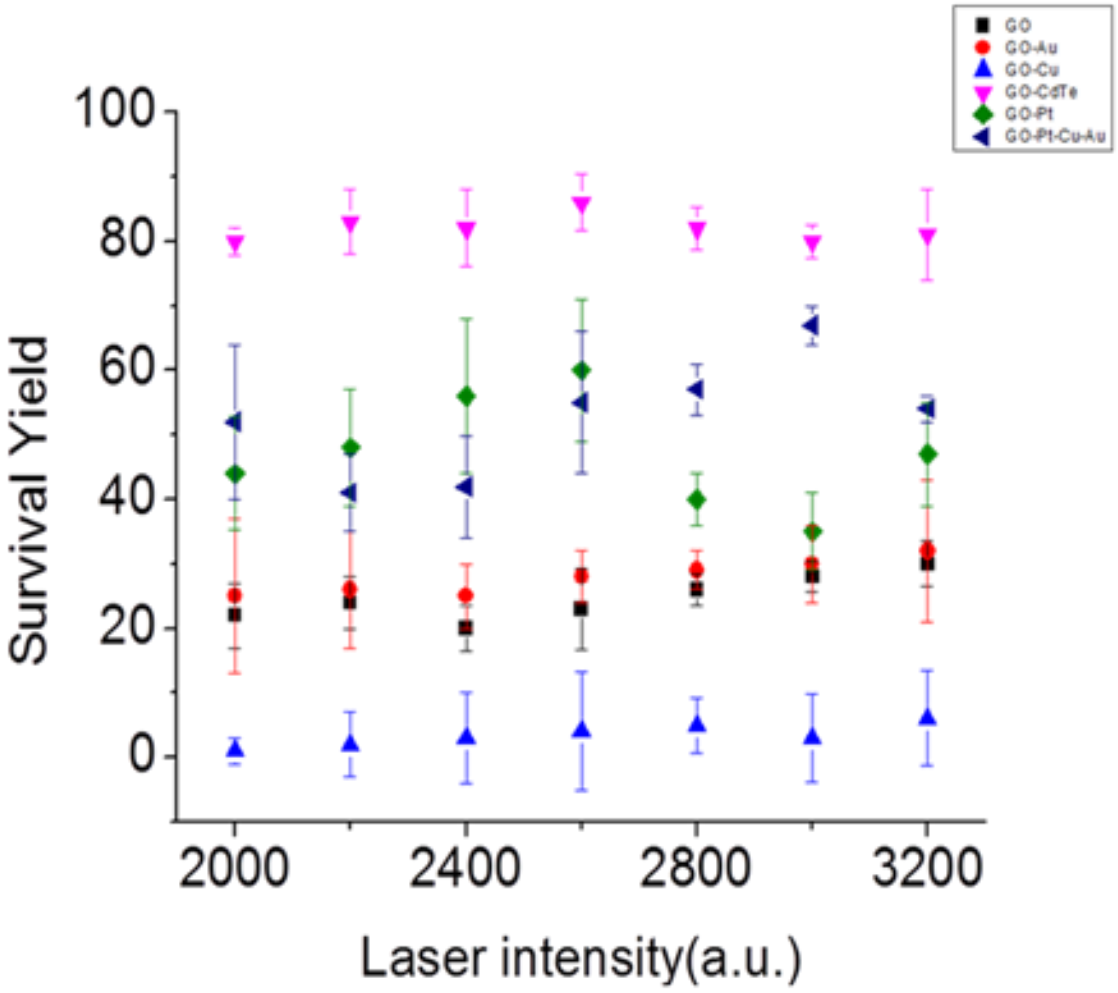

Figure 3-13. Survival yield calculations on GO derivatives

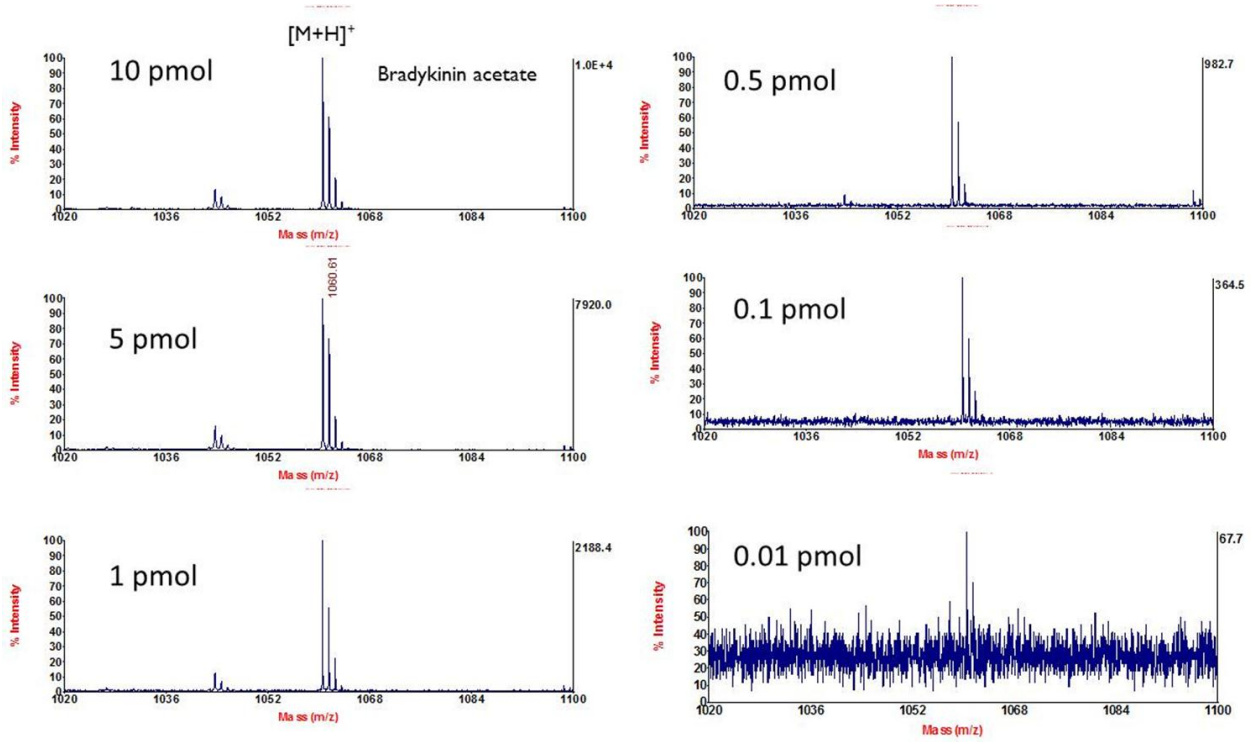

Figure 3-14. Analysis of bradykinin acetate on CdTe-GO

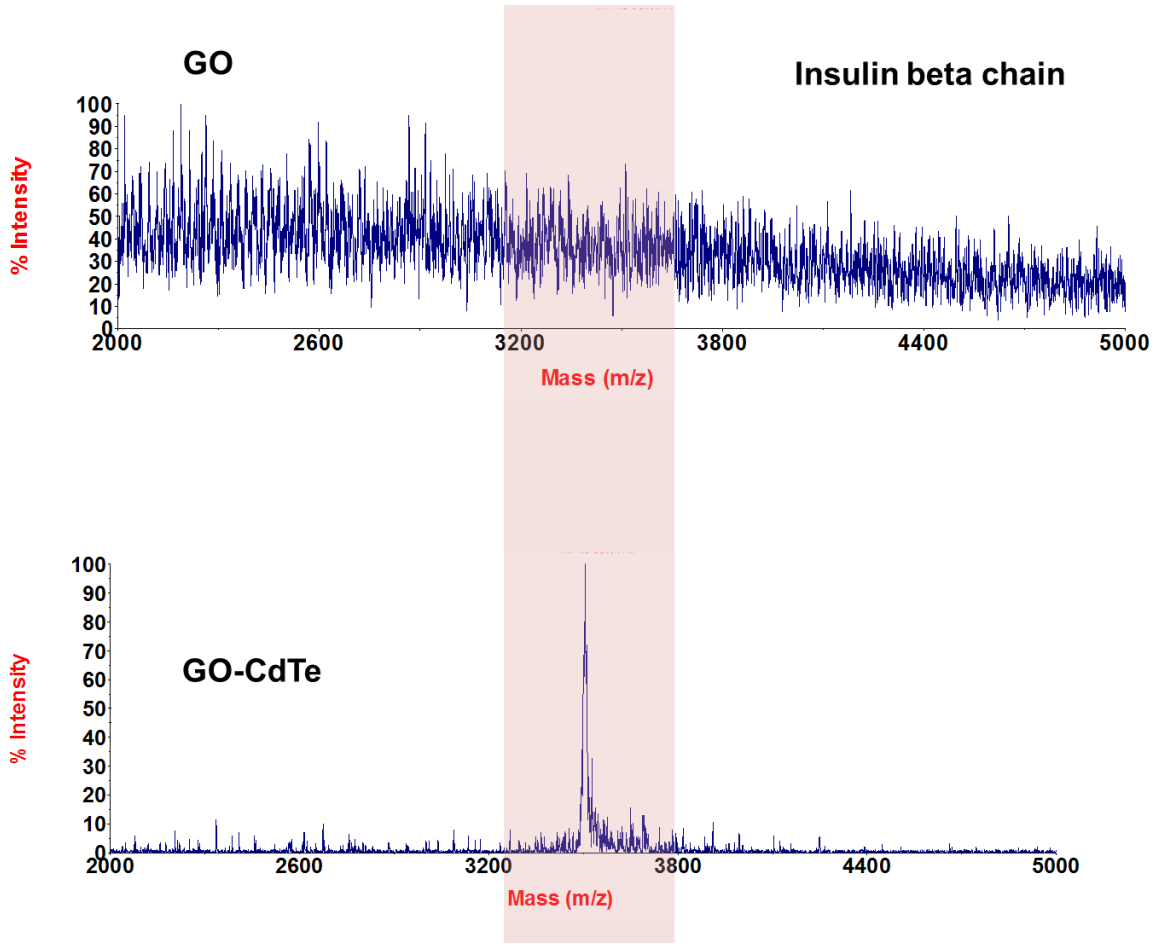

Figure 3-15. Analysis of insulin beta chain on GO (top) and CdTe-GO (bottom)

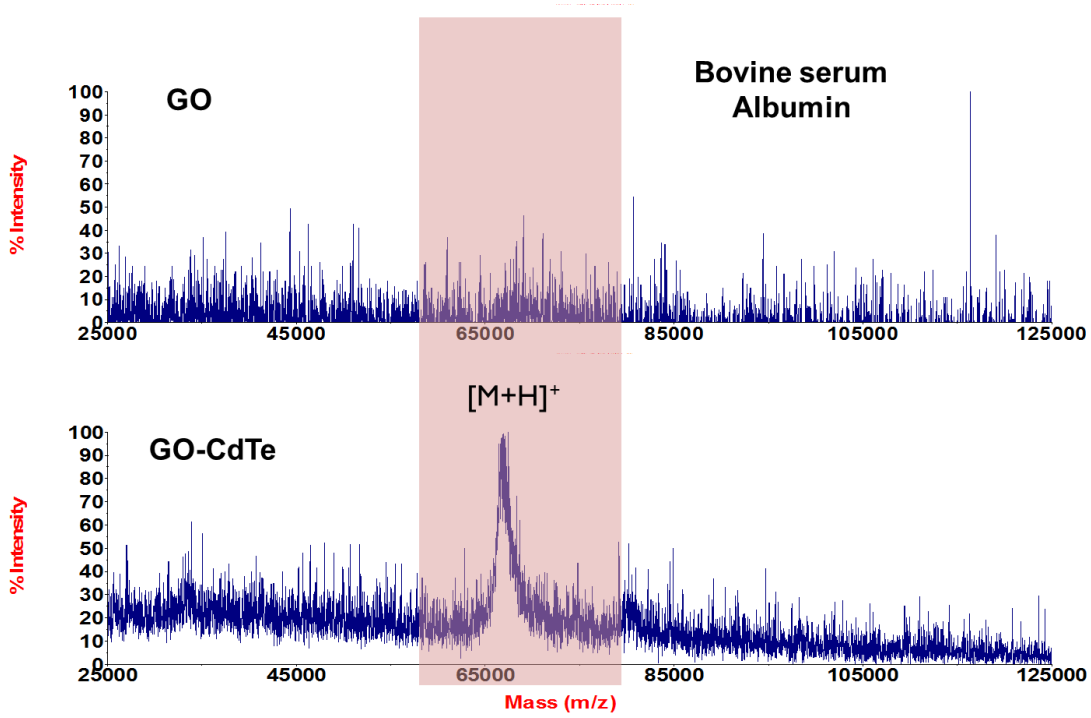

Figure 3-16. Analysis of bovine serum albumin on GO (top) and CdTe-GO (bottom)

CHAPTER 4
HYBRID NANOFLOWERS FOR MASS SPECTROMETRY

The analysis of biologically important small molecules and their subsequent detection in complex biological matrices is an area of growing interest. This challenging task has traditionally been achieved by optical spectroscopy or electrochemistry techniques such as fluorescence, surface plasmon resonance, voltammetry. For example a protocol was developed for label-free quantitative analysis of intracellular carotenoids in cells of red yeast (Phaffia rhodozyma), which makes use of the autofluorescence of these compounds.(*100*) In another study a protein-based nanosensor for was developed for the detection of maltose uptake by living yeast cells.(*101*) The nanosensor was expressed in yeast cells, allowing direct monitoring of changes in cytosolic maltose concentrations in response to the external supply of nutrient. Techniques based on electrochemical measurements were also studied extensively. They can be used as intra—or extracellular probes for label-free detection of metabolites present in the cell and those released to the extracellular microenvironment. However, only electroactive species can be analyzed, which makes the electrochemical methods applicable only to those compounds. Moreover oxidation potentials of coexisting species are generally very close to each other and differentiating their electrochemical response is often times very challenging. For example dopamine which is a very important neurotransmitter coexists with other species such as uric acid and ascorbic acid. The oxidation potentials of these molecules interfere with the each other and create a so-called “fouling effect” which results in overlapping voltammetric response, poor selectivity and reproducibility. (*102*) Optical techniques such as fluorescence and surface plasmon resonance generally require fluorescent tags and

surface immobilization which impede their broad applicability. Electrochemistry techniques as just noted are mostly limited to certain classes of compounds. Mass spectrometry methods have emerged as promising alternatives based on their high sensitivity, speed, reproducibility and label-free readout they offer. MS techniques have also been shown to be capable of detecting biologically important molecules even in single cells. (*103*) On the other hand signal suppression effects and need for very careful sample preparation still limit their overall use. Nanomaterials have been developed and applied as a tool for sample preparation. They have also been used as probes for ionization which allows interference free detection of small molecules especially for metabolomics applications. Various different nanomaterials such as gold, platinum, magnetic nanoparticles and carbon based materials such as graphite, carbon nanotubes and graphene have been tested in this context. This has opened up a relatively new area called “nanomaterial assisted laser desorption ionization”. As discussed in previous chapters because of the complexity of the processes associated to ionization, mechanistic understanding is still very poor. Therefore this recently emerging field requires new nanomaterials to improve their efficiency in MS and to better understand the ionization with nanostructures.

In this chapter two issues are addressed. First, different hybrid nanoparticles were systematically investigated to find an efficient nanoparticle based ionization substrate. Second an aptamer-based affinity mass spectrometry method was developed to extract important biomolecules in very complex biological environments such as cancer cells.

Experimental Section

Chemicals

All chemical were used as received without further purification. Manganese (II) acetylacetonate, oleic acid, oleylamine and phenyl ether, 99%, were obtained from Sigma Aldrich. Gold (III) acetate,>99.9% was purchased from Alfa Aesar. Toluene, >99%, from Sigma-Aldrich and hexane were provided from Fisher. For the synthesis of dopamine-PEG-COOH, Succinic anhydride, N, N-Dicyclohexylcarbodiimide (DCC) and 3,4-Dihydroxyhydrocinnamic acid (3-(3,4-Dihydroxyphenyl)propionic acid were obtained from Alfa-Aesar. O, O′-Bis(2-aminopropyl) polypropylene glycol-block-polyethylene glycol-block-polypropylene glycol, 2,3,4,5,6-Pentafluorophenol (Pentafluorophenol, PFP) and 1,4 Dioxane (Diethylene oxide, Dioxane) were purchased from Sigma-Aldrich.

Synthesis of Hybrid Nanoparticles

Au@MnO nanoflowers

Au@MnO nanoparticles were synthesized following the protocol given elsewhere (*104*) with minor modifications. Briefly, all reactions were completed in standard Schlenk line techniques. The solution of 10 mL of phenylether with 1 mL of oleic acid and 2 mL of oleylamine were injected into 100 mL of three necked flaks containing 1 mM of manganese (II) acetylacetonate and 0.05 mM of gold (III) acetate. The resulting mixture was reflux for 60 min under vigorous stirring. After refluxing, it was allowed to cool down to room temperature. The mixture was precipitated by addition of ethanol and collected by centrifugation. The precipitated product was re-dispersed in toluene.

Au@Fe_3O_4 nanoflowers

Au@Fe_3O_4 nanoparticles were synthesized by following Xie et. al, with minor modification. The solution containing 15 mL of octadecene and 1 mL of oleic acid was

heated at 120^0C for 20 min under argon flow. Sequentially, 0.3mL of Fe $(CO)_5$ and 5 mL of pre-synthesized 8 nm Au NPs in hexane were injected. The temperature was raised up to 220^0C for 15 min and refluxed for 20 min. After refluxing, the mixture was cooled room temperature and washed with 2-propanol three times by centrifugation. The final product was dispersed in hexane.

Au-Fe_3O_4 dimer

Au@Fe_3O_4 nanoparticles were synthesized by following(*105*), with minor modification. The solution containing 15 mL of octadecene, 1 mL of oleic acid and oleylamine was mixed with 1mL of pre synthesized 5 nm Au NPs, then was heated at 120^0C under argon flow. Under argon blanket, 0.1 mL of Fe $(CO)_5$ was injected. Thereafter, the solution was refluxed for 30 min before it was cooled room temperature. The nanoparticles were washed with 2-propanol three times by centrifugation. The final product was dispersed in hexane.

Fe_3O_4@Au core-shell

Fe_3O_4@Au nanoparticles were synthesized using the following protocol. The solution containing 0. 2075 g of gold acetate, 0,775 g of 1, 2 –hexadecanediol, 0.125 mL of oleic acid, 0.75 mL of oleylamine and 8 mL of phenyl ether was mixed with 2.5 mL of phenyl ether reaction solution of Fe_3O_4 NPs. Then resultant mixture was heated up 190^0C and kept at this temperature for 2 hr. After 2hr, it was allowed to cool down to room temperature. The mixture was precipitated by addition of ethanol and collected by centrifuging. The precipitated product was re-dispersed in toluene.

Transfer of Au@MnO FNPs into Aqueous Phase

10 mg of Au@MnO flower nanoparticles were dissolved in 5 mL of tetrahydrofuran anhydrous (THF) and flashed with argon for 15 mins. After degassing, the solution

transferred to a dropping funnel. After 150 mg of heterobiofunctional dopamine-terminated PEG was dissolved in 20 mL of THF anhydrous in 100 mL of three necks flask, nanoparticle solution in dropping funnel was added into PEG ligand solution in a dropwise manner. The resultant mixture was stirred under argon blanket at 500°C for overnight. The NP-PEG ligand conjugation was terminated via addition of ~ 3mL of hexane and collected by centrifugation at 10000 rpm for 20 min. The supernatant was discarded and the product, NPs, at bottom of centrifuge tube was washed with ethanol and centrifuged twice to remove excess and unreacted of PEG ligands. Finally, NP precipitate was dispersed in ultrapure water or PBS buffer for aptamer conjugation.

Characterization

One drop of nanoparticles dispersed in hexane was deposited on carbon-coated copper grids and it was allowed to dry for at least two hours. Transmission electron microscopy (TEM) on a Hitachi H-7000 transmission electron microscope with a working voltage of 100 kV was used to obtain images of nanoparticles. The high-resolution TEM (HRTEM) instrument coupled with spatially resolved energy dispersive X-ray spectroscopy (EDX) was also used for magnified images and further characterization of nanoflowers. The 1800 UV-Vis spectrophotometer (Shimadzu Scientific Instruments, Columbia, MD) was used to show the absorption spectrum of nanoflowers and to determine the concentration of DNA-aptamers. Fluorescence measurements were carried out on a Fluoromax-4 (Horoba Jobin-Yvon, Edison, NJ, USA) was also used for validation of dye-labeled aptamer-nanoflower conjugation. An an Olympus FV 500-IX81 confocal microscope (Olympus, Center Valley, PA, USA) having a 40-oil-dispersion objective was used to image cancer cells incubated with nanoparticles. The demonstration of binding of functionalized nanoparticles to targeting cells was carried

out with a FACScan cytometer (Becton Dickinson Immunocytometry Systems, San Jose, CA, USA).

Synthesis of Aptamers

An ABI 3400 DNA/RNA synthesizer (Applied Biosystems, Foster City, CA) was operated for the synthesis of all aptamer sequences (sgc8: 5`-NH2-ATC TAA CTG CTG CGC CGC CGG GAA AAT ACT GTA CGG TTA GA FITC-3` and ATP aptamer: 5'-SH ACC TGG GGG AGT ATT GCG GAG GAA GGT TMR-3') at the 1 µmol scale. Deprotection was performed in AMA (ammonium hydroxide/ 40% aqueous methylamine 1:1) at 65 °C for 30 min, and deprotected sequences were purified by reversed-phase HPLC (ProStar, Varian, Walnut Creek, CA) with a C_{18} column (Econosil, 5 µm, 250-4.6 mm) from Alltech (Deerfield, IL). Immediately after HPLC purification, purified DNA solution was dried in acid-resistant centriVap centrifugal vacuum concentrators (Labconco, Kansas City, MO). The dried DNA was dissolved in 50 µL DNA grade water, and the concentration of each sequence was determined based on absorbance value at nm using an 1800 UV-Vis spectrophotometer (Shimadzu Scientific Instruments, Columbia, MD).

Functionalization of Au@MnO FNPs

Transferring of Au@MnO FNPs from toluene or hexane to ultrapure water or PBS buffer was completed using dopamine-terminated of heterobicofunctional ligand, dopamine-PEG-carboxylic acid. The OH groups on the dopamine-side of PEG ligand preferentially bind to surface of MnO domain of FNPs, and the other side, carboxyl group contributes water-solubility of FNPs and is free to react with biofunctional groups, aptamers in the presence of 1-ethyl-3-(3-dimethylaminopropyl) carbodiimide), EDC and N-hydroxysulfosuccinimide (Sulfo-NHS). Conventional protein labeling chemistry was

utilized to attach two different aptamers, sgc8 and ATP, to the surface of two different domains, MnO and Au, of FNPs. 30µL of 0.1 M EDC was added to 1.5 mg/mL concentration of 150 µL of FNPs in 10 Mm PBS buffer to activate carboxyl group on PEG ligand for 20 min while gently shaking. After that, 13.1 µL of 228 µM sgc8 aptamer and 30 µL of 0.12 M NHS in 10 Mm PBS buffer were added and incubated 1 h while gently shaking to functionalize the MnO domain of FNPs. After 1 h incubation, to resultant mixture, 7.45 µL of 300 µM ATP aptamer and 77 µL of 10 mM PBS buffer were added and the mixture was placed on shaker for overnight incubation at room temperature to functionalize Au domain of FNPs. After immobilization of the aptamers onto FNPs, the resultant mixture was washed three times with PBS buffer and finally redispersed in 300 µL of PBS buffer.

Cell Culture

CCRF-CEM cells (CCL-119 T-cell, human acute lym- phoblastic leukemia) were obtained from ATCC (American Type Culture Collection). RPMI medium supplemented with 10% fetal bovine serum (FBS) and 100 IU/mL penicillin-streptomycin was used to culture the cells in. A hemocytometer provided the cell density before experiment performed. After suspending two million cells in RPMI cell media buffer, the mixture was centrifuged at 970 rpm for 5 min and redispersed them in [4.5 g/L glucose and 5 mM $MgCl_2$ in Dulbecco's PBS with calcium chloride and magnesium chloride for incubation. During the experiments, the cells were stored in an in incubator at 37°C.

Mass Spectrometry

All mass spectra were acquired using a MALDI-TOF/TOF mass spectrometer (ABI/SCIEX 5800, Applied Biosystems, Foster City, CA). A Nd:YAG laser at 355 nm was used. The spectra were recorded in reflection mode in either positive or negative

mode using an accelerating voltage of 20 kV, a 66% grid voltage, and a 50−200 ns delay extraction. Typically, 10−60 laser shots were collected per spectrum. Applied Biosystems Calibration Mixture 1 was used to calibrate the mass spectrometer. Data analysis and was performed using Date Explorer software.

Results and Discussion

Survival Yield Calculation on Hybrid Nanoparticles

In the first set of experiments Fe_3O_4 NPs, Fe_3O_4 -Au core shell NPs, Fe_3O_4 -Au dimer NPs, Fe_3O_4-Au flower NPs and MnO-Au flower NPs were studied as probes for ionization. The TEM images of these particles are given Figure 4-1. The primary motivation in choosing metal oxide-gold particles was the following; first both metal oxides and gold have been reported to be efficient materials for nanoparticle based laser desorption ionization, second they have relatively easy synthesis procedures and are easily amenable to bioconjugation, finally hybrid nanoparticles made up of metal oxides and gold have not been previously been studied as a substrate for LDI-MS. Driven by this primary motivation, thermometer ions used were used to determine the best hybrid nanoparticle. As extensively discussed in the previous chapter, benzylpyridium ions are ideal molecules to calculate the internal energy deposition and calculation of survival yield in the laser desorption ionization event. Therefore, the mass spectrometry data derived from BP ions therefore serves as a quantitative bench mark to assess the efficiency of different nanostructures and compare them in terms of laser desorption ionization. The results of BP fragmentation experiments are shown in Figure 4-2. As can easily be seen from this figure, survival yields of the studied nanoparticles greatly differ from each other. There was an increasing trend in SY when the particle geometry changes from core-shell to dimer and then to nanoflower. This was an

interesting observation and led us to think us about the reasoning. The first experiment was to compare the UV spectra of the each NP. As can be seen in Figure 4-3 no clear difference exists in UV range of 200-400 nm which rules out the possibility of different UV absorption that might lead to this observation. Even though many studies have been published about nanostructure based MS, no previous data exist in the literature on similar hybrid particles. On the other hand iron oxide-gold particles were previously studied as probes for surface-enhanced raman spectroscopy(SERS).(*106*) It is evident that bare iron oxide NPs does not have any intrinsic plasmonic property which can lead to enhancement in Raman signals. However, when gold is introduced to the system it creates a multiple hot spots where nanogaps can be formed between gold particles which might lead to improved signals. The reason why the SYs improved going from core –shell to nanoflowers can also be understood in the light of this enhancement effect where a large number of hot spots can be formed in flower shaped particles which may not be very operative in the case of core shell structures. Moreover, a great majority of the particles used for MS applications are also useful for SERS applications which might suggest that similar mechanisms govern the nanostructure-based ionization and surface enhancement in Raman spectroscopy. The second plausible reason is that nanoflower shaped structures can accommodate more analytes than that of others owing to a higher surface area. This leads to higher sensitivity and eventually improved ionization. A similar phenomenon was observed previously in the case of carbon nanotube/graphene conjugate materials where CNTs significantly improved the ionization capabilities of graphene in a synergistic manner.(*107*) However, when the petals around the gold core are changed from iron oxide to manganese oxide that is

Au@MnO FNPs is compared to Fe_3O_4@Au FNPs, the former one is superior to the latter one as can be seen from the SY data depicted in Figure 4-2.

Testing Au@MnO FNPs as a Substrate for Ionization

After selecting Au@MnO FNPs as a material for ionization we analyzed a series of different small molecules to show the utility of this particle as an efficient substrate for ionization. The mass spectra are seen in Figures 4-3 to 4-6. When the spectra are analyzed it can easily be seen that most of the analytes are seen as sodium or potassium adducts. As explained in the experimental part, several salts and surfactants were used during synthesis procedure of Au@MnO FNPs. Therefore even after extensive washing steps prior to MS analysis, we were unable to eliminate salt effects. However, we have to note here that even though cationization occurred, no significant background interference was observed and the mass spectra were relatively very clean with very minor background ions. This is especially important for metabolomics applications as most of the important metabolites lie in the m/z range of 50-1000. While MALDI-MS has proven to be a very successful method for proteomics oriented applications, its use has mostly been limited to small molecule analysis. Therefore nanoparticles are the best option for this purpose. We were able to analyze important cellular metabolites such as dopamine, serotonin, melatonin, cholesterol very effectively. A comparison between MALDI-MS and LDI on Au@MnO FNPs is given in Figure 4-7 and significant background ions exist in the MALDI spectra. In the next set of experiments we tested Au@MnO FNPs in the negative ionization mode and and analyzed n-lauryl sarcosine, glutathione and melatonin as the model compounds. As can be seen in Figure 4-8 and 4-9, cation adducts which was observed in the positive ion mode were eliminated and $[M-H]^-$ ions were observed. This suggests that

significant reduction of salt effects can be achieved in the negative ion mode. This is important in the analysis of peptides, fatty acids as well as nucleosides and nucleotides in negative ion mode.

Modification of Au@MnO FNPs with Aptamers

In our experiments we used Au@MnO FNPs with various aptamer modifications. As can be seen in Figure 4-10, Au@MnO FNPs is composed of a gold core surrounded by MnO petals. Therefore both of these domains can be easily modified with different ligands. We have selected acute myeloid leukemia cells (CCRF-CEM) as our model. Our group has previously selected an aptamer for this cell line called sgc8. This aptamer with a K_d value of picomolar, has been a gold standard for many aptamer based cancer cell assays. Our group and others has extensively studied this aptamer for various different applications. Moreover cancer cells in particular leukemia cells are known to be energically more demanding therefore showing more ATP expression. Our ultimate goal was to show that Au@MnO FNPs can be selectively internalized into CCRF-CEM cells, ATP within the cells can be captured and finally ATP can be analyzed by using aptamer modified Au@MnO FNPs as the ionization matrix after cell lysis and washing. So to realize this goal we have modified the Au@MnO FNPs in different ways. In the first modification MnO petals were decorated with FITC labeled sgc8 aptamer and gold core was decorated with TMR labeled ATP aptamer to enable fast cellular uptake and efficient ATP capture in the cell. MnO petals were modified with FITC labeled sgc8 aptamer and gold core was modified with a TMR labeled random aptamer and in the last control we have modified gold domain was not modified with ATP aptames.

We confirmed that FITC labeled-sgc8 aptamer and TMR labeled ATP aptamer were successfully bound to surface of MnO and Au domain of FNPs. These can be

clearly seen in the fluorescence spectra shown in Figure 4-11. It is clearly seen that fluorescence intensity of FITC-labeled aptamers attached onto surface of MnO petals is enhanced with increase of amount of FNPs. When we increase the amount of FNPs, fluorescence intensity is enhanced as more MnO nanoparticles hold a larger number of FITC labeled-scg8. TMR labeled ATP aptamer immobilized on Au nanoparticles of FNPs also exhibits higher fluorescence intensity with increase of amount of FNPs. There was no significant quenching effect generated from the surface of gold to influence fluorescence emission properties of TMR. These two fluorescence spectra proved that modification of two different aptamers onto FNPs were efficiently carried out without seeing a significant interference between the two aptamers.

Internalization of Aptamer Modified Au@MnO FNPs

The internalization and binding of aptamer modified Au@MnO FNPs were performed by following the established procedure in our lab at 37°C and 4°C respectively. Briefly, 4 x10^6 cells were prepared and placed in separate tubes. (2 x10^6 to each),100 µL of 20 ng, 200 ng and 800 ng aptamer conjugated FNPs were added to cell samples and the mixtures were incubated in incubator at 37°C for 2 h for internalization and at 4 °C (on ice) for 30 min for surface binding. The mixtures of cell-particle were centrifuged, washed three times and re-dispersed in 0.5 mL of binding buffer, after incubation. The binding of each sample incubated at 37°C and 4°C was monitored by using flow cytometry counting 10.000 events. (*108*) After incubation of two different benches of FITC-sgc8 aptamer-FNPs conjugates at 37°C for 2h and 40°C for 30 min, internalization of FNPs into cancer cells (CCRF-CEM) and binding of FNPs on surface of cancer cells were monitored by flow cytometry. The results are shown in Figure 4-12. As can be seen in Figure 4-12(a) there was a significant change in the fluorescence

signal observed between lowest (20 ng/mL) and highest (800 ng/mL) amount of FNPs used for cell uptake study. The internalized FITC-labeled sgc8-FNPs into CEM cells at 37°C do not show a strong fluorescence signal compared to incubation of CEM cells with FITC-labeled sgc8-FNPs of carried out at 4°C. When the FITC-labeled sgc8-FNPs were uptaken by CCRF-CEM cells, fluorescence emission intensity of FITC was weakened because of aggregation of particles and intrinsic auto-fluorescence generation from the cells. The same experiments were also performed at 4 °C and flow cytometry data shows that of FITC labeled sgc8 aptamer-FNPs bind to cell surface instead of internalization.(*109*) These results were also confirmed by using confocal microscopy and as can be seen in Figure 4-13 high florescence signals can be observed upon particle internalization.

Extraction of ATP from Cancer Cells Using Aptamer Conjugated Au@MnO FNPs

Motivated by our success in using Au@MnO FNPs for LDI-MS and functionalization of the particle surface with aptamers we then wanted to use this material to extract a very important cellular metabolite, ATP, from cancer cells. ATP is an important molecule for cellular metabolism which works as an intermediate in cellular processes. Many cellular reactions depend on ATP hydrolysis. In cell signaling, for example, the phosphate group is transferred from ATP to key regulatory proteins by protein kinases.(*110*) Apart from its biological importance, ATP was chosen for a couple of other reasons; first there is a very good aptamer available for ATP targeting, second ATP is one of the most abundant yet difficult metabolites to be analyze by MS and third molecular weight of ATP perfectly falls into the m/z range of where Au@MnO FNPs were very efficient. So for all these reasons it serves us as a very good model to demonstrate the aptamer-based affinity mass spectrometry concept in a very complex

biological system. As has been shown in many different applications, nanoparticles can be internalized into the cells by either receptor mediated endocytosis or a passive diffusion mechanism. (*111*) In the first mechanism, a ligand is tethered onto the surface of the nanoparticle and this moiety selectively interacts with one of the surface receptors. As a result of this interaction the particle is easily engulfed by the cell and is internalized. This has been the subject of very intense research and many different particle systems with various molecular recognition ligands have been developed. In the second mechanism, the particle is not decorated with a ligand and particle uptake is simply governed by diffusion, which is not selective. Moreover full uptake of particles takes a long time (>8 h) which is not desirable for analytical and biological applications. (*112*) Therefore our strategy is advantageous from all these respects.

In order to confirm our hypothesis that dual aptamer conjugated Au@MnO FNPs can easily be internalized and used for ATP capture we used it together with the respective controls by following the cell internalization protocols explained in great detail above. After particle internalization, the next step was to test different cell lysis conditions that will enable the most efficient detection of metabolites. Extraction of metabolites from cell lysates is an area of great interest especially in the growing area of metabolomics. (*113, 114*) In the past five years several methods were used with different conditions to release the metabolites from the biological mixtures. (*115*) While many protocols were suggested in the literature, success still depends on trial and error based optimization. Organic solvents such as cold acetone, methanol, and ethanol have been generally used for metabolite extraction. In our first attempts we used cold methanol for cell lysis and after 10 mins of treatment with cold methanol, the final cell

lysis was brought to room temperature and particles were centrifuged and removed from the cell lysate. After several cycles of washing, an aliquot of the particles were spotted onto the plate and analyzed. However in any of the particles we have been unable to observe a significant signal associated to ATP. The results are depicted in Figure 4-14 and the molecular weight region for ATP and its secondary metabolites ADP and AMP is highlighted for clarity. This might have been for a couple reasons. First, not enough particles were internalized, second ATP aptamers were not functional within the cells because of the cellular complexity or they are cleaved of by endonucleases .Third the cell lysis with organic solvents might distrupt the interaction of the aptamer with its target. The first two reasons are very unlikely because aptamers can be easily internalized and can recognize their targets even in the cells. Although there is a possibility that aptamers might be cleaved of by cellular endonucleases, recent studies showed that nanoparticles provide a strong barrier for such kind of unwanted enzymatic reactions.(*116*) Most notable example of this phenomenon has recently been demonstrated.(*117*) (*20*)The method developed to monitor mRNA activity called “”nanoflares” relies on immobilizing an oligonucleotide and a reporter complementary strand onto a gold nanoparticle surface which fluoresces upon target binding. It has been shown endonucleases cannot cleave off nanoparticle immobilized oligonucleotides. This has also been exemplified in a similar work called “aptamer nanoflares”. (*118*) The last and the most likely reason is the use of an organic solvent during the cell lysis and metabolite extraction. Aptamers are very stable molecules compared to antibodies against changes in pH, temperature, ionics strength but still their target recognition depends on their 3D conformation. We think that that cold

methanol treatment irreversibly disrupts the aptamer-target interaction and therefore target cannot be captured by the aptamer as a result no significant signal was observed.

In the next set of experiments we therefore replaced cold methanol with boiling water for metabolite extraction and cell lysis. While aptamers can be denatured with heat they can easily refold to their proper 3D conformation upon cooling. The main workhorse for oligonucleotide amplification, PCR, actually relies on thermal cycling and therefore oligonucleotides can survive even at 100° C. Moreover previous studies have shown that boiling water is a better solvent for extracting nucleotides from the cells. We repeated the same experiments using “hot water” as our metabolite extraction solvent. However, we were also challenged by the fast turnover rate of ATP molecule.(*8*) ATP is a very labile metabolite and can easily be converted to ADP and AMP upon losing its phosphate groups. The kinetics of the reaction is very fast and ATP binding aptamer can also capture ADP and AMP and as we can see in Figure 4-15 we were only able to detect ADP and AMP. To overcome this problem we have slightly modified the metabolite extraction step by incorporating another step using cold NH_4HCO_3 buffer and dipping the cells into liquid N_2 to quench the metabolism prior to metabolite extraction and cell lysis. This has previously been proven successful to quench metabolism. (*119*)The results are seen in Figure 4-16 and we can clearly see that ATP can be detected and no significant ATP decompositon is observed. The respective control experiments show to a great extent that ATP can only be captured and detected by dual aptamer modified Au@MnO FNPs.

In conclusion, we have developed a new and efficient nanoparticle-based matrix for laser desorption ionization through investigating the properties of different

nanoparticles. The developed nanoparticles are the first such material to be used in laser desorption ionization mass spectrometry. The utility of Au@MnO FNPs have been demonstrated for sensitive detection of several different metabolites in both positive ion and negative ion modes. Moreover selective detection of cellular metabolites within cancer cells can be achived through utilizing the unique properties of Au@MnO FNPs and the excellent selectivity of aptamers. The Au@MnO FNPs developed herein were used for multiple tasks in one single system. First they are used as a novel ionization substrate, second the surface of the Au@MnO FNPs is decorated in such a way that they are used for fast and efficient internalization to cancer cells using molecular aptamers directly selected from whole cells and at the same time can be used for extracting cellular metabolites. Future work will include the further development of the assay including analyzing different cancer cell lines with varying degree of ATP expression. The particle size, incubation times, and sample preparation methods for complex samples are also important variables that still need more optimization. Although we have used ATP to demonstrate the potential and utility of the aptamer based affinity mass spectrometry, the assay can be easily extended to other cellular targets such as membrane proteins or cytoplasmic proteins such as lysozyme or insulin for which high quality aptamers exist. This assay has shown the potential that aptamers when combined with mass spectrometry provide a rapid, high throughput, sensitive, and cost effective detection of targets of interest.

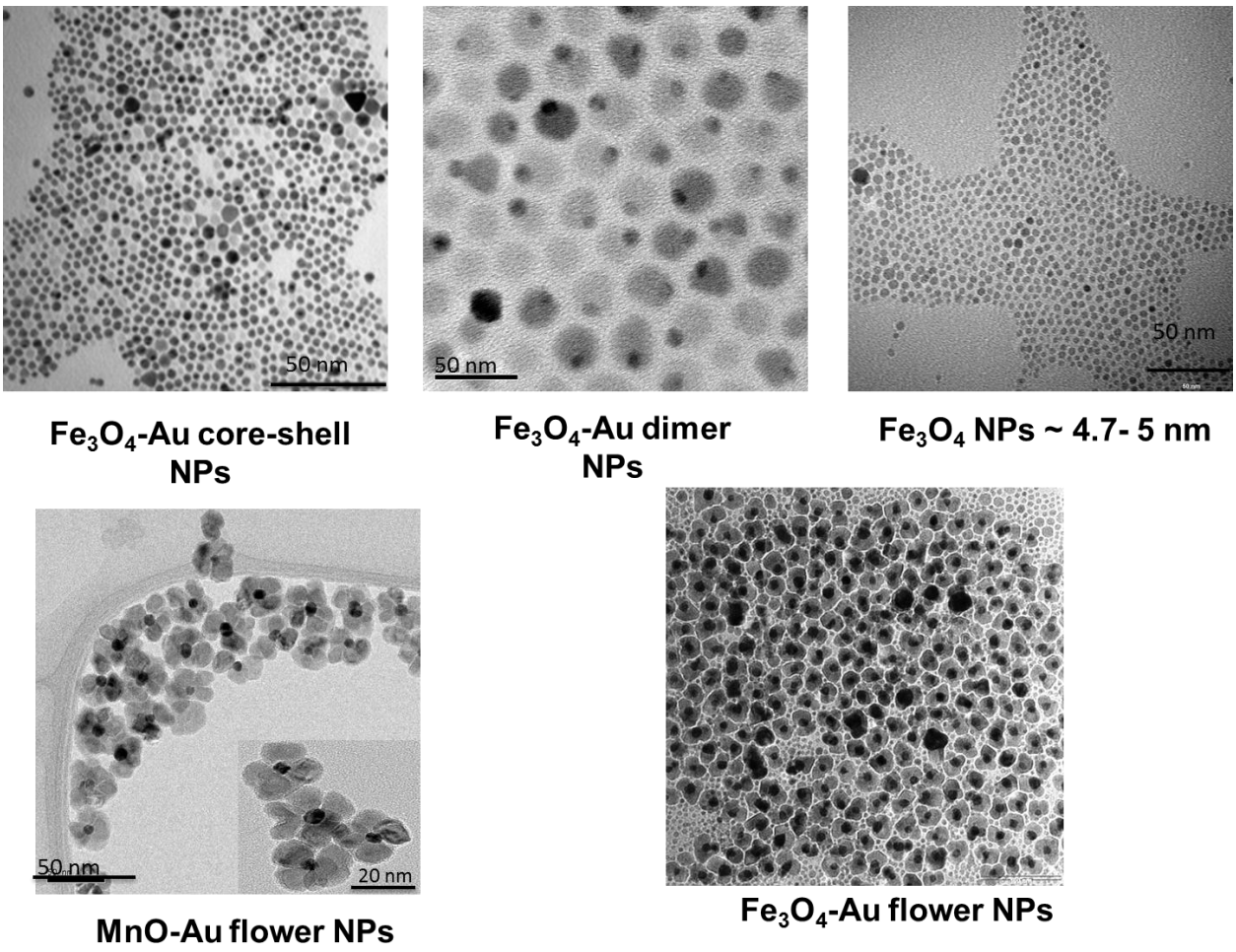

Figure 4-1. TEM images of hybrid nanostructures.

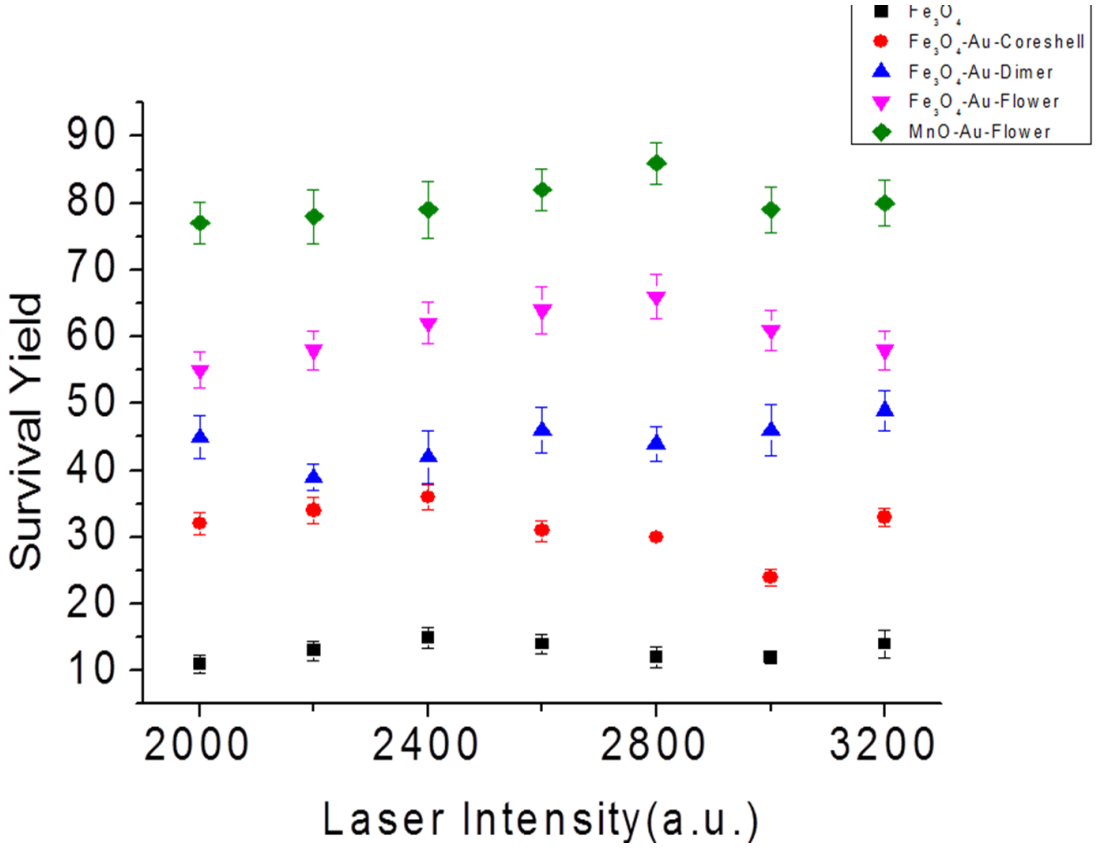

Figure 4-2. Survival yield calculations on metal oxide-Au heteronanostructures

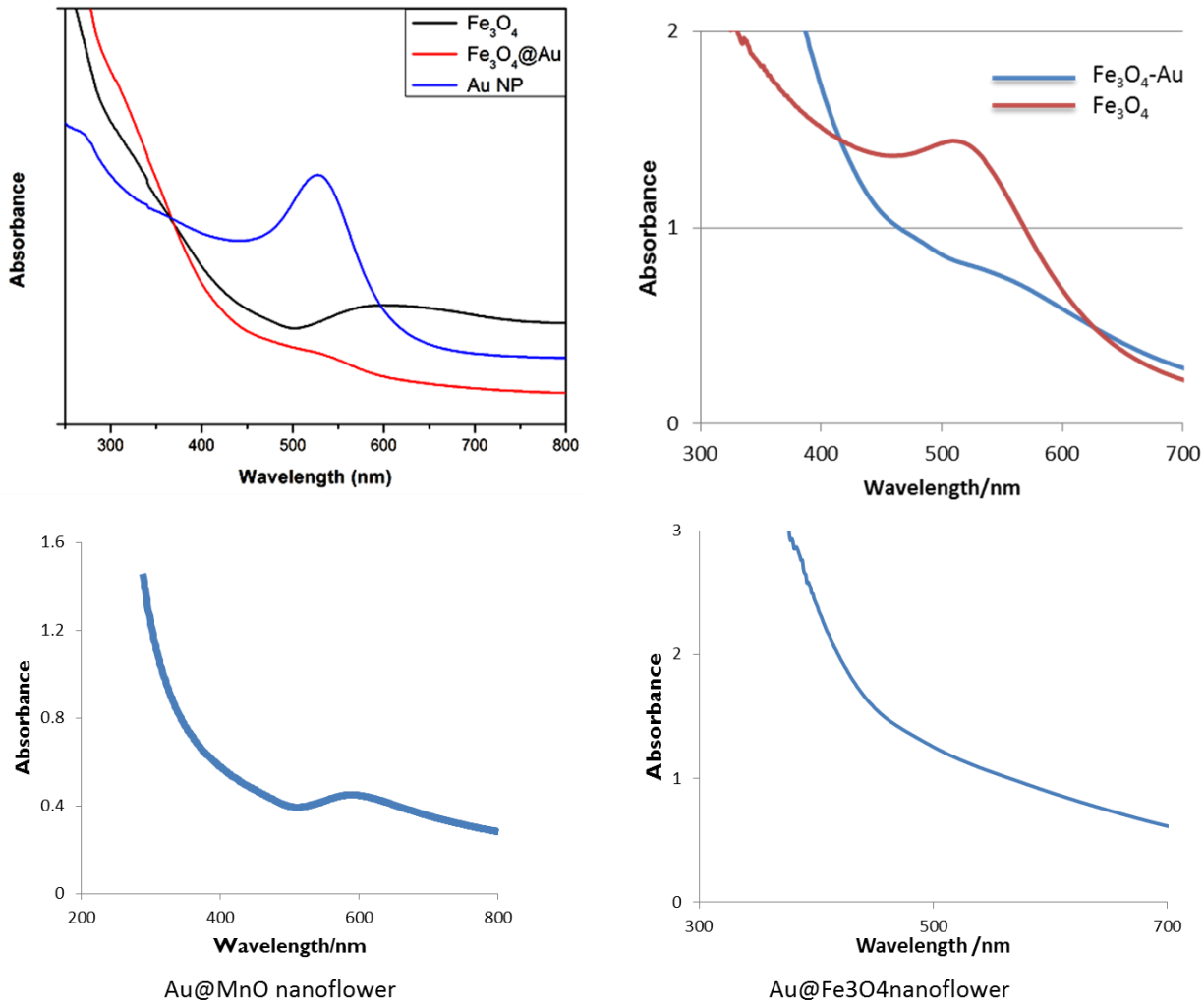

Figure 4-3. UV spectra of the hybrid NPs

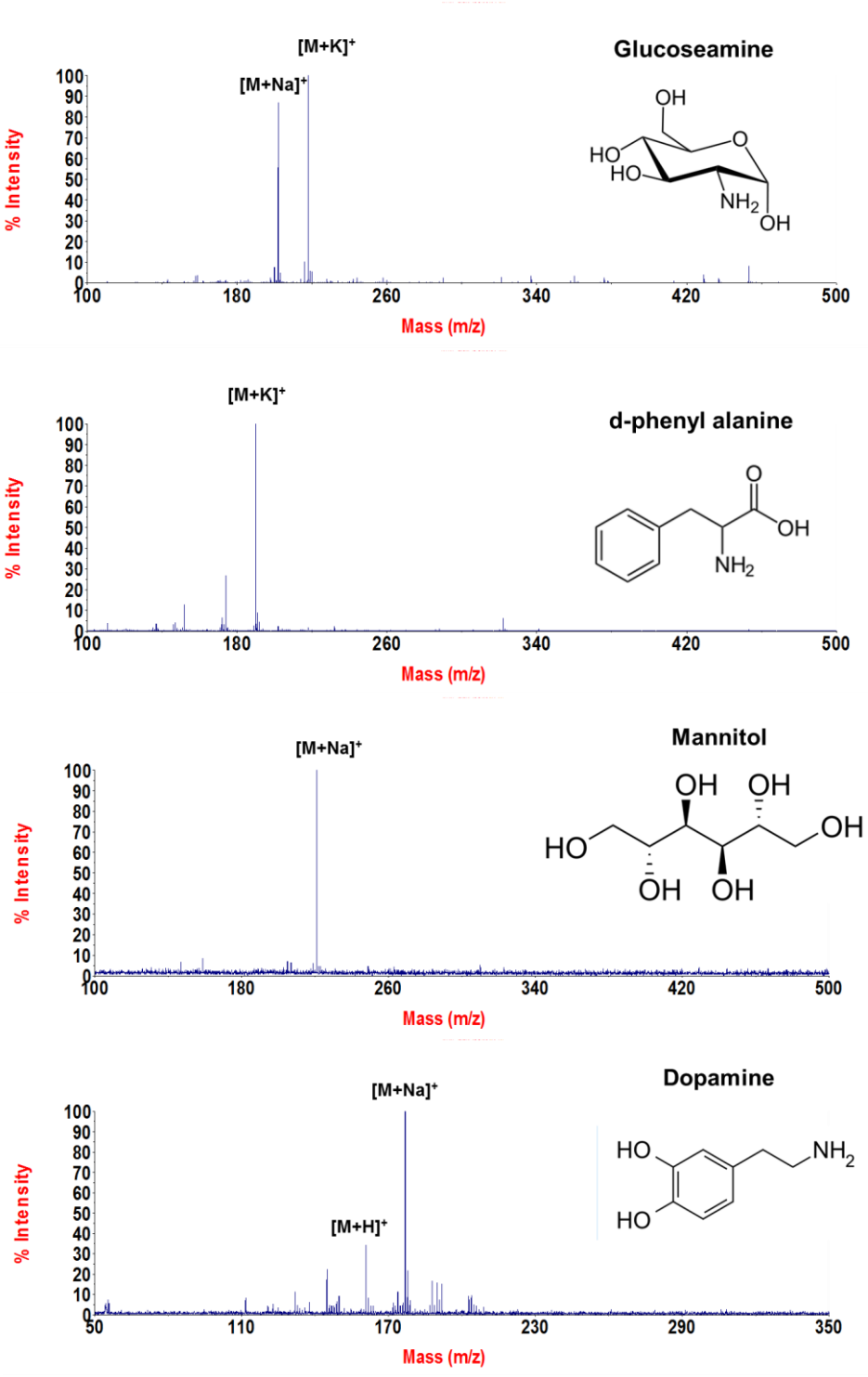

Figure 4-4. LDI analysis of glucoseamine, phenylalanine,mannitol and dopamine on FNPs

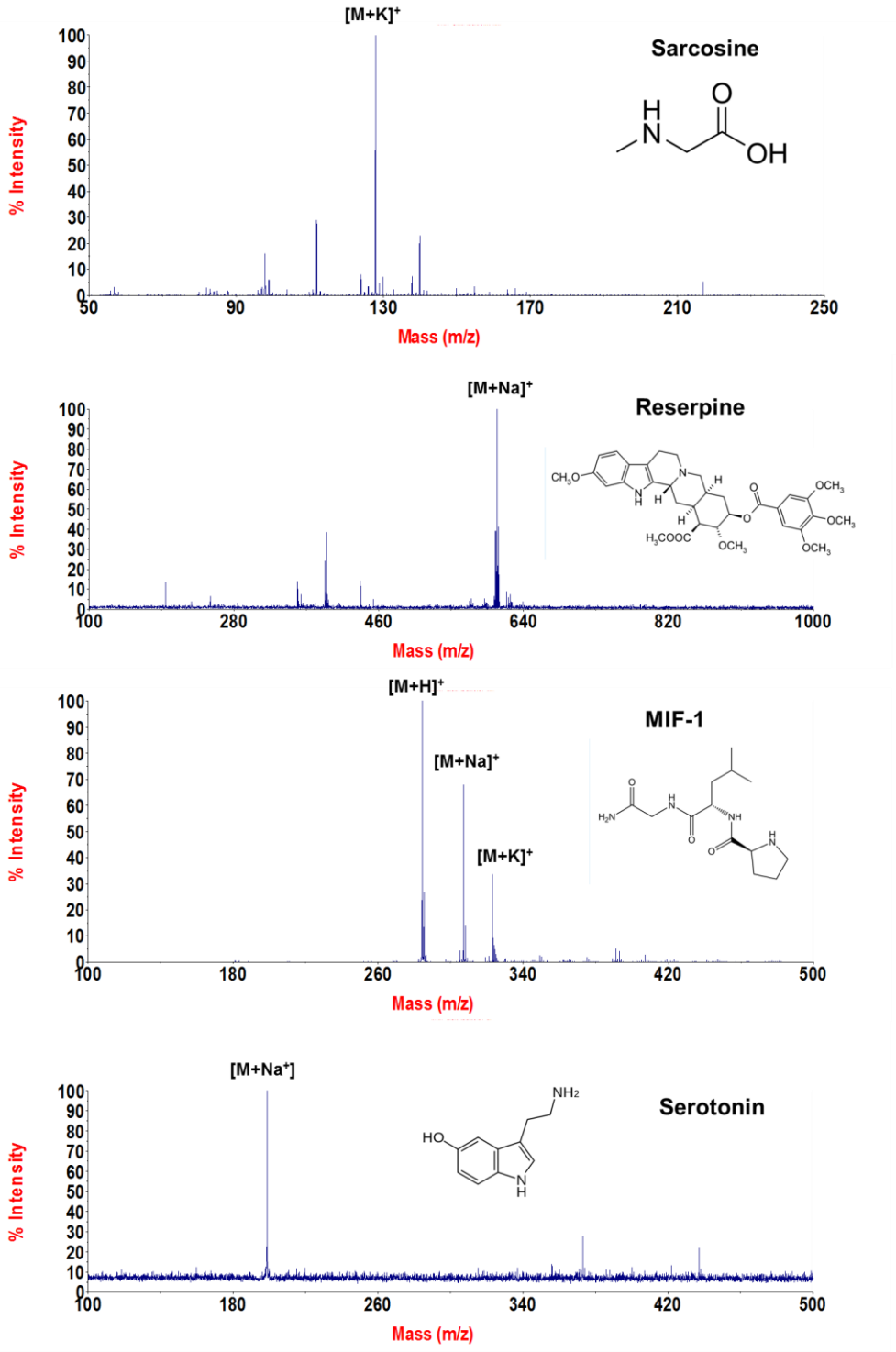

Figure 4-5. LDI analysis of sarcosine, reserpine, MIF-1 and serotonin on FNPs

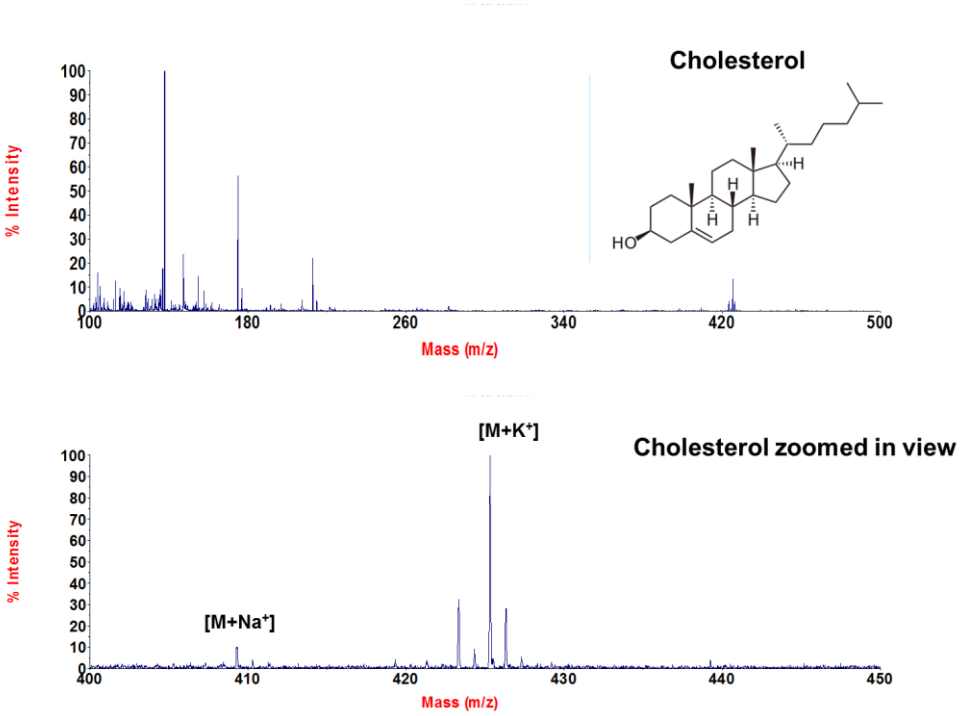

Figure 4-6. LDI analysis of cholesterol on FNPs

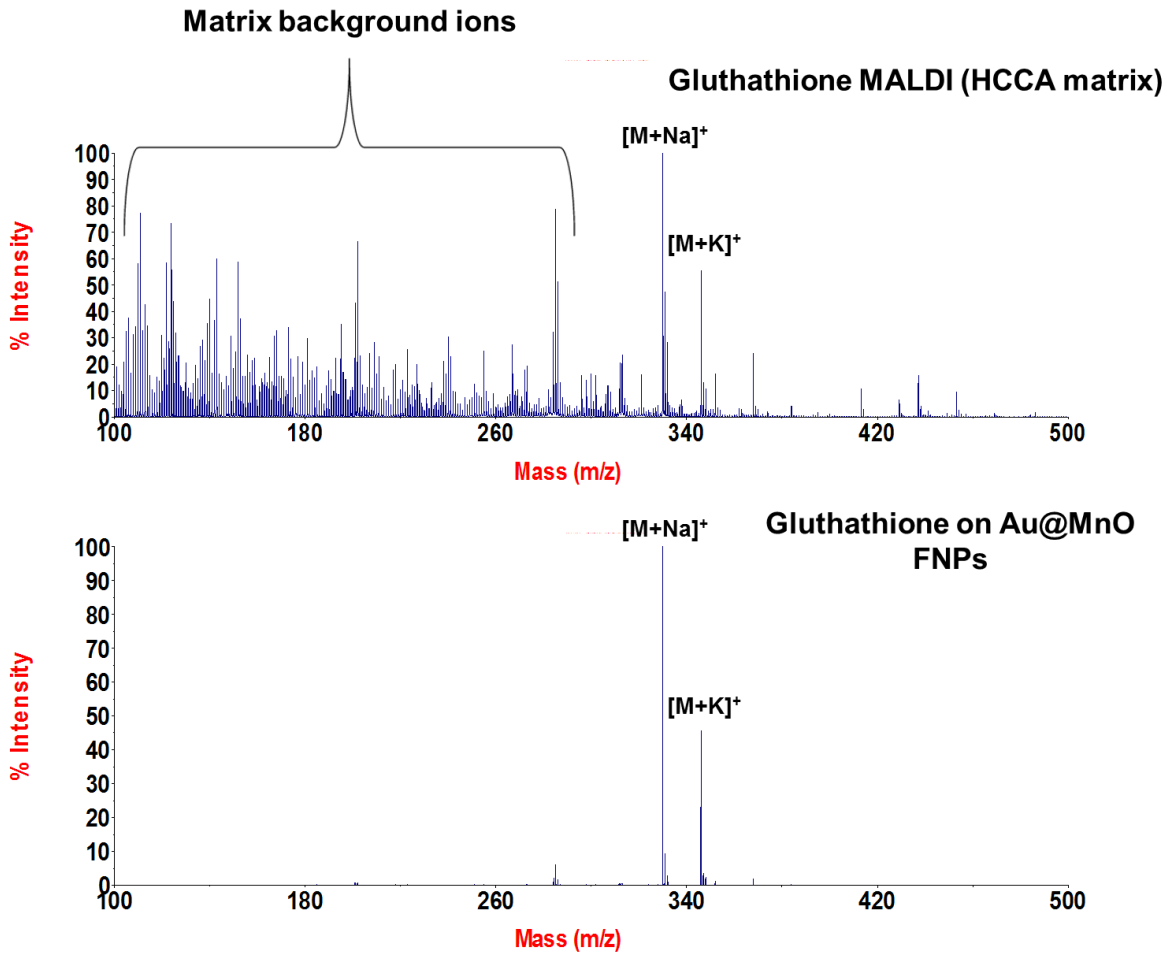

Figure 4-7. Comparison of LDI analysis of glutatione using HCCA matrix and FNPs

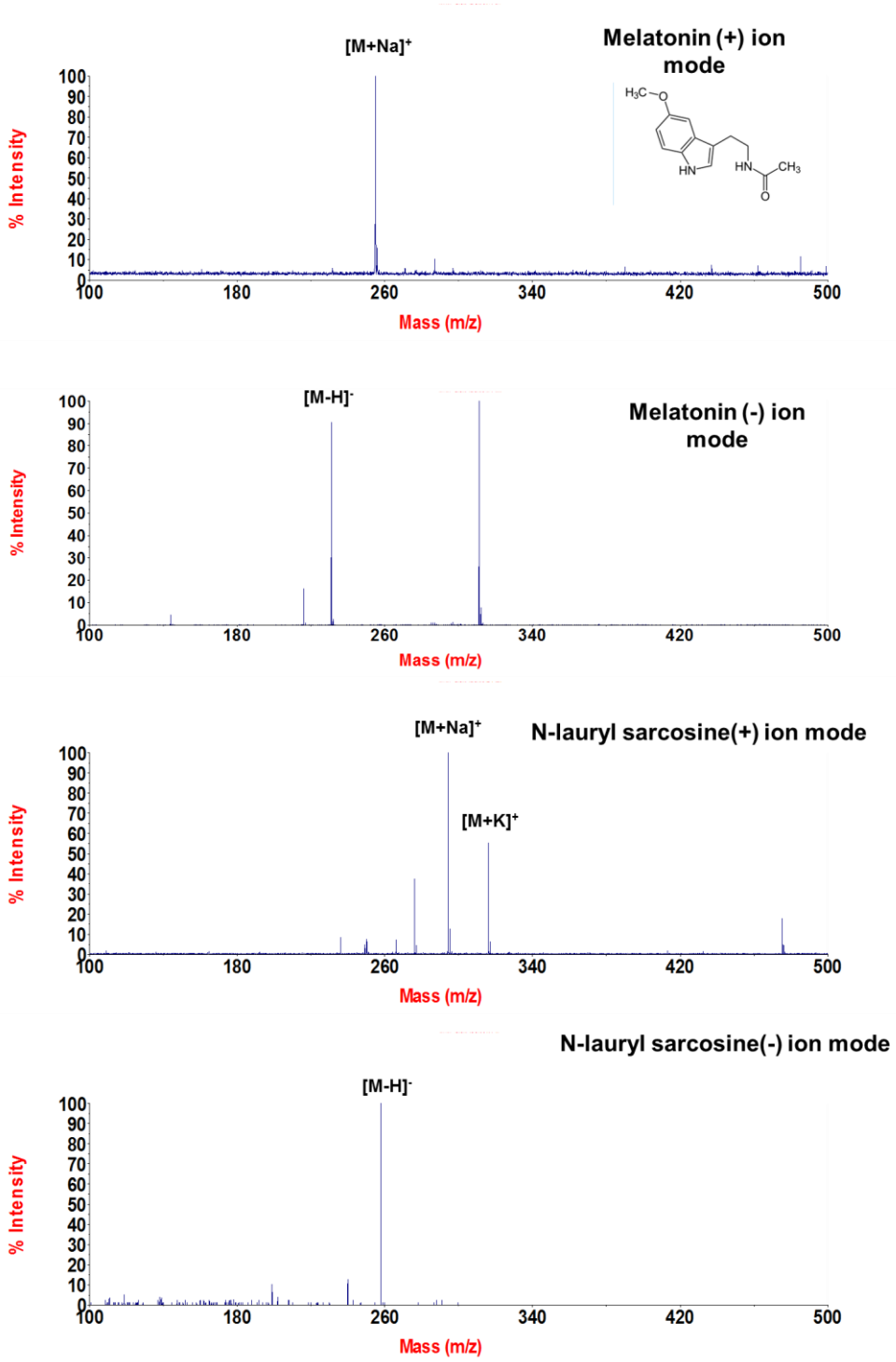

Figure 4-8. Comparison of LDI analysis of melatonin and n-lauryl sarcosine in positive and negative ion mode

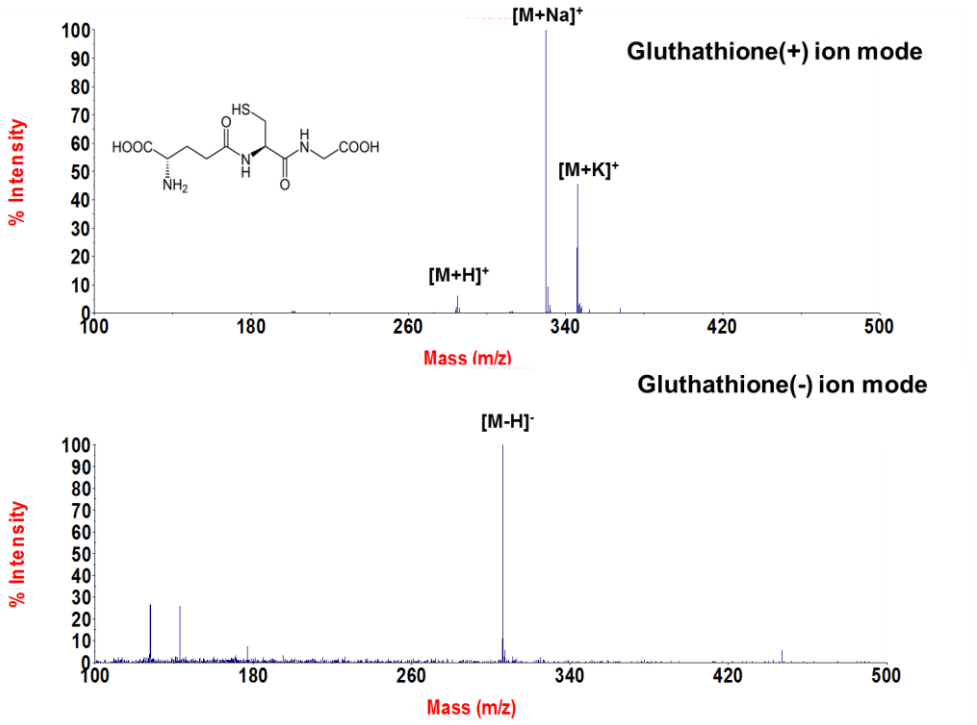

Figure 4-9. Comparison of LDI analysis of glutatione in positive and negative ion mode

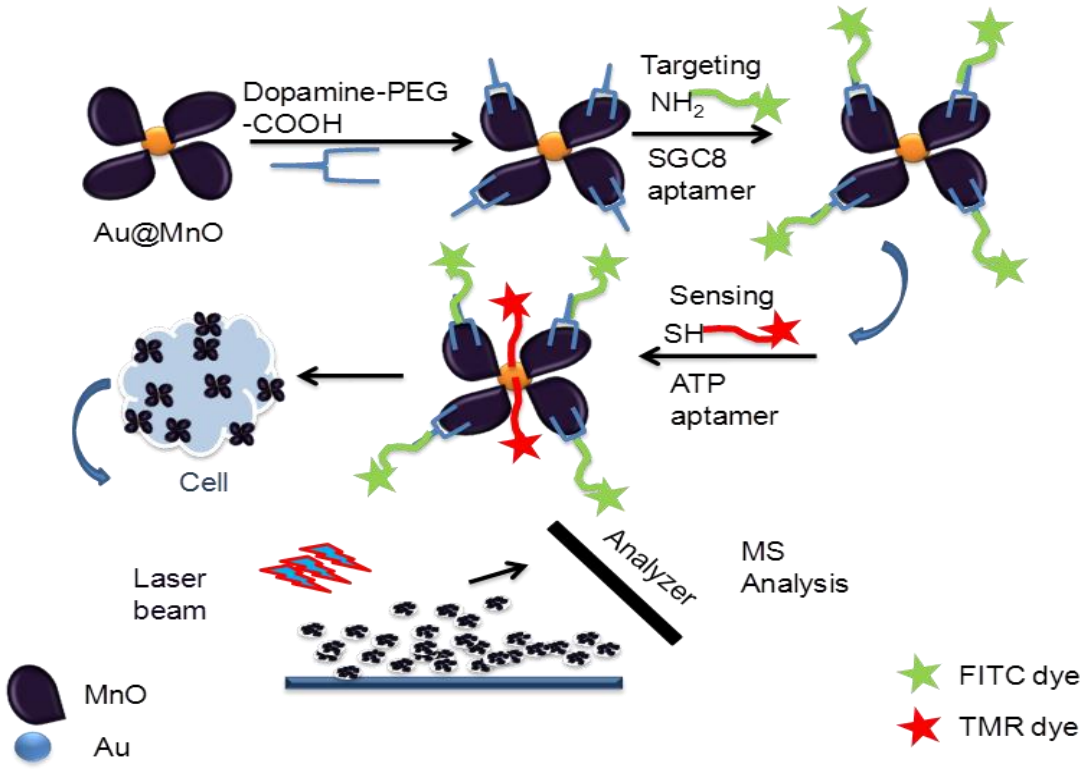

Figure 4-10. Schematic diagram of aptamer modification of FNPs and MS analyses

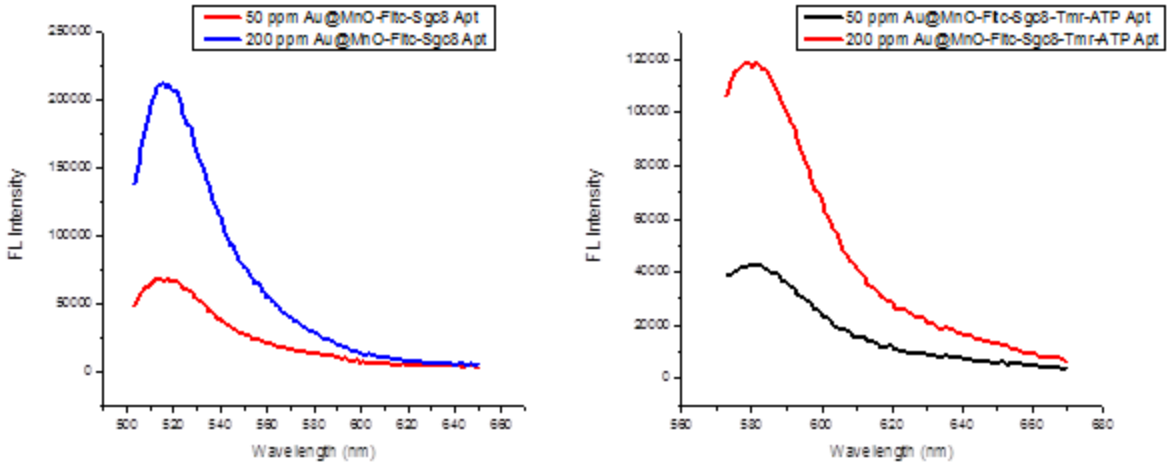

Figure 4-11. Fluorescence spectra of FNPs after aptamer conjugations

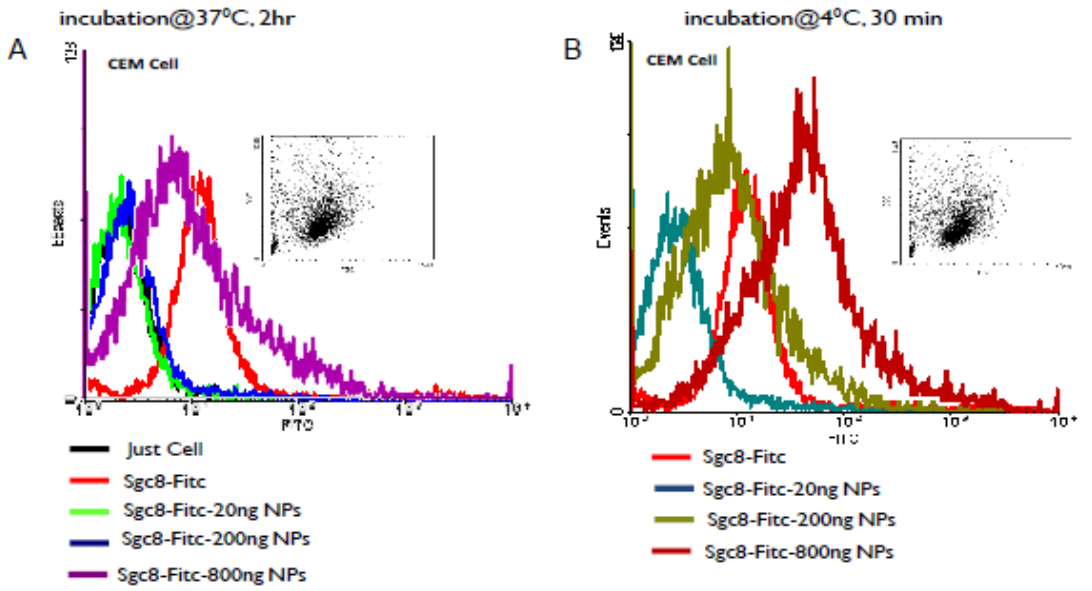

Figure 4-12. Flow cytometric assay to monitor the binding

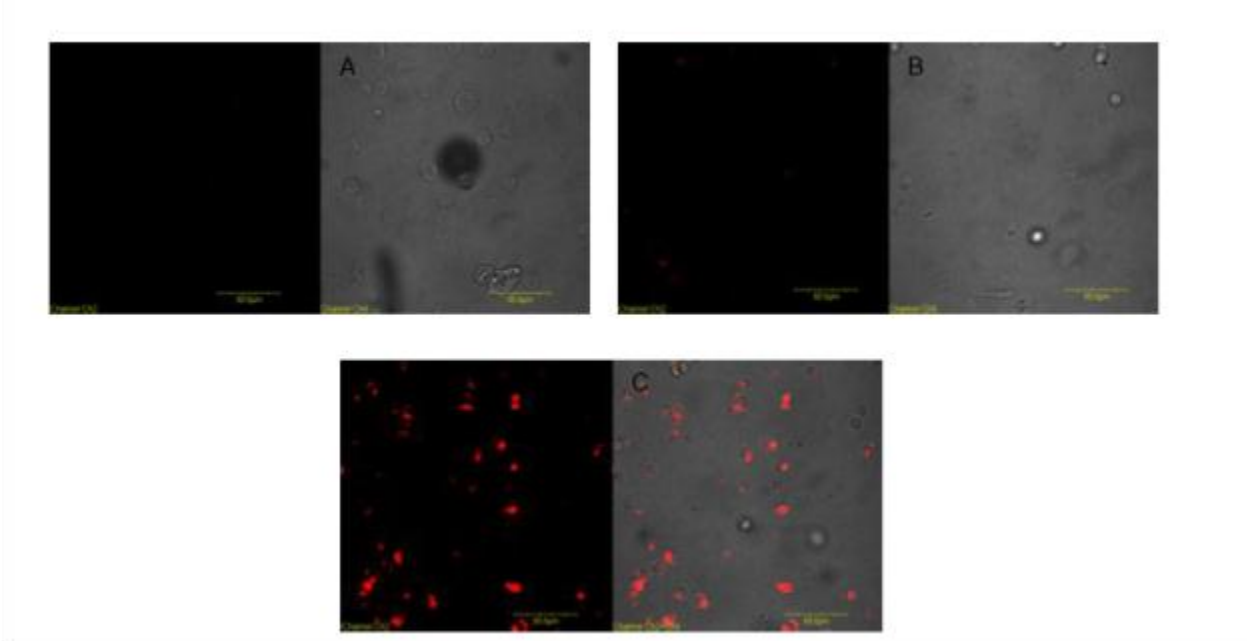

Figure 4-13. Images of cancer cells (A), cells incubated with bare FNPs without aptamer functionalization (B), cancer cells incubated with aptamer functionalized FNPs(C)

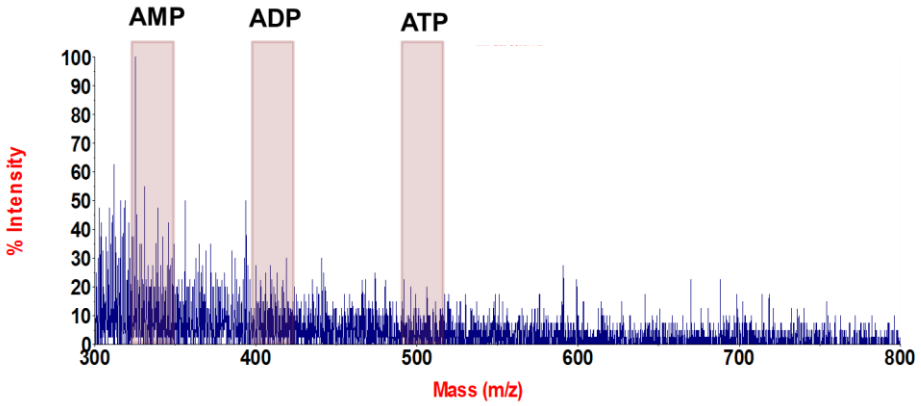

Figure 4-14. LDI analysis of CEM cell lysate after metabolite extraction by cold methanol using FNPs

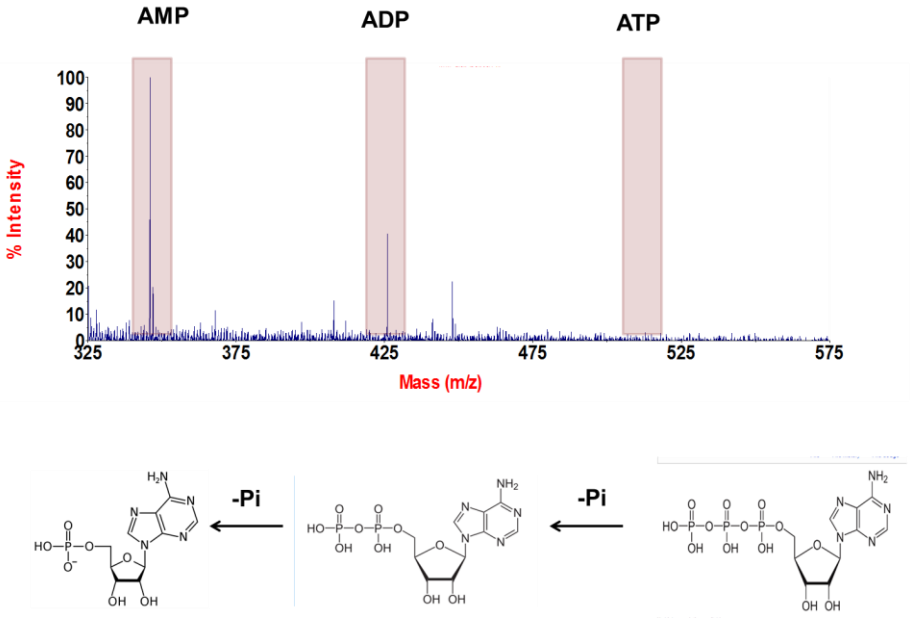

Figure 4-15. LDI analysis of CEM cell lysate after metabolite extraction by hot water using FNPs

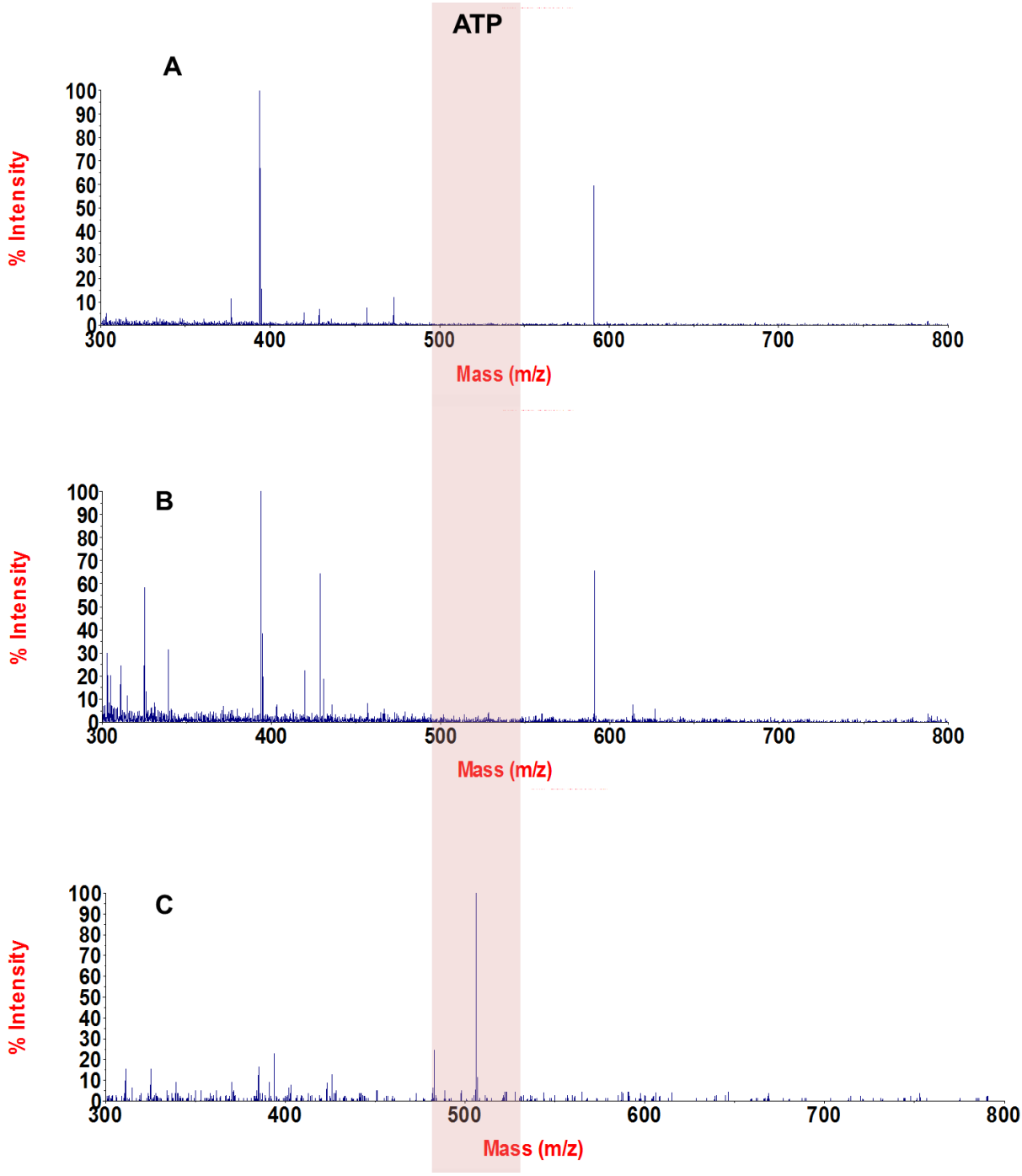

Figure 4-16. LDI analysis of CEM cell lysate after metabolite extraction by hot water using FNPs after quenching the metabolism A-) only sgc8 control B-)sgc-random control C-) sgc8-ATP particle

CHAPTER 5
BIOMARKER DISCOVERY OF HEPATOCELLULAR CARCINOMA USING CELL SPECIFIC APTAMER PROBES AND MASS SPECTROMETRY

Hepatocellular carcinoma (HCC) is one of the most common neoplasms worldwide. It is ranked as the fifth most common cause of cancer-related deaths and approximately 500000 people died by complications caused by HCC. (*120*) According to the World Health Organization, the deaths from HCC are expected to continue to increase until 2030, and these tumors are projected to have the second highest increase in overall death rates.(*121*) As other cancer types, exact mechanism of cancer initiation and progression in HCC are largely unknown. Many different risk factors such as alcohol consumption, hepatitis B virus infection, exposure to toxic chemicals such as aflatoxin, unhealthy fat-rich diet and rare genetic diseases, such as a1-antitrypsin deficiency are associated with HCC.(*121*)

Liver is a very central organ involved in hormonal regulation and digestion system. Therefore HCC can easily metastasize which is a very big complication as metastasis is not easily controllable and decreases the likelihood of survival. Currently, the disease status in HCC is usually determined by physical assessment, either by ultrasound imaging of the liver or pathological examination of biopsy samples.(*122*) However as all other cancer types, early detection is of utmost importance. Accurate detection of HCC is necessary to identify the need for intervention because early surgical and chemotherapeutic intervention is the best hope for patient survival. However, the interpretation of ultrasound imaging is subjective and can be difficult in persons who are obese or have underlying cirrhosis. Moreover pathological examination of biopsy samples is also highly dependent on clinicians' experience. In either case liver cancer cannot be accurately diagnosed until the tumor reaches to a certain size. (>1 cm) When

it reaches that size and detected, it also often reaches to stage 2 or stage 3. On the other hand curative therapy for HCC is possible if it is diagnosed early. Surgical options, including resection and liver transplantation, offer the best chance of a successful outcome.(*123-125*) Local regional therapies, such as radiofrequency ablation and chemoembolization, provide effective local control in those with acceptable hepatic function. The multi-kinase inhibitor sorafenib has also been the first molecular targeted oral agent that was recently shown to provide a survival benefit for selected patients with HCC.(*126*) However all these strategies can be successful only if early diagnosis can be achieved.

Application of new technologies is therefore necessary to extend our knowledge about the molecular pathogenesis, improve therapeutic approaches and patient life in HCC. Discovery of new biomarkers which might lead to early diagnosis, and to define new therapeutic targets for HCC is of great interest. At present, only five biomarkers are used for HCC. They are alpha-Fetoprotein (AFP), DCP (PIVKA-II), AFP-L3, Golgi phosphoprotein 2 and Glypican3 (GPC3). (*127*) AFP is the most common and classical tumor marker for HCC. In adults, under normal conditions, the serum AFP concentration is approximately 5–10 mg/L. AFP is presumed to function as a transport molecule for several ligands, such as bilirubin, fatty acids, retinoid, steroids, heavy metals, dyes, flavonoids, phytoestrogens, dioxin, and various drugs. AFP is also suggested to exhibit immunosuppressive activity and to play a role in the regulation of cell proliferation. Despite the uncertainty concerning its biologic role, an increase in the serum concentration of AFP is mainly used as a tumor marker for HCC. The AFP

concentration is slightly increased in patients with active chronic liver diseases and the low specificity of AFP for a diagnosis for HCC is a clinical problem. (*128*)

Changes in glycosylation are associated with the development of many types of cancer, including HCC. In particular, fucosylation is one of the most important models of glycosylation involved in hepatocarcinogenesis. The amount of fucosylated N-linked glycans in the sera of patients with advanced liver diseases including HCC is significantly increased compared with that of healthy controls or patients with mild liver diseases. Fucosylated AFP (AFP-L3) is a more specific marker for HCC compared with AFP alone. DCP is a protein induced by vitamin K absence or antagonist II (PIVKA-II), DCP may be useful primarily as a prognostic biomarker in HCC cell lines, predictive of rapid tumor progression and poor prognosis. Glycoprotein GP73 (Golgi phosphoprotein 2), a potential biomarker for liver diseases, is elevated in the liver in acute hepatitis (51, 52). GP73 is a single membrane-spanning domain near the short cytoplasmic amino terminus of the protein. GP73 and related protein GPP130 may also be redistributed to the cell surface and endosomes.(*129*) Although the biologic function of GP73 remains uncertain and it is unclear which cells are the source of circulating GP73 and how it arrives in the circulation in vivo, the correlation with HCC is sufficiently high to warrant its further investigation as a potential disease marker. GPC-3 is an oncofetal protein being one of the members of heparan sulfate proteoglycans anchored to the plasma membrane through glycosylphosphatidyinositol.(*130*) However even though all these markers are clinically practiced none of them has yet proven to be an effective indicator of hepatocellular carcinoma. Therefore there is still a big gap in this fied and new biomarkers or panel of biomarkers are needed.

As briefly discussed in the introduction chapter, our lab has developed a hybrid SELEX technique known as cell-based SELEX, or cell-SELEX, for aptamer selection to produce probes for molecular analysis of tumor cells. Instead of using a single type of molecule as the target, the cell-SELEX process uses the whole cells as targets to select single-stranded DNA aptamers that can distinguish target cells from control cells. In addition to the advantages of aptamers such as low molecular weight, easy and reproducible synthesis, easy modification, fast tissue penetration, low toxicity or immunogenicity, easy storage, and high binding affinity and specificity comparable to antibodies, the most significant advantage of the cell-SELEX technology is the absence of the requirement for prior knowledge about the potential biomarkers for cancer on these cells. Also, under these circumstances, a group of cell-specific aptamers can be selected using a subtraction strategy in a relatively short period without knowing which target molecules are present on the cell surface. Once the aptamers are selected, target molecules that might be important cancer biomarkers can be determined as the elucidation of the aptamer binding receptors on the cell surface will reveal the molecular structure of these receptors. This is very unique way to determine molecular characteristics of cells. Also, the generation of a group of aptamers during the process provides multiple molecular probe candidates for surface biomarker recognitions. On the other hand, there is no easy way to produce a similar panel of monoclonal antibodies in such a short time without purified antigens for any unknown antigens.

Moreover most FDA-approved clinically proven cancer drugs target cell surface proteins and inhibit their functions. So the there is a great chance that discovered proteins have importance as biomarkers or understanding the pathways involved.

However membrane proteins constitute the most underrepresented family of proteins in proteomics studies. Because of their poor water solubility, high hydrophobicity, high molecular weight characteristics they cannot easily be separated and identified by MS. Many methods have been proposed to address these issues but with very limited success has been achived so far. Our group has previously shown that aptamers can be used as pull-down probes to identify new biomarkers. In the most striking example protein tyrosine kinase PTK7 was identified as the binding receptor on the cell membrane surface for aptamer Sgc8 which is selected against CCRF-CEM leukemia cells. Protein tyrosine kinase-7 (PTK7), also known as colon carcinoma kinase-4 (CCK4), is a relatively new and little studied member of the RTK superfamily. It was identified as a novel regulator of non-canonical WNT or planar cell polarity (PCP) signaling.(*131*) So it is very clear from this accumulating evidence that aptamer targets have important implications in cancer. This chapter discusses how the aptamer based affinity mass spectrometry is applied in the discovery of a new candidate biomarker for HCC.

Experimental

Cell Line

LH86 human liver cancer cell line is cultured at 37 °C and 5% CO_2 in DMEM supplemented with 10% FBS, 100 U/mL penicillin−streptomycin (Cellgro). Cells were washed before and after incubation with washing buffer (4.5 g/L glucose and 5 mM $MgCl_2$ in Dulbecco's phosphate-buffered saline with calcium chloride and magnesium chloride (Sigma).

Synthesis of Aptamers

An ABI 3400 DNA/RNA synthesizer (Applied Biosystems, Foster City, CA) was operated for the synthesis of all aptamer sequences for liver cancer :TLS11a: 5`-ACAGCATCCCCATGTGAACAATCGCATTGTGATTGTTACGGTTTCCGCCTCATGGACGTGCTG biotin-3` and ATP aptamer: 5'-AGTCCATTTTATTCCTGAATATTTGTTAACCTCATGGAC biotin -3') at the 1 µmol scale. Deprotection was performed in AMA (ammonium hydroxide/ 40% aqueous methylamine 1:1) at 65 °C for 30 min, and deprotected sequences were purified by reversed-phase HPLC (ProStar, Varian, Walnut Creek, CA) with a C18 column (Econosil, 5 µm, 250-4.6 mm) from Alltech (Deerfield, IL). Immediately after HPLC purification, purified DNA solution was dried in acid-resistant centriVap centrifugal vacuum concentrators (Labconco, Kansas City, MO). The dried DNA was dissolved in 50 µL DNA grade water, and the concentration of each sequence was determined based on absorbance value at nm using an 1800 UV-Vis spectrophotometer (Shimadzu Scientific Instruments, Columbia, MD).

Biomarker Identification

LH86 (100X106) cells were washed three times at 4 °C with a PBS buffer and lysed in 5 mL of hypotonic buffer [50 mM Tris-HCl (pH 7.5) containing protease inhibitors (0.1 mM PMSF and 2 µg/mL pepstatin, leupeptin, and aprotinin)] at 4 °C for 30 min. After centrifugation, the debris was washed three times with 5 mL of hypotonic buffer and dissolved in 1.5 mL of lysis buffer (PBS containing 5 mM MgCl2 and 1% Triton X-100) at 4 °C for 30 min. In other cell experiments IP lysis kit from Pierce was used following manufacturer`s instructions.

In a typical procedure the supernatant was incubated with with TLS11 sequence in the presence or absence of 1000-fold excess of random DNA sequence library as a nonspecific competitor, at 4 °C for 30 min. The protein−TLS11a complex was captured by incubating it with 2 mg (200 µL) of magnetic streptavidin beads at 4 °C for 15 min and collected on a magnet ic stand. The collected magnetic beads were washed four times with 1 mL of PBS containing 5 mM MgCl2. The proteins were eluted by heating in 30 µL of loading buffer and analyzed by polyacrylamide gel electrophoresis (12%) (SDS-PAGE) stained with colloidal blue or mass spectrometry compatible silver stains. When in solution sample processing was performed the proteins were eluted by heating and supernatant was removed and transferred to another eppendorf tube for further processing.

Protein Identification by Nano-LC-ESI MS

Proteins captured by aptamers as described above were digested according to manufacturer's instructions in solution. When gel samples are processed, the gel bands excised digested according to manufacturer's instructions. The peptides were loaded onto a C_{18} capillary trap cartridge (LC Packings) and then separated on a 15-cm nanoflow C_{18} column (PepMap, 75-µm inner diameter, 3 µmm, 100 Å) (LC Packings) at a flow rate of 200 nl/min. Quadrupole time-of-flight (QSTAR XL) MS system was used for protein identification. Two different chromatographic separation profiles were used: In the first one which is performed for in gel digested samples, peptides were eluted from the HPLC column by a linear gradient from 5% Solvent B (96.9% acetonitrile (v/v), 0.1% (v/v) acetic acid) to 20% Solvent B for 30 mins followed by ramping up to 80% Solvent B in 5 min. In the second one which is perfomed for in solution digestion samples 3% Solvent B (96.9% acetonitrile (v/v), 0.1% (v/v) acetic acid) to 40% Solvent

B for 2 h followed by ramping up to 90% Solvent B in 10 min. Peptides were sprayed into the orifice of the mass spectrometer, which was operated in an information-dependent data acquisition mode where an MS scan followed by three MS/MS scans of the five highest abundance peptide ions were acquired in each cycle. Spectra and product ion spectra were acquired using Analyst QS software.

Data Analysis

The peptide tandem mass spectra were searched against using MASCOT search engine (http://www.matrixscience.com). The search was performed to allow for carbamidomethylation, oxidation, and a maximum of one missed trypsin cleavage. Peptide tolerance and MS/MS tolerance were both 0.2 Da.

Results and Discussion

Our group had previously selected aptamers which can recognize HCC cells. The binding profile of the aptamers was depicted in Figure 5-1. As the first step of the protein identification procedure we applied the procedure reported by our group previously. A general workflow of the aptamer assisted membrane protein extraction and mass spectrometric identification procedure is schematically represented in Figure 5-2. Typically $100X10^6$cells were first lysed in hypotonic cell lysis buffer and incubated with TLS11a aptamer which recognizes human liver cancer cells. In a separate control experiment cell lysates were incubated with TLS9 control sequence (scrambled sequence) to differentiate the specific capture from non-specific capturing. The results are depicted in Figure 5-3. As can be seen from the coomassie stained gel image, several proteins were observed in the total cell lysate and there was only a very faint band around 50 kDa which did not show up with the control sequence. The results were seen in Figure 5-3. As can be seen from this western blot, there was indeed a band at

around 50 Kd. We excised this band, performed in-gel digestion and nano-LC-MS/MS based protein identification. The protein list after the identification is shown in Figure 5-5. The protein hit was “vimentin” which has a molecular weight of 54 kDa. We have identified the same protein together with other non-specifically bound proteins. However while our results consistently showed the same protein, vimentin, we ruled out the possility that this is the target protein. Vimentin is a class-III intermediate filament protein found in various non-epithelial cells, especially mesenchymal cells. It is attached to the nucleus, endoplasmic reticulum, and mitochondria, either laterally or terminally. While recent data suggest its role in cancer initiation and growth(*132*), it is a cytoplasmic protein not a membrane protein; therefore it probably interacted with the aptamer in a nonspecific manner.

In the next set of experiments we performed the same pull –down procedure but performed the gel staining using silver. While coomassie blue has been shown to be more compatible with mass spectrometry it is also known to have poor sensitivity in staining rare proteins. While aptamers can recognize their targets with very high specificity, the expression levels of their membrane targets are unknown. Moreover besides their intrinsic difficulties in handling, membrane proteins have also low copy numbers on the cell surface. Silver staining has been shown to detect proteins as low as picogram levels. For this reason we have proceeded with silver staining to enable a more clear protein staining and to pick the band of interest more easily. The gel image stained with silver is shown in Figure 5-4. As we had previously seen in the coammassie staining we have seen a band around the same molecular weight region. When we excised the band and perfomed nano-LC-MS/MS based protein identification

results were very similar. We also repeated the same experiment and performed in solution digestion followed by nano-LC MS/MS to confirm the validity of the experiments. Results of in gel and in solution digestion are seen in Figure 5-6 and Figure 5-7 While the results were consistent with the previous experiments, the protein hit was not a membrane protein suggesting that: 1) protein target of the aptamer has a low copy number 2) binding is masked by cytoplasmic and nuclear proteins 3) the cell lysis protocol do not liberate membrane proteins sufficiently. The results also showed that running gel samples do not have any significant advantage in protein ID results as very similar results were obtained in both cases.

Being unable to get any membrane protein identified after aptamer based membrane protein extraction, we have made small changes in the experimental procedure. To address the first issue we have first increased the cell number to $1X10^9$ cells which would give sufficient proteins. Secondly, instead of using a hypotonic cell lysis buffer, immunoprecipitation lysis buffer (IP lysis buffer) was used in liberating the proteins from the cells. This buffer has successfully been used for antibody based pull down experiments. This buffer has a formulation to help maintain protein complexes for co-immunoprecipitation. As we have discussed previously, membrane proteins can easily lose their structural integrity and aptamer-protein complexes might not be maintained when the proteins are extracted from the cell membrane. Third an additional clean-up step was incorporated into aptamer based protein pull-down. As the aptamers are oligonucleotides there are many proteins in the cell lysate which have natural tendency to bind to oligonucleotides. To eliminate this and minimize the effect of non-

specifically bound proteins, cell lysate was first incubated with a 1000 fold excess the random DNA library. Aptamer was then incubated with this library treated lysate.

The results of the protein identification of only random library treated samples are seen Figure 5-8. This protein list was largely dominated with different histones and other cytoplasmic proteins. Histones are the proteins which surround chromosomal DNA and control formation of nucleosomes. The results of the protein identification of after a non-specific aptamer (TLS9) are seen Figure 5-9.

When the same experiment was performed using a human liver cancer specific aptamer TLS11a we have observed a protein called “Plexin B3” in the protein list as shown in Figure 5-10. This was a single pass trans-membrane protein. Being the only membrane protein in the protein list this lead us to think that this might be the potential target of the TLS11a aptamer in LH86 HCC cell lysate samples.

Plexin B3 is a 260 kDa type I transmembrane glycoprotein in the Plexin B subfamily of semaphorin receptors. Its identified ligand is the transmembrane semaphorin Sema5A, and are both expressed during differentiation and migration of central nervous system oligodendrocytes. Plexin B3 can interact with the transmembrane scatter factor receptors Met and Ron, activating these receptors and the signaling molecule RhoA upon semaphorin engagement. Up to date, plexin B3 were shown to be expressed specifically in pancreatic and prostate cancer cell lines derived from metastatic tumors which suggest its potential role in cancer growth. (*133-135*) A very recent report also suggests that Plexin B3 has very important roles in glioma which is a very aggressive type of brain cancer.(*136*) We have also mapped its interactions using the program Pathway Studio to get a clearer picture about its potential role. As

can be seen from this map in Figure 5-11, Plexin B3 interacts with GTP-binding protein Rit2 and Sema5A and is involved in neoplastic growth and cell metastasis. Our results also explain why the gel images didn`t show any differential band. As the molecular weight of Plexin B-3 is 260 Da it is difficult to isolate this protein by using a 1D gel. While the functional role of of Plexin B3 in is still elusive as there is no previous data in HCC our data suggests that it might be a very important novel biomarker for HCC and might shed light into complex cellular mechanisms of hepatocellular carcinoma and identify new and more effective biomarkers and identify new drug targets.

Here, we have presented novel aptamer based affinity mass spectrometry strategy for identifying differentially expressed proteins in hepatocellular carcinoma (HCC). This method integrates the selection of molecular probes targeting specific cells and the use of cell specific aptamers for effective identification of target proteins. Our group's previous work with aptamer selection for HCC has showed that selective targeting can be achieved through aptamer probes. In here we show that it is also feasible to discover previously unidentified proteins that may have a important role in transforming normal cells into diseased HCC cells. As there is no previous data on the role of Plexin B3 in HCC, future work will involve validation of Plexin B3 in tumour tissue samples and screening this protein in proximal tumor tissue using targeted based protein identification methods such as MRM or ELISA.

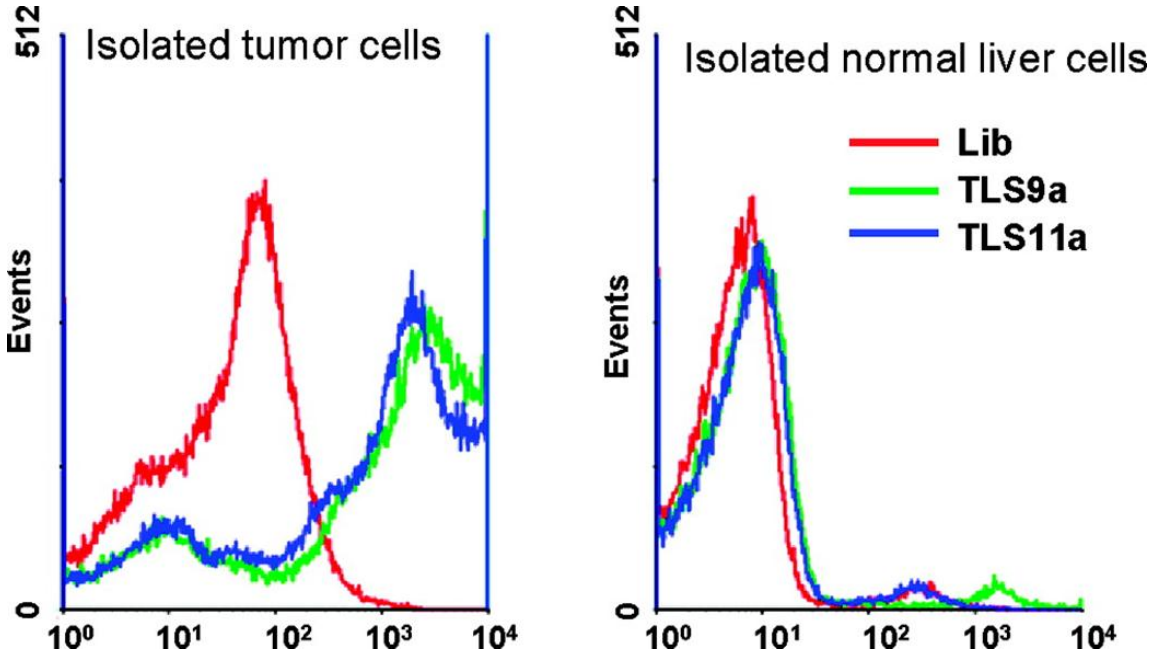

Figure 5-1. Flow cytometry assay for the binding of the HCC aptamers TLS9a and TLS911a(*137*)

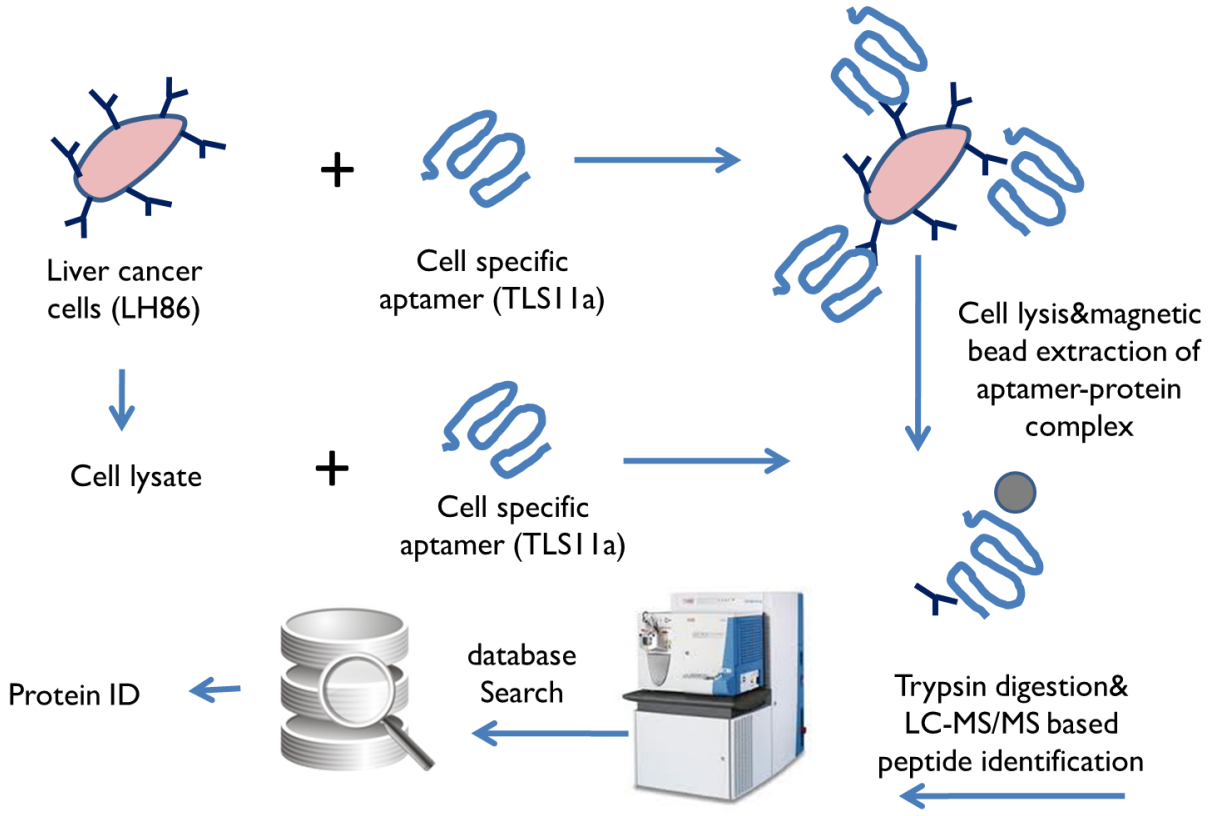

Figure 5-2. Aptamer based affinity mass spectrometry for cancer biomarker discovery

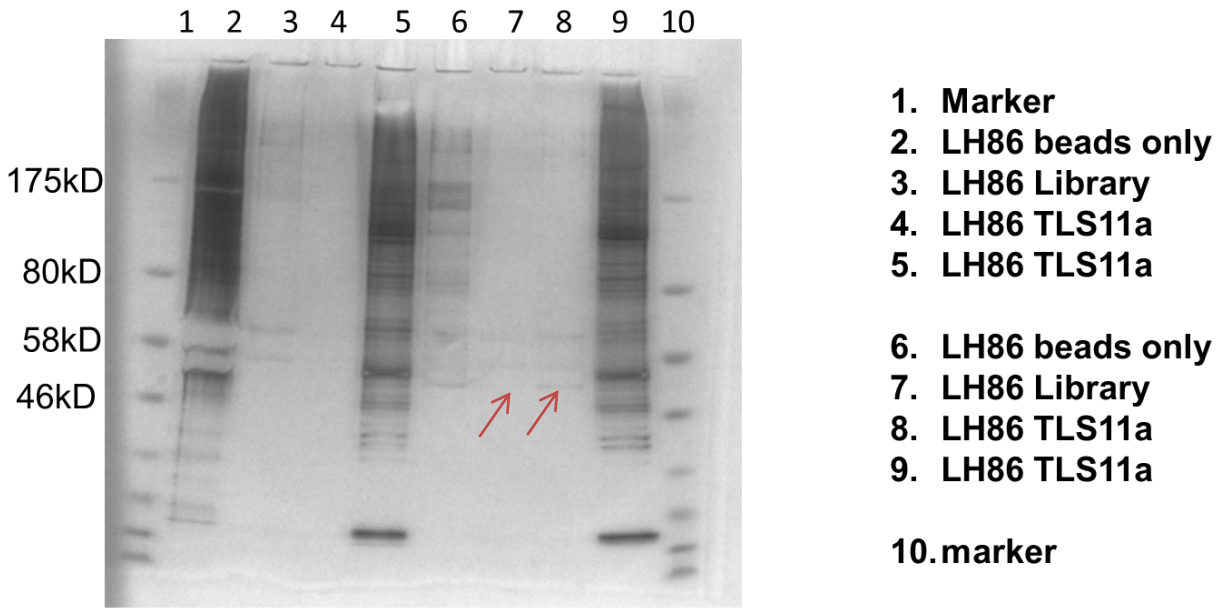

Figure 5-3. 1D gel electrophoresis image of HCC cell lysate after aptamer based affinity enrichment. (Coamassie staining)

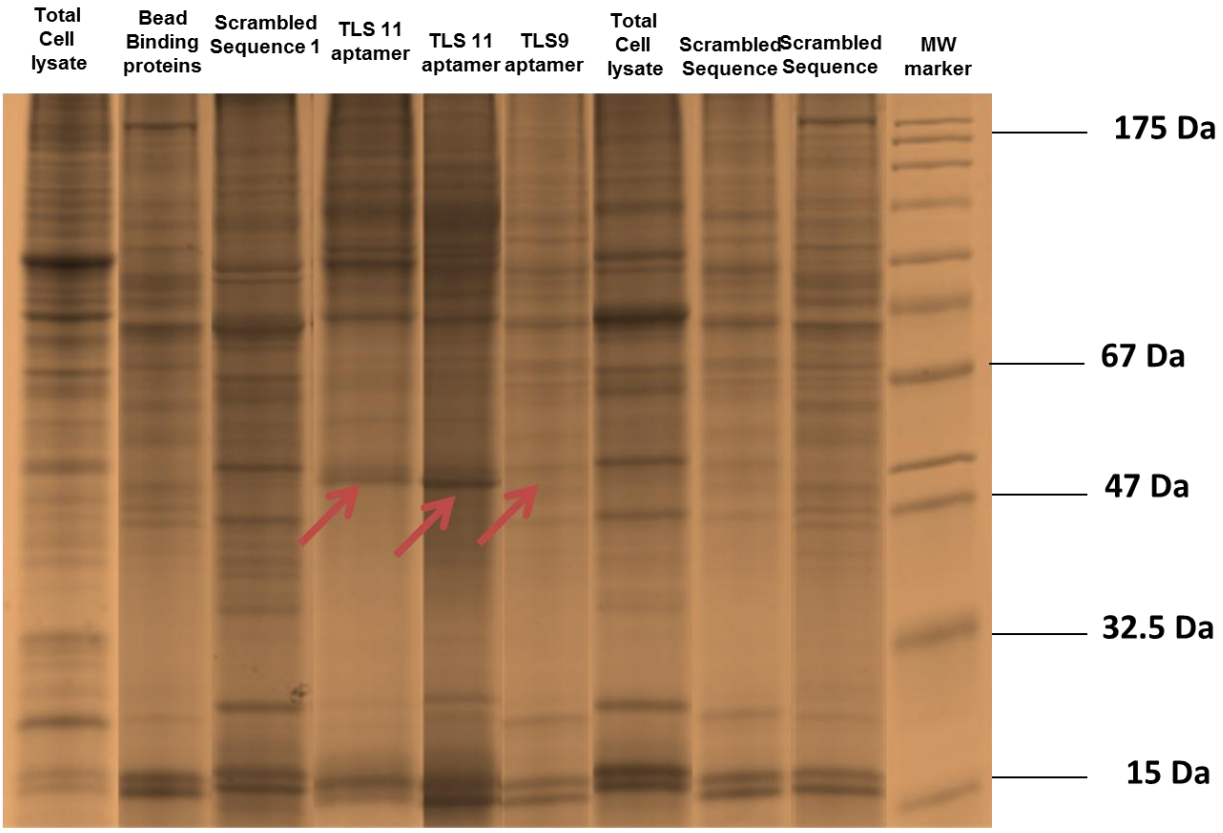

Figure 5-4. 1D gel electrophoresis image of HCC cell lysate after aptamer based affinity enrichment. (Silver staining)

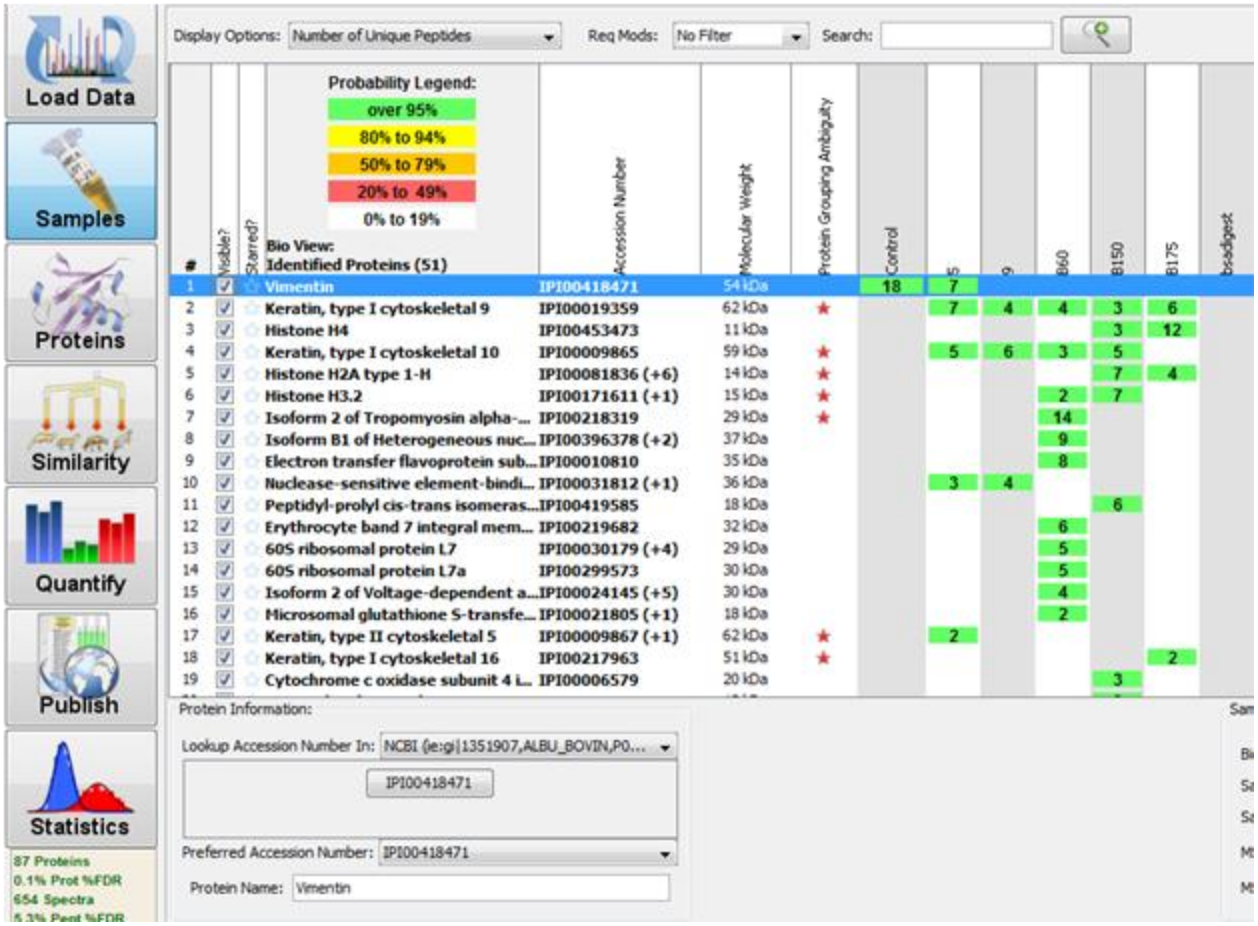

Figure 5-5. Protein ID results of the excised band after aptamer based affinity enrichment.(coammassie stained gel)

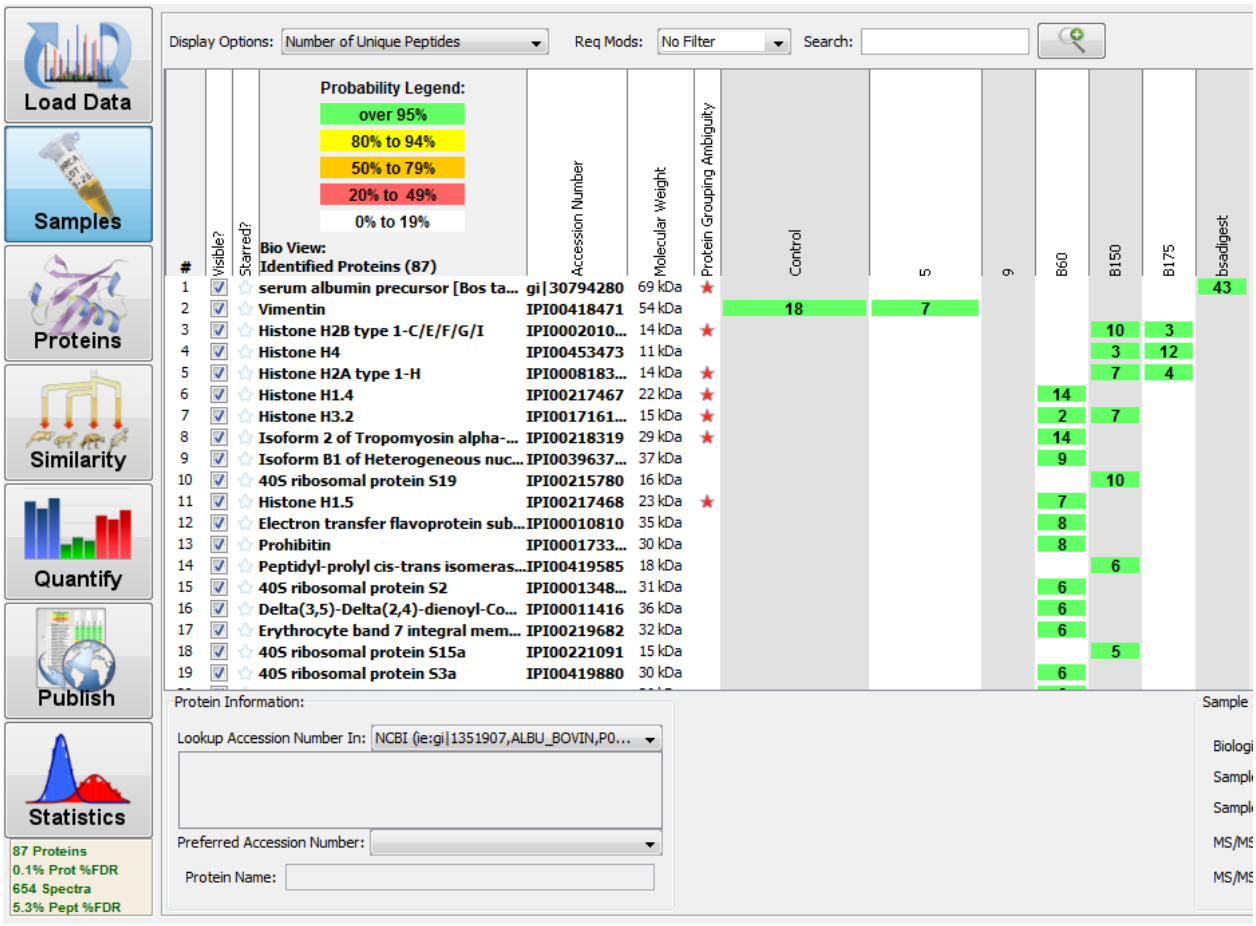

Figure 5-6. Protein ID results of the excised band after aptamer based affinity enrichment. (Silver stained gel)

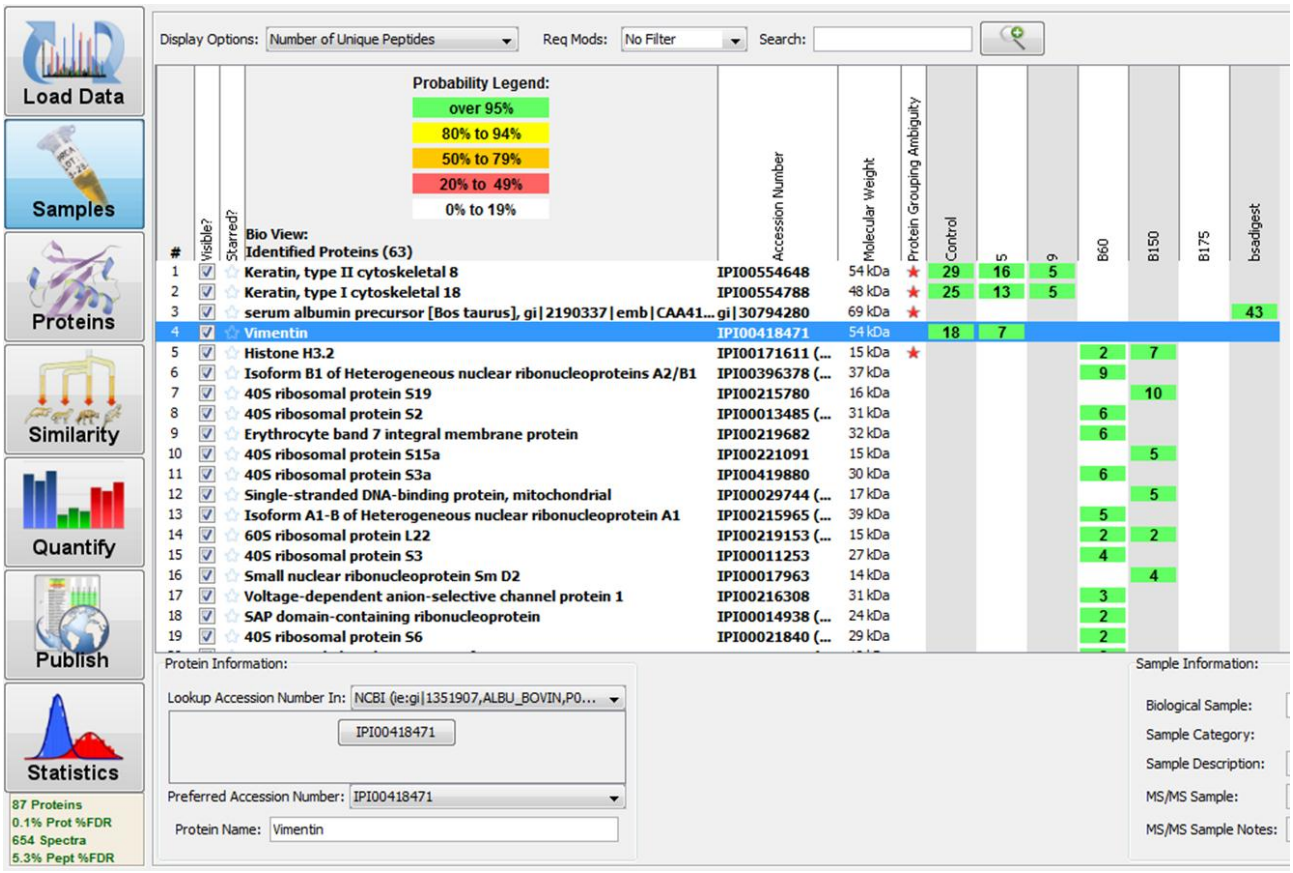

Figure 5-7. Protein ID results of the excised band after aptamer based affinity enrichment (in solution digestion)

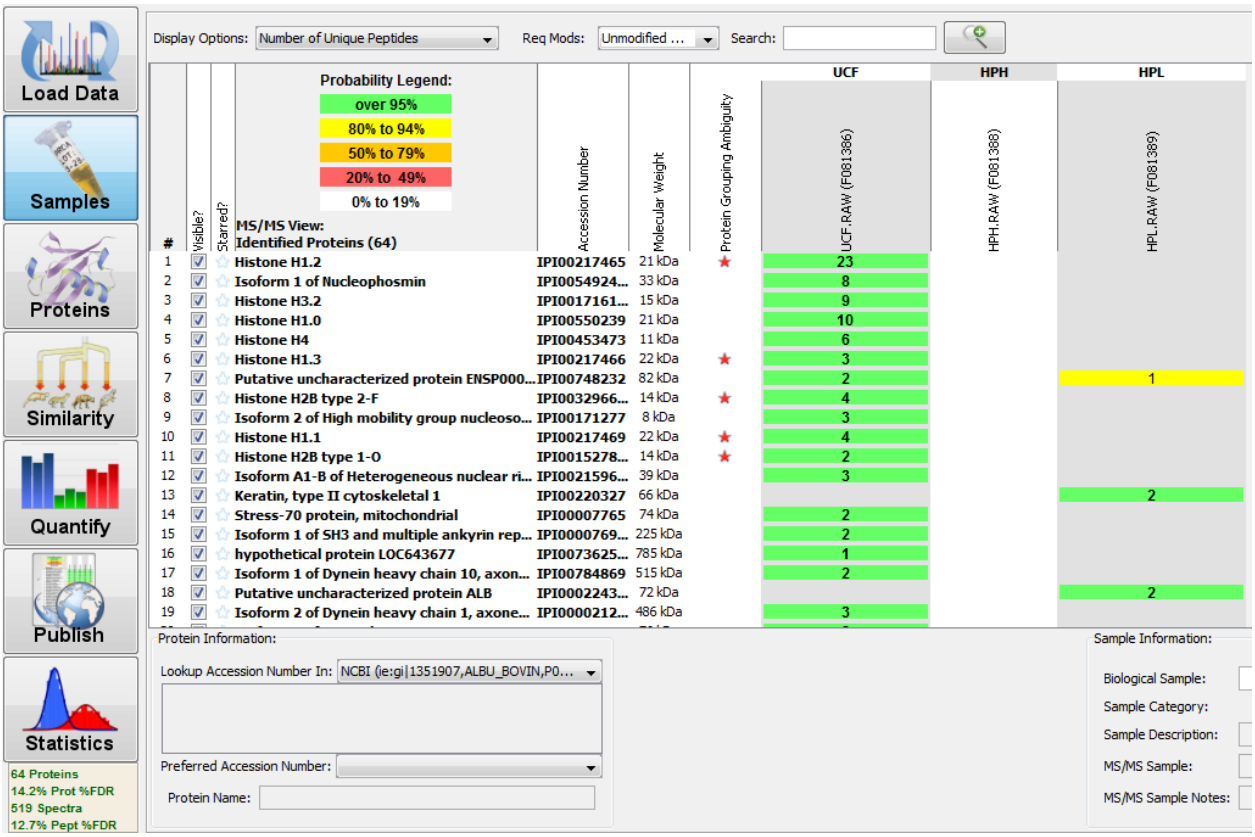

Figure 5-8. Protein ID results of the excised band after aptamer based affinity enrichment. (Library treated)

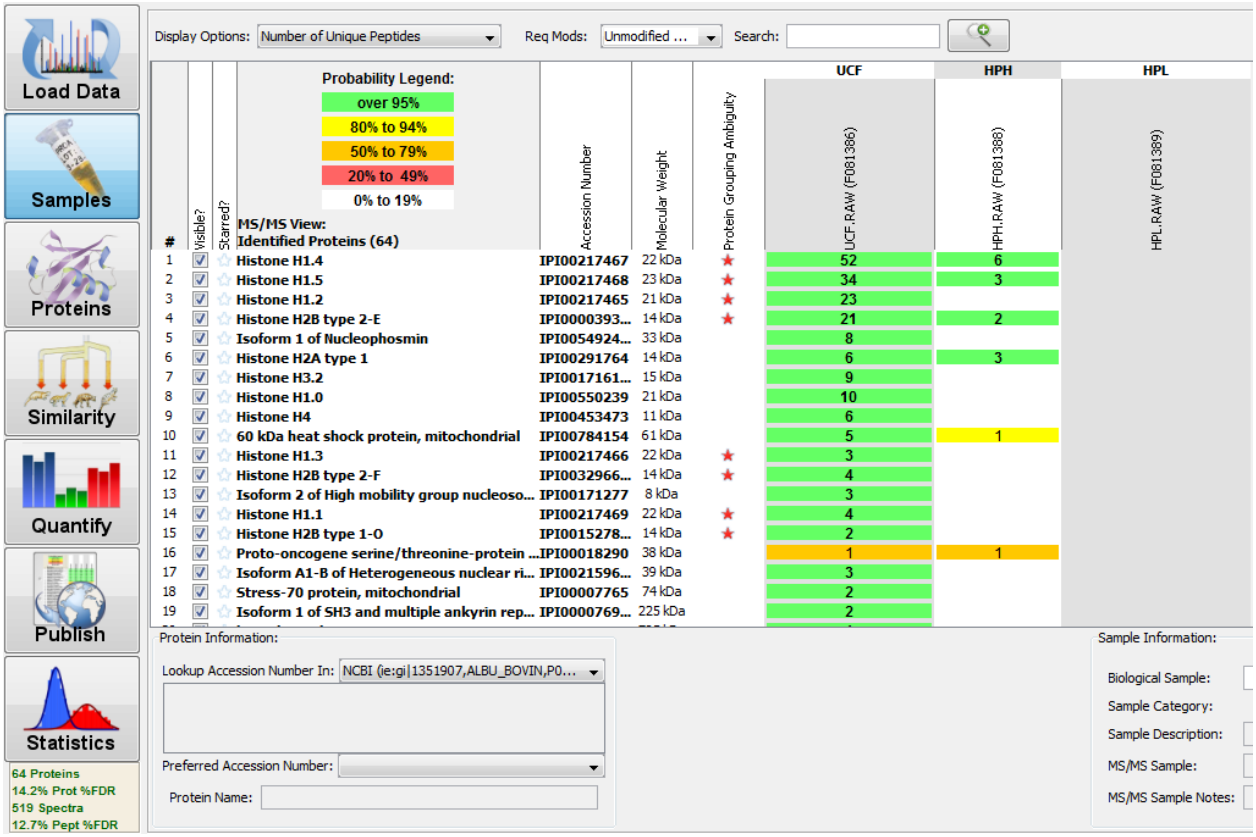

Figure 5-9. Protein ID results of the excised band after aptamer based affinity enrichment. (Library+TLS9 control aptamer treated)

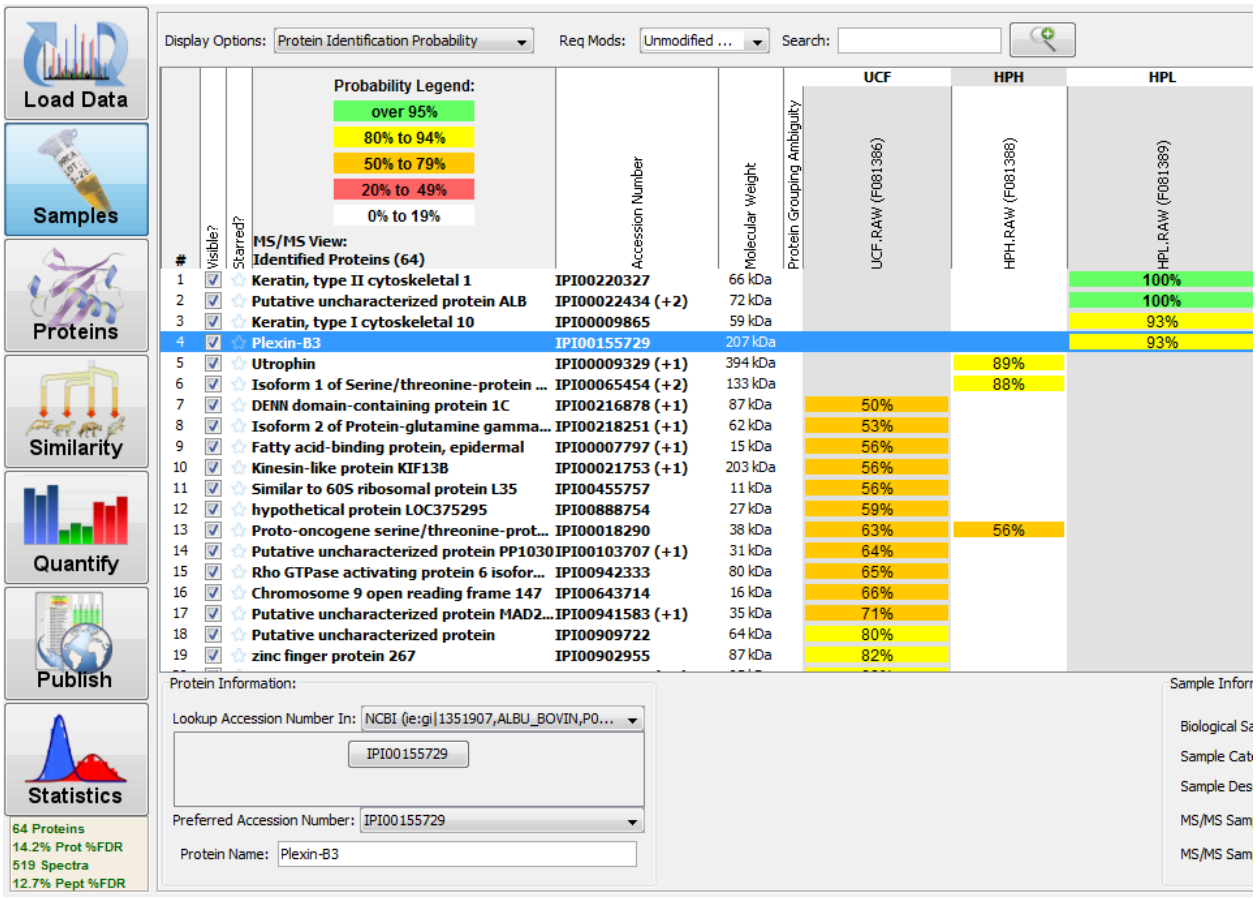

Figure 5-10. Protein ID results of the excised band after aptamer based affinity enrichment. (Library+TLS11a HCC aptamer treated)

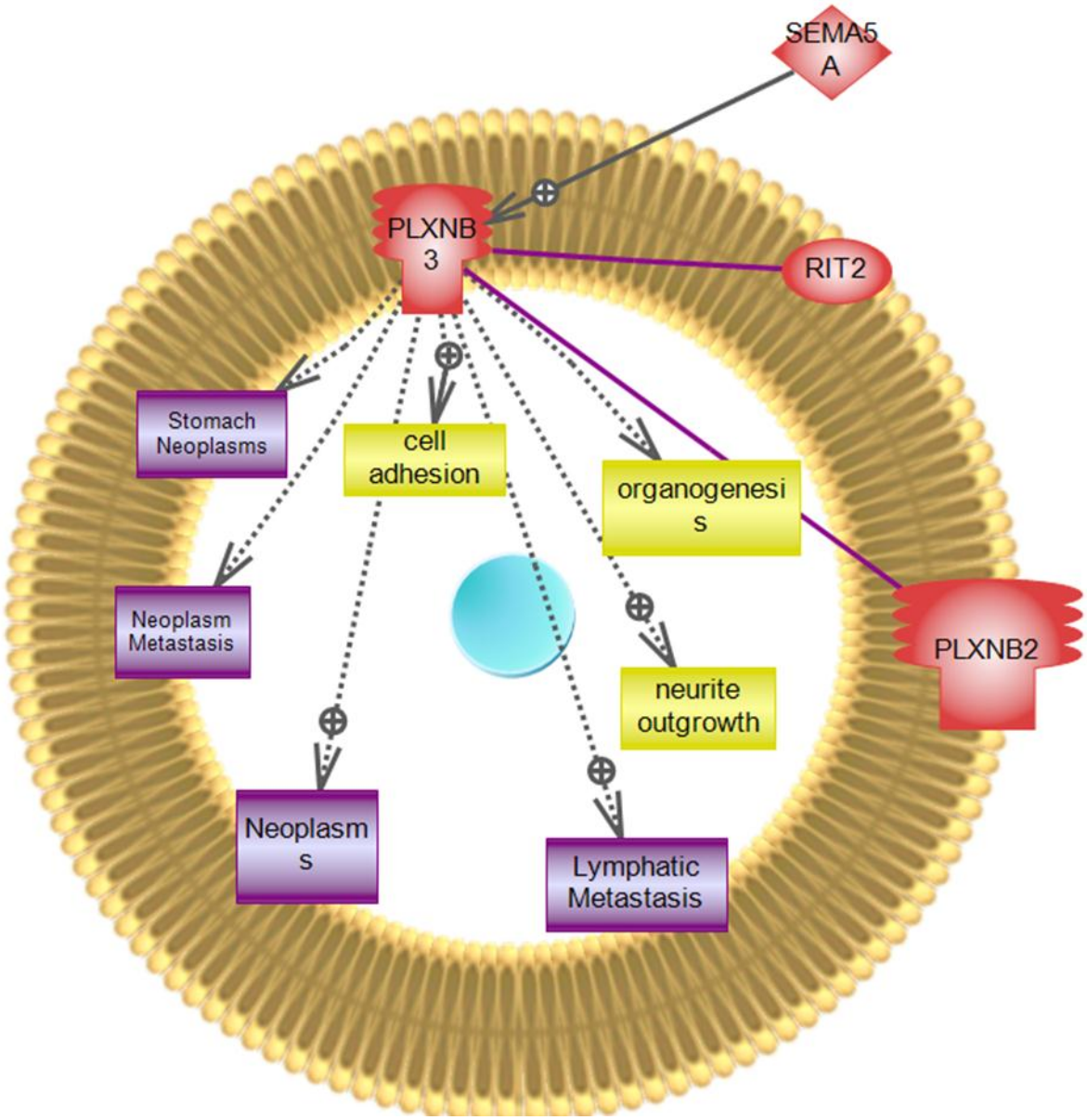

Figure 5-11. Analysis of interaction maps of Plexin B3

CHAPTER 6
CONCLUDING REMARKS AND FUTURE WORK

In this dissertation different aptamer based affinity methods were developed for improving the efficiency of mass spectrometry in identifying biological molecules of interest in complex biological mixtures. The results clearly suggest that the use of both aptamers- and mass spectrometry are complementary and can serve as an advantageous complement to conventional methods for separation. The methodologies described in the current thesis dealt with samples without any kind of derivatization, thus achieving a less complex, less expensive, and less time-consuming way to carry out the analysis of the biologically important molecules In addition, this fact differentiates this study and its procedures from other approaches normally reported in the literature for the tedious separation and/or determination of important compounds in clinical samples. Using the features provided by the proposed aptamer techniques plus the mass accuracy and sensitivity characteristics of the mass spectrometer, targeted analytes were efficiently separated and accurately detected. The aim of this study was to achieve a comprehensive understanding of the aptamer based structures for mass spectrometry. The development of a reliable analytical workflow based on the utilization of cutting-edge technology together with sophisticated data processing and analysis software tools enabled us to find a new biomarker candidate for HCC.

In fact, the unequivocal identification of target compounds is still one of the bottlenecks of biomarker discovery studies. In this sense, it is well-known that tandem mass spectrometry provides the ability to positively identify the proteins, the information provided by characteristics fragmentation patterns is far from being clinically useful. It also comes at the expense of enourmous amount of effort careful optimization of

experimental and instrumental paramaters. As we have demonstrated in four different examples aptamer based strategies can overcome many of the problems that the analytical chemistry and biomarker discovery community has been facing for many years.

Therefore, implementation of these aptamer based affinity mass spectrometry methodologies to improve the identification of the tentative biomarkers will be the part of the future work. In addition while working towards heavily on developing aptamer based strategies, different nanostructures methodologies have also been demonstrated to contribute to the detection of unique analytes. This study also generated many biological questions to be answered through further experimentation. Given the complexity and diversity of cancers, even within similar categories, multiple cancer-specific molecular probes are needed to delineate unique fingerprints of tumor cells. In most of our investigations, aptamers recognized their targets in very complex media such as cell lysates or plasma samples. However, aptamers that are applied the as proof of concept using cultured cell lines, should also be tested on real clinical specimens to determine their applicability in clinical diagnosis. Considering that very big organizations such as Human Proteome Organization (HUPO) and National Institutes of Health (NIH) support developing new protein capturing agents aimed at biomarker discovery, aptamer based affinity mass spectrometry method will gain more and more importance in the next 10 years. Most of the initial patents, which has been a roadblocker for their broad use, about aptamers will expire very soon and it is anticipated that aptamers will be more useful.

LIST OF REFERENCES

1. Gao, J., Garulacan, L.-A., Storm, S. M., Opiteck, G. J., Dubaquie, Y., Hefta, S. A., Dambach, D. M., and Dongre, A. R. (2005) Biomarker discovery in biological fluids, *Methods 35*, 291-302.

2. Want, E. J., Nordström, A., Morita, H., and Siuzdak, G. (2006) From Exogenous to Endogenous: The Inevitable Imprint of Mass Spectrometry in Metabolomics, *Journal of Proteome Research 6*, 459-468.

3. Griffin, J. L., and Kauppinen, R. A. (2006) Tumour Metabolomics in Animal Models of Human Cancer, *Journal of Proteome Research 6*, 498-505.

4. Kurihara, K., Konishi, F., Kanazawa, K., Fujii, T., and Saito, K. (1997) Alpha-Fetoprotein-Producing carcinoma of the colon: Report of a case, *Surgery Today 27*, 453-456.

5. Duffy, M. J. (2001) Carcinoembryonic Antigen as a Marker for Colorectal Cancer: Is It Clinically Useful?, *Clinical Chemistry 47*, 624-630.

6. Makarov, D. V., Loeb, S., Getzenberg, R. H., and Partin, A. W. (2009) Biomarkers for Prostate Cancer, *Annual Review of Medicine 60*, 139-151.

7. Forsberg, K., Valyi-Nagy, I., Heldin, C. H., Herlyn, M., and Westermark, B. (1993) Platelet-derived growth factor (PDGF) in oncogenesis: development of a vascular connective tissue stroma in xenotransplanted human melanoma producing PDGF-BB, *Proceedings of the National Academy of Sciences 90*, 393-397.

8. Dietmair, S., Timmins, N. E., Gray, P. P., Nielsen, L. K., and Krömer, J. O. (2010) Towards quantitative metabolomics of mammalian cells: Development of a metabolite extraction protocol, *Analytical Biochemistry 404*, 155-164.

9. Sreekumar, A., Poisson, L. M., Rajendiran, T. M., Khan, A. P., Cao, Q., Yu, J., Laxman, B., Mehra, R., Lonigro, R. J., Li, Y., Nyati, M. K., Ahsan, A., Kalyana-Sundaram, S., Han, B., Cao, X., Byun, J., Omenn, G. S., Ghosh, D., Pennathur, S., Alexander, D. C., Berger, A., Shuster, J. R., Wei, J. T., Varambally, S., Beecher, C., and Chinnaiyan, A. M. (2009) Metabolomic profiles delineate potential role for sarcosine in prostate cancer progression, *Nature 457*, 910-914.

10. Wikoff, W. R., Gangoiti, J. A., Barshop, B. A., and Siuzdak, G. (2007) Metabolomics Identifies Perturbations in Human Disorders of Propionate Metabolism, *Clinical Chemistry 53*, 2169-2176.

11. Aebersold, R., Anderson, L., Caprioli, R., Druker, B., Hartwell, L., and Smith, R. (2005) Perspective: A Program to Improve Protein Biomarker Discovery for Cancer, *Journal of Proteome Research 4*, 1104-1109.

12. Stein, L. D. (2004) Human genome: End of the beginning, *Nature 431*, 915-916.

13. Hamacher, M., Stephan, C., Eisenacher, M., van Hall, A., Marcus, K., Martens, L., Park, Y. M., Gutstein, H. B., Herberg, F., and Meyer, H. E. (2007) Proteomics for everyday use: Activities of the HUPO Brain Proteome Project during the 5th HUPO World Congress, *Proteomics 7*, 1012-1015.

14. Robertson, K. D. (2005) DNA methylation and human disease, *Nat Rev Genet 6*, 597-610.

15. Alderton, G. K. (2010) Transcriptomics: Common disease pathogenesis pathways, *Nat Rev Cancer 10*, 387-387.

16. Srivastava, S., and Srivastava, R.-G. (2005) Proteomics in the Forefront of Cancer Biomarker Discovery†, *Journal of Proteome Research 4*, 1098-1103.

17. Good, D. M., Thongboonkerd, V., Novak, J., Bascands, J.-L., Schanstra, J. P., Coon, J. J., Dominiczak, A., and Mischak, H. (2007) Body Fluid Proteomics for Biomarker Discovery: Lessons from the Past Hold the Key to Success in the Future, *Journal of Proteome Research 6*, 4549-4555.

18. Flemming, A. (2012) Therapeutics: Opening the door to a new class of proteasome inhibitors, *Nat Rev Cancer 12*, 5-5.

19. Levinson, S. S., Elin, R. J., and Yam, L. (2002) Light Chain Proteinuria and Lysozymuria in a Patient with Acute Monocytic Leukemia, *Clinical Chemistry 48*, 1131-1132.

20. Prigodich, A. E., Seferos, D. S., Massich, M. D., Giljohann, D. A., Lane, B. C., and Mirkin, C. A. (2009) Nano-flares for mRNA Regulation and Detection, *ACS Nano 3*, 2147-2152.

21. Hood, L., and Friend, S. H. (2011) Predictive, personalized, preventive, participatory (P4) cancer medicine, *Nat Rev Clin Oncol 8*, 184-187.

22. LaBaer, J. (2005) So, You Want to Look for Biomarkers (Introduction to the Special Biomarkers Issue)†, *Journal of Proteome Research 4*, 1053-1059.

23. Steen, H., and Mann, M. (2004) The abc's (and xyz's) of peptide sequencing, *Nat Rev Mol Cell Biol 5*, 699-711.

24. Hawkridge, A. M., and Muddiman, D. C. (2009) Mass Spectrometry–Based Biomarker Discovery: Toward a Global Proteome Index of Individuality, *Annual Review of Analytical Chemistry 2*, 265-277.

25. JF, K., JC, T., JE, L., DR, A., and HM, T. (2010) The emerging process of top down mass spectrometry for protein analysis: biomarkers, protein-therapeutics, and achieving high throughput, *Mol. Biosyst. 6*, 1532.

26. MP, W., R, U., C, D., DM, S., and JR, Y. (2002) Analysis of quantitative proteomic data generated via multidimensional protein identification technology, *Anal. Chem. 74*, 1650.

27. Coon, J. J. (2009) Collisions or Electrons? Protein Sequence Analysis in the 21st Century, *Analytical Chemistry 81*, 3208-3215.

28. Nesvizhskii, A. I., Vitek, O., and Aebersold, R. (2007) Analysis and validation of proteomic data generated by tandem mass spectrometry, *Nat Meth 4*, 787-797.

29. Albala, J. S. (2001) Array-based proteomics: the latest chip challenge, *Expert Review of Molecular Diagnostics 1*, 145-152.

30. Gulmann, C., Sheehan, K. M., Kay, E. W., Liotta, L. A., and Petricoin, E. F. (2006) Array-based proteomics: mapping of protein circuitries for diagnostics, prognostics, and therapy guidance in cancer, *The Journal of Pathology 208*, 595-606.

31. Rifai, N., Gillette, M. A., and Carr, S. A. (2006) Protein biomarker discovery and validation: the long and uncertain path to clinical utility, *Nat Biotech 24*, 971-983.

32. Horvatovich, P., Govorukhina, N., and Bischoff, R. (2006) Biomarker discovery by proteomics: challenges not only for the analytical chemist, *Analyst 131*.

33. L, A., and CL, H. (2006) Quantitative mass spectrometric multiple reaction monitoring assays for major plasma proteins, *Mol. Cell Proteomics 5*, 573.

34. Han, X., Aslanian, A., and Yates Iii, J. R. (2008) Mass spectrometry for proteomics, *Current Opinion in Chemical Biology 12*, 483-490.

35. Knochenmuss, R. (2006) Ion formation mechanisms in UV-MALDI, *Analyst 131*, 966-986.

36. Tang, K., Shvartsburg, A. A., Lee, H.-N., Prior, D. C., Buschbach, M. A., Li, F., Tolmachev, A. V., Anderson, G. A., and Smith, R. D. (2005) High-Sensitivity Ion Mobility Spectrometry/Mass Spectrometry Using Electrodynamic Ion Funnel Interfaces, *Analytical Chemistry 77*, 3330-3339.

37. Mæland Nilsen, M., Uleberg, K.-E., Janssen, E. A. M., Baak, J. P. A., Andersen, O. K., and Hjelle, A. (2011) From SELDI-TOF MS to protein identification by on-chip elution, *Journal of Proteomics 74*, 2995-2998.

38. Zhang, H., Kong, B., Qu, X., Jia, L., Deng, B., and Yang, Q. (2006) Biomarker discovery for ovarian cancer using SELDI-TOF-MS, *Gynecologic Oncology 102*, 61-66.

39. Hutchens, T. W., Magnuson, J. S., and Yip, T.-T. (1989) Interaction of Human Lactoferrin with DNA[colon] One-Step Purification by Affinity Chromatography on Single-Stranded DNAAgarose, *Pediatr Res 26*, 618-619.

40. Forler, D., Kocher, T., Rode, M., Gentzel, M., Izaurralde, E., and Wilm, M. (2003) An efficient protein complex purification method for functional proteomics in higher eukaryotes, *Nat Biotech 21*, 89-92.

41. Bauer, A., and Kuster, B. (2003) Affinity purification-mass spectrometry, *European Journal of Biochemistry 270*, 570-578.

42. Johnson, C. J., Zhukovsky, N., Cass, A. E. G., and Nagy, J. M. (2008) Proteomics, nanotechnology and molecular diagnostics, *Proteomics 8*, 715-730.

43. Bischoff, S., Kahn, M., Powell, M., and Kirlin, W. (2002) SELDI-TOF-MS Analysis of Transcriptional Activation Protein Binding to Response Elements Regulating Carcinogenesis Enzymes, *International Journal of Molecular Sciences 3*, 1027-1038.

44. Terracciano, R., Casadonte, F., Pasqua, L., Candeloro, P., Di Fabrizio, E., Urbani, A., and Savino, R. (2010) Enhancing plasma peptide MALDI-TOF-MS profiling by mesoporous silica assisted crystallization, *Talanta 80*, 1532-1538.

45. Ressine, A., Ekström, S., Marko-Varga, G., and Laurell, T. (2003) Macro-/Nanoporous Silicon as a Support for High-Performance Protein Microarrays, *Analytical Chemistry 75*, 6968-6974.

46. Finnskog, D., Jaras, K., Ressine, A., Malm, J., Marko-Varga, G., Lilja, H., and Laurell, T. (2006) High-speed biomarker identification utilizing porous silicon nanovial arrays and MALDI-TOF mass spectrometry, *Electrophoresis 27*, 1093-1103.

47. Meng, J.-c., Siuzdak, G., and Finn, M. G. (2004) Affinity mass spectrometry from a tailored porous silicon surface, *Chemical Communications*.

48. Tanaka, K., Waki, H., Ido, Y., Akita, S., Yoshida, Y., Yoshida, T., and Matsuo, T. (1988) Protein and polymer analyses up to m/z 100 000 by laser ionization time-of-flight mass spectrometry, *Rapid Communications in Mass Spectrometry 2*, 151-153.

49. Chiang, C.-K., Chen, W.-T., and Chang, H.-T. (2011) Nanoparticle-based mass spectrometry for the analysis of biomolecules, *Chemical Society Reviews 40*, 1269-1281.

50. Trauger, S. A., Go, E. P., Shen, Z., Apon, J. V., Compton, B. J., Bouvier, E. S. P., Finn, M. G., and Siuzdak, G. (2004) High Sensitivity and Analyte Capture with Desorption/Ionization Mass Spectrometry on Silylated Porous Silicon, *Analytical Chemistry 76*, 4484-4489.

51. Kong, X. L., Huang, L. C. L., Hsu, C. M., Chen, W. H., Han, C. C., and Chang, H. C. (2004) High-Affinity Capture of Proteins by Diamond Nanoparticles for Mass Spectrometric Analysis, *Analytical Chemistry 77*, 259-265.

52. Wang, K.-Y., Chuang, S.-A., Lin, P.-C., Huang, L.-S., Chen, S.-H., Ouarda, S., Pan, W.-H., Lee, P.-Y., Lin, C.-C., and Chen, Y.-J. (2008) Multiplexed Immunoassay: Quantitation and Profiling of Serum Biomarkers Using Magnetic Nanoprobes and MALDI-TOF MS, *Analytical Chemistry 80*, 6159-6167.

53. Chiang, C.-K., Yang, Z., Lin, Y.-W., Chen, W.-T., Lin, H.-J., and Chang, H.-T. (2010) Detection of Proteins and Protein−Ligand Complexes Using HgTe Nanostructure Matrixes in Surface-Assisted Laser Desorption/Ionization Mass Spectrometry, *Analytical Chemistry 82*, 4543-4550.

54. Thakare, V. S., Das, M., Jain, A. K., Patil, S., and Jain, S. (2010) Carbon nanotubes in cancer theragnosis, *Nanomedicine 5*, 1277-1301.

55. Hsu, W.-Y., Lin, W.-D., Hwu, W.-L., Lai, C.-C., and Tsai, F.-J. Screening Assay of Very Long Chain Fatty Acids in Human Plasma with Multiwalled Carbon Nanotube-Based Surface-Assisted Laser Desorption/Ionization Mass Spectrometry, *Analytical Chemistry 82*, 6814-6820.

56. Najam-ul-Haq, M., Rainer, M., Huck, C. W., Hausberger, P., Kraushaar, H., and Bonn, G. n. K. (2008) Nanostructured Diamond-Like Carbon on Digital Versatile Disc as a Matrix-Free Target for Laser Desorption/Ionization Mass Spectrometry, *Analytical Chemistry 80*, 7467-7472.

57. Tang, L. A. L., Wang, J., and Loh, K. P. (2010) Graphene-Based SELDI Probe with Ultrahigh Extraction and Sensitivity for DNA Oligomer, *Journal of the American Chemical Society 132*, 10976-10977.

58. Dong, X., Cheng, J., Li, J., and Wang, Y. (2010) Graphene as a Novel Matrix for the Analysis of Small Molecules by MALDI-TOF MS, *Analytical Chemistry 82*, 6208-6214.

59. Sefah, K., Shangguan, D., Xiong, X., O'Donoghue, M. B., and Tan, W. (2010) Development of DNA aptamers using Cell-SELEX, *Nat. Protocols 5*, 1169-1185.

60. Keefe, A. D., Pai, S., and Ellington, A. (2010) Aptamers as therapeutics, *Nat Rev Drug Discov 9*, 537-550.

61. Ng, E. W. M., Shima, D. T., Calias, P., Cunningham, E. T., Guyer, D. R., and Adamis, A. P. (2006) Pegaptanib, a targeted anti-VEGF aptamer for ocular vascular disease, *Nat Rev Drug Discov 5*, 123-132.

62. Tim, S. (2003) Aptamers and SELEX: the technology, *World Patent Information 25*, 123-129.

63. Wu, C. C., and Yates, J. R. (2003) The application of mass spectrometry to membrane proteomics, *Nat Biotech 21*, 262-267.

64. Siuti, N., and Kelleher, N. L. (2007) Decoding protein modifications using top-down mass spectrometry, *Nat Meth 4*, 817-821.

65. Phizicky, E., Bastiaens, P. I. H., Zhu, H., Snyder, M., and Fields, S. (2003) Protein analysis on a proteomic scale, *Nature 422*, 208-215.

66. F, H., M, K., RC, B., and BT, C. (1991) Matrix-assisted laser desorption/ionization mass spectrometry of biopolymers, *Anal. Chem. 63*, A1193.

67. Towers, M. W., McKendrick, J. E., and Cramer, R. (2010) Introduction of 4-Chloro-α-cyanocinnamic Acid Liquid Matrices for High Sensitivity UV-MALDI MS, *Journal of Proteome Research 9*, 1931-1940.

68. Shen, Z., Thomas, J. J., Averbuj, C., Broo, K. M., Engelhard, M., Crowell, J. E., Finn, M. G., and Siuzdak, G. (2000) Porous Silicon as a Versatile Platform for Laser Desorption/Ionization Mass Spectrometry, *Analytical Chemistry 73*, 612-619.

69. Shenar, N., Martinez, J., and Enjalbal, C. (2008) Laser desorption/ionization mass spectrometry on porous silica and alumina for peptide mass fingerprinting, *Journal of the American Society for Mass Spectrometry 19*, 632-644.

70. Walker, B. N., Razunguzwa, T., Powell, M., Knochenmuss, R., and Vertes, A. (2009) Nanophotonic Ion Production from Silicon Microcolumn Arrays, *Angewandte Chemie International Edition 48*, 1669-1672.

71. Walker, B. N., Stolee, J. A., Pickel, D. L., Retterer, S. T., and Vertes, A. (2010) Tailored Silicon Nanopost Arrays for Resonant Nanophotonic Ion Production, *The Journal of Physical Chemistry C 114*, 4835-4840.

72. Finkel, N. H., Prevo, B. G., Velev, O. D., and He, L. (2005) Ordered Silicon Nanocavity Arrays in Surface-Assisted Desorption/Ionization Mass Spectrometry, *Analytical Chemistry 77*, 1088-1095.

73. Okuno, S., Arakawa, R., Okamoto, K., Matsui, Y., Seki, S., Kozawa, T., Tagawa, S., and Wada, Y. (2005) Requirements for Laser-Induced Desorption/Ionization on Submicrometer Structures, *Analytical Chemistry 77*, 5364-5369.

74. Wada, Y., Yanagishita, T., and Masuda, H. (2007) Ordered Porous Alumina Geometries and Surface Metals for Surface-Assisted Laser Desorption/Ionization of Biomolecules: Possible Mechanistic Implications of Metal Surface Melting, *Analytical Chemistry 79*, 9122-9127.

75. Li, N., Mitchell, D. T., Lee, K.-P., and Martin, C. R. (2003) A Nanostructured Honeycomb Carbon Anode, *Journal of The Electrochemical Society 150*, A979-A984.

76. Touboul, D., Bouchoux, G., and Zenobi, R. (2008) Gas-Phase Protonation Thermochemistry of Adenosine, *The Journal of Physical Chemistry B 112*, 11716-11725.

77. Northen, T., Woo, H.-K., Northen, M., Nordström, A., Uritboonthail, W., Turner, K., and Siuzdak, G. (2007) High surface area of porous silicon drives desorption of intact molecules, *Journal of the American Society for Mass Spectrometry 18*, 1945-1949.

78. Hsu, N.-Y., Tseng, S. Y., Wu, C.-Y., Ren, C.-T., Lee, Y.-C., Wong, C.-H., and Chen, C.-H. (2008) Desorption Ionization of Biomolecules on Metals, *Analytical Chemistry 80*, 5203-5210.

79. Chen, S.-Y., Li, K.-I., Yu, C.-S., Wang, J.-S., Hu, Y.-C., and Lai, C.-C. (2010) A Radiate Microstructure MALDI Chip for Sample Concentration and Detection, *Analytical Chemistry 82*, 5951-5957.

80. Jones, L. L., McDonald, D. A., and Borum, P. R. (2010) Acylcarnitines: Role in brain, *Progress in Lipid Research 49*, 61-75.

81. Brittain, S. M., Ficarro, S. B., Brock, A., and Peters, E. C. (2005) Enrichment and analysis of peptide subsets using fluorous affinity tags and mass spectrometry, *Nat Biotech 23*, 463-468.

82. Curran, D. P. (2008) Fluorous Tags Unstick Messy Chemical Biology Problems, *Science 321*, 1645-1646.

83. Northen, T. R., Yanes, O., Northen, M. T., Marrinucci, D., Uritboonthai, W., Apon, J., Golledge, S. L., Nordstrom, A., and Siuzdak, G. (2007) Clathrate nanostructures for mass spectrometry, *Nature 449*, 1033-1036.

84. Vallès-Miret, M., and Bradley, M. (2011) A generic small-molecule microarray immobilization strategy, *Tetrahedron Letters 52*, 6819-6822.

85. Lu, Z., Zhou, X., Hu, S., Shu, X., Tian, Y., and Zhu, J. (2010) Interfacial Assembly of Nanoparticles with Fluorous-Tagged Organic Molecules, *The Journal of Physical Chemistry C 114*, 13546-13550.

86. Cametti, M., Crousse, B., Metrangolo, P., Milani, R., and Resnati, G. (2012) The fluorous effect in biomolecular applications, *Chemical Society Reviews 41*.

87. Mamidyala, S. K., Ko, K.-S., Jaipuri, F. A., Park, G., and Pohl, N. L. (2006) Noncovalent fluorous interactions for the synthesis of carbohydrate microarrays, *Journal of Fluorine Chemistry 127*, 571-579.

88. Collet, B. Y. M., Nagashima, T., Yu, M. S., and Pohl, N. L. B. (2009) Fluorous-based peptide microarrays for protease screening, *Journal of Fluorine Chemistry 130*, 1042-1048.

89. Edwards, H. D., Nagappayya, S. K., and Pohl, N. L. B. (2012) Probing the limitations of the fluorous content for tag-mediated microarray formation, *Chemical Communications 48*.

90. Whiteaker, J. R., Zhao, L., Lin, C., Yan, P., Wang, P., and Paulovich, A. G. (2011) Sequential multiplexed analyte quantification using peptide immunoaffinity enrichment coupled to mass spectrometry, *Molecular & Cellular Proteomics*.

91. Chou, P.-H., Chen, S.-H., Liao, H.-K., Lin, P.-C., Her, G.-R., Lai, A. C.-Y., Chen, J.-H., Lin, C.-C., and Chen, Y.-J. (2005) Nanoprobe-Based Affinity Mass Spectrometry for Selected Protein Profiling in Human Plasma, *Analytical Chemistry 77*, 5990-5997.

92. Shen, J., Shi, M., Yan, B., Ma, H., Li, N., Hu, Y., and Ye, M. (2010) Covalent attaching protein to graphene oxide via diimide-activated amidation, *Colloids and Surfaces B: Biointerfaces 81*, 434-438.

93. Chattopadhyay, J., de Jesus Cortez, F., Chakraborty, S., Slater, N. K. H., and Billups, W. E. (2006) Synthesis of Water-Soluble PEGylated Single-Walled Carbon Nanotubes, *Chemistry of Materials 18*, 5864-5868.

94. Barylyuk, K., Chingin, K., Balabin, R., and Zenobi, R. (2010) Fragmentation of benzylpyridinium “thermometer” ions *Journal of the American Society for Mass Spectrometry 21*, 172-177.

95. Greisch, J. F., Gabelica, V., Remacle, F., and De Pauw, E. (2003) Thermometer ions for matrix-enhanced laser desorption/ionization internal energy calibration, *Rapid Communications in Mass Spectrometry 17*, 1847-1854.

96. Pak, A., Lesage, D., Gimbert, Y., Vékey, K., and Tabet, J.-C. (2008) Internal energy distribution of peptides in electrospray ionization : ESI and collision-induced dissociation spectra calculation, *Journal of Mass Spectrometry 43*, 447-455.

97. Medintz, I. L., Uyeda, H. T., Goldman, E. R., and Mattoussi, H. (2005) Quantum dot bioconjugates for imaging, labelling and sensing, *Nat Mater 4*, 435-446.

98. Liu, C.-W., Chien, M.-W., Chen, G.-F., Chen, S.-Y., Yu, C.-S., Liao, M.-Y., and Lai, C.-C. (2011) Quantum Dot Enhancement of Peptide Detection by Matrix-Assisted Laser Desorption/Ionization Mass Spectrometry, *Analytical Chemistry 83*, 6593-6600.

99. Chen, W.-T., Chiang, C.-K., Lee, C.-H., and Chang, H.-T. (2012) Using Surface-Assisted Laser Desorption/Ionization Mass Spectrometry to Detect Proteins and Protein–Protein Complexes, *Analytical Chemistry 84*, 1924-1930.

100. An, G. H., Suh, O. S., Kwon, H. C., Kim, K., and Johnson, E. A. (2000) Quantification of carotenoids in cells of Phaffia rhodozyma by autofluorescence, *Biotechnology Letters 22*, 1031-1034.

101. Fehr, M., Frommer, W. B., and Lalonde, S. (2002) Visualization of maltose uptake in living yeast cells by fluorescent nanosensors, *Proceedings of the National Academy of Sciences 99*, 9846-9851.

102. Kim, Y.-R., Bong, S., Kang, Y.-J., Yang, Y., Mahajan, R. K., Kim, J. S., and Kim, H. (2010) Electrochemical detection of dopamine in the presence of ascorbic acid using graphene modified electrodes, *Biosensors and Bioelectronics 25*, 2366-2369.

103. Amantonico, A., Oh, J. Y., Sobek, J., Heinemann, M., and Zenobi, R. (2008) Mass Spectrometric Method for Analyzing Metabolites in Yeast with Single Cell Sensitivity, *Angewandte Chemie International Edition 47*, 5382-5385.

104. Schladt, T. D., Shukoor, M. I., Schneider, K., Tahir, M. N., Natalio, F., Ament, I., Becker, J., Jochum, F. D., Weber, S., Köhler, O., Theato, P., Schreiber, L. M., Sönnichsen, C., Schröder, H. C., Müller, W. E. G., and Tremel, W. (2010) Au@MnO Nanoflowers: Hybrid Nanocomposites for Selective Dual Functionalization and Imaging, *Angewandte Chemie International Edition 49*, 3976-3980.

105. Wei, Y., Klajn, R., Pinchuk, A. O., and Grzybowski, B. A. (2008) Synthesis, Shape Control, and Optical Properties of Hybrid Au/Fe3O4 “Nanoflowers”, *Small 4*, 1635-1639.

106. Zhai, Y., Zhai, J., Wang, Y., Guo, S., Ren, W., and Dong, S. (2009) Fabrication of Iron Oxide Core/Gold Shell Submicrometer Spheres with Nanoscale Surface Roughness for Efficient Surface-Enhanced Raman Scattering, *The Journal of Physical Chemistry C 113*, 7009-7014.

107. Kim, Y.-K., Na, H.-K., Kwack, S.-J., Ryoo, S.-R., Lee, Y., Hong, S., Hong, S., Jeong, Y., and Min, D.-H. (2011) Synergistic Effect of Graphene Oxide/MWCNT Films in Laser Desorption/Ionization Mass Spectrometry of Small Molecules and Tissue Imaging, *ACS Nano 5*, 4550-4561.

108. Estévez, M., O’Donoghue, M., Chen, X., and Tan, W. (2009) Highly fluorescent dye-doped silica nanoparticles increase flow cytometry sensitivity for cancer cell monitoring, *Nano Research 2*, 448-461.

109. Chen, T., Shukoor, M. I., Chen, Y., Yuan, Q. A., Zhu, Z., Zhao, Z. L., Gulbakan, B., and Tan, W. H. (2011) Aptamer-conjugated nanomaterials for bioanalysis and biotechnology applications, *Nanoscale 3*, 546-556.

110. Acin-Perez, R., Gatti, Domenico L., Bai, Y., and Manfredi, G. (2011) Protein Phosphorylation and Prevention of Cytochrome Oxidase Inhibition by ATP: Coupled Mechanisms of Energy Metabolism Regulation, *Cell metabolism 13*, 712-719.

111. Jiang, W., KimBetty, Y. S., Rutka, J. T., and ChanWarren, C. W. (2008) Nanoparticle-mediated cellular response is size-dependent, *Nat Nano 3*, 145-150.

112. Zhu, Z.-J., Ghosh, P. S., Miranda, O. R., Vachet, R. W., and Rotello, V. M. (2008) Multiplexed Screening of Cellular Uptake of Gold Nanoparticles Using Laser Desorption/Ionization Mass Spectrometry, *Journal of the American Chemical Society 130*, 14139-14143.

113. Sellick, C. A., Hansen, R., Stephens, G. M., Goodacre, R., and Dickson, A. J. (2011) Metabolite extraction from suspension-cultured mammalian cells for global metabolite profiling, *Nat. Protocols 6*, 1241-1249.

114. Shin, M. H., Lee, D. Y., Liu, K.-H., Fiehn, O., and Kim, K. H. (2010) Evaluation of Sampling and Extraction Methodologies for the Global Metabolic Profiling of Saccharophagus degradans, *Analytical Chemistry 82*, 6660-6666.

115. Yanes, O., Tautenhahn, R., Patti, G. J., and Siuzdak, G. (2011) Expanding Coverage of the Metabolome for Global Metabolite Profiling, *Analytical Chemistry 83*, 2152-2161.

116. Cutler, J. I., Auyeung, E., and Mirkin, C. A. (2012) Spherical Nucleic Acids, *Journal of the American Chemical Society 134*, 1376-1391.

117. Seferos, D. S., Giljohann, D. A., Hill, H. D., Prigodich, A. E., and Mirkin, C. A. (2007) Nano-Flares: Probes for Transfection and mRNA Detection in Living Cells, *Journal of the American Chemical Society 129*, 15477-15479.

118. Zheng, D., Seferos, D. S., Giljohann, D. A., Patel, P. C., and Mirkin, C. A. (2009) Aptamer Nano-flares for Molecular Detection in Living Cells, *Nano Letters 9*, 3258-3261.

119. Sellick, C. A., Hansen, R., Maqsood, A. R., Dunn, W. B., Stephens, G. M., Goodacre, R., and Dickson, A. J. (2008) Effective Quenching Processes for Physiologically Valid Metabolite Profiling of Suspension Cultured Mammalian Cells, *Analytical Chemistry 81*, 174-183.

120. El-Serag, H. B. (2011) Hepatocellular Carcinoma, *New England Journal of Medicine 365*, 1118-1127.

121. Villanueva, A., Minguez, B., Forner, A., Reig, M., and Llovet, J. M. (2010) Hepatocellular Carcinoma: Novel Molecular Approaches for Diagnosis, Prognosis, and Therapy, *Annual Review of Medicine 61*, 317-328.

122. Kudo, M. (2011) Diagnostic Imaging of Hepatocellular Carcinoma: Recent Progress, *Oncology 81*, 73-85.

123. Murakami, T., Imai, Y., Okada, M., Hyodo, T., Lee, W. J., Kim, M. J., Kim, T., and Choi, B. I. (2011) Ultrasonography, Computed Tomography and Magnetic Resonance Imaging of Hepatocellular Carcinoma: Toward Improved Treatment Decisions, *Oncology 81*, 86-99.

124. Lee, I. J., and Seong, J. (2011) Radiotherapeutic Strategies in the Management of Hepatocellular Carcinoma, *Oncology 81*, 123-133.

125. Yu, L., Dai, Z., Wang, Z., Fan, J., and Zhou, J. (2011) Prognostic Indicators for Tumor Recurrence after Liver Transplantation in Hepatocellular Carcinoma and Related Molecular Targeted Therapy, *Oncology 81*, 116-122.

126. Llovet, J. M., Ricci, S., Mazzaferro, V., Hilgard, P., Gane, E.,., Häussinger, D., Giannaris, T., Shan, M., Moscovici, M., Voliotis, D., and Bruix, J. (2008) Sorafenib in Advanced Hepatocellular Carcinoma, *New England Journal of Medicine 359*, 378-390.

127. Mínguez, B., and Lachenmayer, A. (2011) Diagnostic and prognostic molecular markers in hepatocellular carcinoma, *Disease Markers 31*, 181-190.

128. Zinkin, N. T., Grall, F., Bhaskar, K., Otu, H. H., Spentzos, D., Kalmowitz, B., Wells, M., Guerrero, M., Asara, J. M., Libermann, T. A., and Afdhal, N. H. (2008) Serum Proteomics and Biomarkers in Hepatocellular Carcinoma and Chronic Liver Disease, *Clinical Cancer Research 14*, 470-477.

129. Llovet, J. M., Pena, C., Lathia, C., Shan, M., Meinhardt, G., and Bruix, J. (2012) Plasma Biomarkers as Predictors of Outcome in Patients with Advanced Hepatocellular Carcinoma, *Clinical Cancer Research*.

130. Shafizadeh, N., Ferrell, L. D., and Kakar, S. (2008) Utility and limitations of glypican-3 expression for the diagnosis of hepatocellular carcinoma at both ends of the differentiation spectrum, *Mod Pathol 21*, 1011-1018.

131. Peradziryi, H., Kaplan, N. A., Podleschny, M., Liu, X., Wehner, P., Borchers, A., and Tolwinski, N. S. (2011) PTK7/Otk interacts with Wnts and inhibits canonical Wnt signalling, *EMBO J 30*, 3729-3740.

132. Lahat, G., Zhu, Q.-S., Huang, K.-L., Wang, S., Bolshakov, S., Liu, J., Torres, K., Langley, R. R., Lazar, A. J., Hung, M. C., and Lev, D. (2010) Vimentin Is a Novel Anti-Cancer Therapeutic Target; Insights from In Vitro and In Vivo Mice Xenograft Studies, *PLoS ONE 5*, e10105.

133. Balakrishnan, A., Penachioni, J. Y., Lamba, S., Bleeker, F. E., Zanon, C., Rodolfo, M., Vallacchi, V., Scarpa, A., Felicioni, L., Buck, M., Marchetti, A., Comoglio, P. M., Bardelli, A., and Tamagnone, L. (2009) Molecular profiling of the “plexinome” in melanoma and pancreatic cancer, *Human Mutation 30*, 1167-1174.

134. Sadanandam, A., Varney, M. L., Singh, S., Ashour, A. E., Moniaux, N., Deb, S., Lele, S. M., Batra, S. K., and Singh, R. K. (2010) High gene expression of semaphorin 5A in pancreatic cancer is associated with tumor growth, invasion and metastasis, *International Journal of Cancer 127*, 1373-1383.

135. Li, X., and Lee, A. Y. W. (2010) Semaphorin 5A and Plexin-B3 Inhibit Human Glioma Cell Motility through RhoGDIα-mediated Inactivation of Rac1 GTPase, *Journal of Biological Chemistry 285*, 32436-32445.

136. Li, X., Law, J. W. S., and Lee, A. Y. W. (2012) Semaphorin 5A and plexin-B3 regulate human glioma cell motility and morphology through Rac1 and the actin cytoskeleton, *Oncogene 31*, 595-610.

137. Shangguan, D., Meng, L., Cao, Z. C., Xiao, Z., Fang, X., Li, Y., Cardona, D., Witek, R. P., Liu, C., and Tan, W. (2008) Identification of Liver Cancer-Specific Aptamers Using Whole Live Cells, *Analytical Chemistry 80*, 721-728.

BIOGRAPHICAL SKETCH

Basri Gulbakan was born in Balikesir, Turkey. After completing the high school, he attended the Hacettepe University to get his B.S degree. He obtained his B.S. (2004) in chemistry and his master of science (2006) in physical chemistry. He joined the University of Florida in 2007 and pursued his PhD training under the supervision of Dr. Weihong Tan and co-supervision of Dr.David H.Powell